

UNCLASSIFIED

AD NUMBER

AD832225

LIMITATION CHANGES

TO:

Approved for public release; distribution is unlimited.

FROM:

Distribution authorized to U.S. Gov't. agencies and their contractors; Critical Technology; MAY 1968. Other requests shall be referred to Air Force Technical Application Center, Washington, DC 20333. This document contains export-controlled technical data.

AUTHORITY

usaf ltr, 25 jan 1972

THIS PAGE IS UNCLASSIFIED

TR 68-2

AD832225

TECHNICAL REPORT NO. 68-2

STRAIN SEISMOGRAPH OPERATING PROCEDURES AND APPLICATIONS

STATEMENT #2 UNCLASSIFIED

This document is subject to special export controls and each transmittal to foreign governments or foreign nationals may be made only with prior approval of *USIA/NSA/DoD*

Seismological Center, Wash DC 20333

DDC
MAY 20 1968



GEOTECH

A TELEDYNE COMPANY

TECHNICAL REPORT NO. 68-2

STRAIN SEISMOGRAPH OPERATING PROCEDURES AND APPLICATIONS

by

R. H. Kirklin

and

B. W. Girard

Sponsored by

Advanced Research Projects Agency
Nuclear Test Detection Office
ARPA Order No. 624

Availability

Qualified users may request copies
of this document from:
Defense Documentation Center
Cameron Station
Alexandria, Virginia 22341

Acknowledgement

This research was supported by the
Advanced Research Projects Agency,
Nuclear Test Detection Office, and
was monitored by the Air Force
Technical Applications Center under
Contract No. AF 33(657)-15288.

GEOTECH
A TELEDYNE COMPANY
3401 Shiloh Road
Garland, Texas

1 May 1968

IDENTIFICATION

AFTAC Project No.	VELA T/5081
Project Title:	Multicomponent Strain Seismograph
ARPA Order No.	624
ARPA Code No.	8100
Contractor:	The Geotechnical Corporation Garland, Texas
Date of Contract:	1 July 1965
Amount of Contract:	\$393,361
Contract No.	AF 33(657)-15288
Contract Expiration Date:	31 December 1967
Project Manager:	R. C. Shopland, BR1-2561

CONTENTS

	<u>Page</u>
ABSTRACT	
1. INTRODUCTION	1
2. THEORY	2
3. EQUATING STRAIN AND INERTIAL RESPONSES	3
3.1 Seismometer installation	4
3.2 Matched strain and inertial seismographs	4
4. STRAIN-INERTIAL SEISMOGRAPH RESPONSES TO SEISMIC WAVES	9
4.1 Surface waves	9
4.1.1 Love waves	10
4.1.2 Rayleigh waves	10
4.2 Body waves	15
4.2.1 Longitudinal waves	18
4.2.2 Transverse waves	18
4.2.2.1 SH component	18
4.2.2.2 SV component	21
4.2.3 Earthquake phases	21
5. APPLICATION OF STRAIN SEISMOGRAPHS	28
5.1 Horizontal strain-inertial combination	28
5.1.1 Microseismic rejection	31
5.1.2 Signal addition	36
5.2 Vertical strain-inertial combination	36
5.3 Seismic wave identification	41
5.3.1 Earthquake phases	41
5.3.2 Microseisms	43
6. SYSTEM DESCRIPTION AND OPERATING PROCEDURES	46
6.1 System description	46
6.2 System calibration procedures	51
6.2.1 Determination of calibration constants	51
6.2.1.1 Strain seismometers	51
6.2.1.2 Inertial seismometers	54
6.2.2 Daily calibration procedures	54
6.2.2.1 Horizontal strain seismographs	54
6.2.2.2 Vertical strain seismograph	55
6.2.2.3 Inertial seismographs	56

CONTENTS, continued

	<u>Page</u>
6.2.3 Determination of seismograph response curves	56
6.2.3.1 Amplitude response for strain seismographs	56
6.2.3.2 Amplitude response for inertial seismographs	58
6.2.3.3 Phase measurement techniques	59
6.2.3.4 Determination of the amplitude and phase response match between strain and inertial seismographs	59
6.2.4 Determination of strain seismograph polarity	59
6.3 Recording procedures	72
6.3.1 Recorder requirements	72
6.3.2 Recorder signal levels	72
6.3.2.1 Develocorders	72
6.3.2.2 Magnetic-tape recorders	77
7. SELECTED REFERENCES	80

ILLUSTRATIONS

<u>Figure</u>		<u>Page</u>
1	Horizontal strain seismometer installation showing orientation of instruments	5
2	Vertical strain seismometer installation	6
3	Block diagram of matched horizontal short-period strain and inertial seismographs at WMSO	7
4	Asymptotic amplitude responses of matched short-period strain and inertial seismographs and their components	8
5	Azimuthal response of a horizontal strain seismometer, solid curve, and a horizontal inertial seismometer, dashed curve, to horizontally polarized transverse waves (SH)	11
6	Ratios of horizontal and vertical differential displacement to surface displacement due to Rayleigh waves plotted as a function of frequency. The dashed line is the horizontal ratio and is for an 18 meter strain rod. The solid lines are the vertical ratios for different positions and lengths of the strain rod	12
7	Seismogram illustrating the difference between responses of summed orthogonal horizontal strains (ESNE, SNW) and vertical strain (SZ) to high frequency Rayleigh when equal for longer period microseisms	13
8	Displacement-depth and phase-depth relationships for Rayleigh and longitudinal waves. Longitudinal wave incident at 30°	14
9	Azimuthal response of a horizontal strain seismometer, solid curve, and horizontal inertial seismometer, dashed curve, to apparent longitudinal waves	16
10	Displacement-depth relationship for Rayleigh waves using an earth model for WMSO	17

ILLUSTRATIONS, continued

<u>Figure</u>		<u>Page</u>
11	Polar plots of the relative vertical displacement, vertical differential displacement, horizontal displacement, and horizontal differential displacement due to incident longitudinal waves plotted as a function of the angle of incidence. The values of vertical and horizontal differential displacement have been multiplied by 144 and 28 respectively	19
12	Phase of the vertical displacement, vertical differential displacement, horizontal displacement, and horizontal differential displacement due to incident longitudinal waves as a function of the angle of incidence at a frequency of 1.0 Hz	20
13	Polar plots of the relative horizontal displacement and horizontal differential displacement due to incident SH waves plotted as a function of the angle of incidence. The values of horizontal differential displacement have been multiplied by 28	22
14	Polar plots of the relative vertical displacement, vertical differential displacement, horizontal displacement, and horizontal differential displacement due to incident SV waves plotted as a function of the angle of incidence. The values of vertical and horizontal differential displacement have been multiplied by 144 and 28 respectively	23
15	Phase of the vertical displacement, vertical differential displacement, horizontal displacement, and horizontal differential displacement due to incident SV waves as a function of the angle of incidence at a frequency of 1.0 Hz	24
16	Seismogram illustrating the sensitivity of a vertical strain seismograph to the SV component of transverse waves. The recording is of the S-phase from an earthquake whose epicenter was in the Kurile Islands	25

ILLUSTRATIONS, continued

<u>Figure</u>		<u>Page</u>
17	Ratios of the theoretical amplitudes of the vertical strain to vertical inertial for several earthquake body phases. The ratios are based on a value of unity for Rayleigh waves. The SV component of transverse waves is used	26
18	Ratios of the theoretical amplitudes of the horizontal strain to horizontal inertial for several earthquake body phases. The ratios are based on a value of unity for Rayleigh waves. The SH component of transverse waves is used	27
19	Azimuthal response to Rayleigh waves of the summed outputs of horizontal strain and inertial seismographs that are oriented in the same direction	29
20	Azimuthal response to Love waves of the summed outputs of the horizontal strain and inertial seismographs that are oriented in the same direction	30
21	Seismogram illustrating the ability of the strain directional array to azimuthally discriminate between microseisms exhibiting directional properties	32
22	Azimuthal response to Rayleigh waves of the summed outputs of a horizontal inertial seismograph and either a vertical strain or two orthogonal horizontal strain seismographs	33
23	Seismograms showing results obtained from the sine-cosine technique. Maximum cancellation of 4 to 6 second microseisms occurred on the west and southwest traces (6 and 7), indicating that the microseisms are arriving from the east and the northeast	34
24	Seismograms illustrating the reduction of microseisms by the west component of the WMSO directional array (W) thereby enhancing the horizontal component of body phases (figure 24a) and surface waves (24b) from an earthquake. The horizontal east inertial (SPE) recording is also shown	35

ILLUSTRATIONS, continued

<u>Figure</u>		<u>Page</u>
25	Seismograms illustrating increased improvement in recorded P-waves by the NW component of the WMSO directional array as the epicentral distance decreases	37/38
26	Enhancement of surface waves from Central Alaska by the north component of the WMSO directional array	39
27	Azimuthal discrimination of surface waves from Central Alaska and South America superimposed to simulate simultaneous recording. The surface waves from South America have been rejected, enhancing those from Central Alaska	40
28	Seismograms illustrating limited reduction of microseisms over sustained periods of time attained by the summation (Σ SPZ, SZ) of the filtered outputs of a vertical strain (SZ) and a vertical inertial (SPZ) seismograph	42
29	Seismograms illustrating how vertical strain and inertial recordings can be used to discriminate between the phases pP and PcP by inspection. The strain/inertial amplitude ratio for pP is about the same as for P, but much smaller for PcP. The earthquake epicenter was in the western part of Brazil	44
30	Seismogram illustrating the 180° phase difference between the orthogonal horizontal strains (SN and SE) for Love waves, and 0° phase difference for Rayleigh waves. The phase difference between the orthogonal horizontal inertials (SPN and SPE) for both Love and Rayleigh will be dependent on azimuth	45
31	Block diagram of strain-inertial seismograph system at WMSO	47
32	Schematic diagram of a typical two channel strain directional array	52
33	Calibration Control Unit, Model 17123	53

ILLUSTRATIONS, continued

<u>Figure</u>		<u>Page</u>
34	Curves A and B are theoretical amplitude and phase response curves for the short-period strain seismograph at constant differential ground displacement. Curve C is curve A compensated 6 dB/octave to allow determination of match between strain and inertial seismograph responses	60
35	Curves A and B are theoretical amplitude and phase response curves for the long-period strain seismograph at constant differential ground displacement. Curve C is curve A compensated 6 dB/octave to allow determination of match between strain and inertial seismograph responses	61
36	Theoretical amplitude and phase response curves for the short-period inertial seismograph for constant ground displacement	62
37	Theoretical amplitude and phase response curves for the long-period inertial seismograph at constant ground displacement	63
38	Recommended operating levels for the magnetic tape recorders in the strain inertial system	78

TABLES

<u>Table</u>		<u>Page</u>
1	Strain-inertial seismograph operating parameters	48
2	Strain and inertial seismometer characteristics	49
3	Strain-inertial seismograph galvanometer characteristics	50
4	Theoretical SP strain seismograph amplitude response data for constant differential ground displacement	64
5	Theoretical SP strain seismograph phase response data for constant differential ground displacement	65
6	Theoretical LP strain seismograph amplitude response data for constant differential ground displacement	66
7	Theoretical LP strain seismograph phase response data for constant differential ground displacement	67
8	Theoretical SP inertial seismograph amplitude response data for constant ground displacement	68
9	Theoretical SP inertial seismograph phase response data for constant ground displacement	69
10	Theoretical LP inertial seismograph amplitude response data for constant ground displacement	70
11	Theoretical LP inertial seismograph phase response data for constant ground displacement	71

ABSTRACT

Procedures necessary to operate the multicomponent strain seismograph facility located at the Wichita Mountains Seismological Observatory (WMSO) and the applications of these seismographs to the enhancement and identification of seismic waves are discussed. The theory of strain seismometers and their response to seismic waves are examined to assist in the interpretation of strain seismograms. A description of the WMSO strain seismograph system is also included.

BLANK PAGE

STRAIN SEISMOGRAPH OPERATING PROCEDURES AND APPLICATIONS

1. INTRODUCTION

This report was published by Geotech, A Teledyne Company, in fulfillment of the requirements set forth in Subtask 4f of "Statement of Work to Be Done" Amendments 2 and 3 of Contract AF 33(657)-15288, Project VELA T/5081.

The purpose of this report is to provide the procedures necessary to operate a multicomponent strain seismograph facility, comparable to that located at the Wichita Mountains Seismological Observatory (WMSO) and to acquaint the reader with the applications of strain seismographs to the enhancement and identification of seismic waves. A brief review of the theory of strain seismology is presented first, followed by a discussion on the matching of strain and inertial seismograph frequency responses. The response of strain seismographs to seismic waves is then discussed. This necessitates the examination of displacement caused by the waves, which in turn readily allows for a comparison of the strain with the more familiar inertial seismograph response to seismic waves. The analysis of and methods of applying strain seismograms for signal enhancement and identification are examined. A description of the strain and inertial seismograph systems at WMSO and detailed procedures for the operation are given.

A linear strain seismograph responds differently to seismic waves than does a conventional inertial seismograph. As a consequence, comparing simultaneous seismograms from the two types of instruments can provide information on wave characteristics, which cannot be determined from either seismogram alone. Furthermore, by combining in different ways the outputs of matched co-located strain and inertial seismographs, various wave types can be enhanced and others suppressed.

Several specific seismic wave discrimination techniques involving strain and inertial seismograph combinations have been described explicitly in the literature. These include a combination of vertical strain and inertial seismograph outputs to enhance teleseismic P-waves, and a combination of horizontal strain and inertial seismograph outputs to enhance surface waves. These techniques plus others are reviewed in this report, and their effectiveness illustrated.

Before examining the strain and inertial seismographs, the reason for selecting the names strain and inertial for the seismometers that respond to differential displacement and displacement, respectively, should be mentioned.

A strain seismometer records the difference in a component of displacement between two locations. This is accomplished by measuring the distance between the two locations by means of a rod, fixed to a pier at one location but allowed to move in a transducer that is fixed at the second location. Linear strain may be defined as the rate of change of a component of displacement with respect to the coordinate along which the component of displacement occurs. That is, strain is the spatial derivative of displacement. This rate can be closely approximated by measuring the ratio of the change in distance between two piers, resulting, for example, from a seismic disturbance, to the distance between the piers when undisturbed. This may be expressed as $\frac{\Delta L}{L}$, where ΔL is the change in distance and L is the undisturbed distance between the piers. The change in distance between piers or differential displacement, therefore, provides a good approximation of strain; hence, the name strain is applied to the seismograph.

A displacement seismometer generally consists of a mass suspended by a spring to provide an undisturbed reference relative to which the displacement of the frame of the seismometer can be measured. That is, inertia of the mass-spring system provides the reference, hence the name inertial.

2. THEORY

The theory of strain seismometers has been thoroughly covered in the literature, Benioff (1935), Romney (1964), and, therefore, will not be presented here. Those expressions necessary to compute the theoretical response of strain seismometers to seismic waves, however, are given below.

Linear differential displacement (δ) is defined as the instantaneous difference between a component of displacement (\mathcal{D}_1) at a point and the same component of displacement (\mathcal{D}_2) at a second point where the component is directed parallel to a straight line connecting the points; that is,

$$\delta = \mathcal{D}_2 - \mathcal{D}_1 \quad (1)$$

In the case of horizontal differential displacement, where for any given propagating seismic wave \mathcal{D}_1 and \mathcal{D}_2 differ only in phase, equation (1) can be expressed as

$$\delta_h = - \frac{L}{c} \cos^2 \alpha \frac{\partial \xi}{\partial t} \quad (2)$$

for apparent longitudinal waves, including Rayleigh, P, and SV waves; and as

$$\delta_h = - \frac{L}{c} \cos \alpha \sin \alpha \frac{\partial \xi}{\partial t} \quad (3)$$

for all horizontally polarized transverse waves, such as Love and SH waves.

In these expressions

L = length of strain

c = apparent phase velocity in a horizontal plane

α = angle between the horizontal strain rod and the direction of wave propagation

ξ = particle displacement in a horizontal plane

$\frac{\partial \xi}{\partial t}$ = particle velocity in a horizontal plane

In the case of vertical differential displacement, where the phase and/or amplitudes of \mathcal{D}_1 and \mathcal{D}_2 are likely to differ, no general expression can be given for all wave types. An approximation of vertical differential displacement, however, can be obtained by examining strain. At the surface of the earth where the vertical stress is zero, vertical strain is proportional to the total horizontal strain, independent of wave type,

$$\frac{\partial u}{\partial x} + \frac{\partial v}{\partial y} = - \frac{2\mu + \lambda}{\lambda} \frac{\partial w}{\partial z} \quad (4)$$

Here u , v , and w are the displacements in the orthogonal directions x , y , and z , respectively (z normal to the surface), and λ and μ are the Lamé constants. Applying this relationship to vertical differential displacement and using (2) and (3) gives

$$\delta_z = \frac{\lambda}{2\mu + \lambda} \frac{L}{c} \frac{\partial \xi}{\partial t} \quad (5)$$

for apparent longitudinal waves and $\delta_z=0$ for horizontally polarized transverse waves. Note that $\frac{\partial \xi}{\partial t}$ is the particle velocity in a horizontal plane, not in the z direction.

3. EQUATING STRAIN AND INERTIAL RESPONSES

This section of the report discusses the concept of equating the strain and inertial seismograph responses to earth motion, and describes the instrumentation of a typical pair of matched strain and inertial seismographs. This is preceded by a brief description of the WMSO strain installation. The complete strain-inertial system is described in section 6.

3.1 SEISMOMETER INSTALLATION

The WMSO strain-inertial seismograph system contains four short-period (SP) horizontal strain seismometers, four SP horizontal inertial seismometers, one long-period (LP) horizontal inertial seismometer, one SP vertical strain seismometer, one SP vertical inertial seismometer, and one LP vertical inertial seismometer. The horizontal strain rods are 19.3 meters long. The system is capable of recording earth motion in the period range of 0.1 sec to 200 sec.

The horizontal strain seismometers and horizontal and vertical inertial seismometers are located in a central subsurface concrete vault with four strain-member housings extending radially toward the northeast, north, northwest, and west as shown in figure 1. The concrete vault and strain-member housings are rigidly anchored to competent bedrock. The vault is sealed against rapid pressure changes that produce noise in the frequency band of interest.

The 18.6 m vertical strain seismometer is located in a borehole about 30 m north of the concrete vault. The borehole is cased with a 178 mm (7 in.) i.d. steel casing and is 39 m deep. The upper end of the seismometer is anchored at a depth of 18 m as shown in figure 2. The seismometer is submerged in heavy motor oil to damp spurious horizontal vibrations of the rod, and the borehole is sealed against wind-induced pressure changes. By operating at a depth of 18 m, the seismometer is sufficiently insensitive to local surface disturbances, yet shallow enough to avoid a large reduction of signal at short wavelengths.

3.2 MATCHED STRAIN AND INERTIAL SEISMOGRAPHS

In order that instrument responses can be neglected when comparing the outputs of strain and inertial seismographs, the system has been designed with matched outputs. The systems are considered to be matched if the response of the strain seismographs to differential displacement exactly duplicates the response of the horizontal inertial seismographs to particle velocity. The reason for this is indicated by expressions (2), (3), and (5).

These expressions show that differential displacement differs from particle velocity only by the factors $\frac{L}{c}$ and a function of α , the azimuthal angle of propagation, whereas it differs from particle displacement by these factors and by the angular frequency and a phase difference of 90 degrees as well.

Thus, the frequency and phase difference are removed by matching the responses of the strain and inertial seismographs to differential displacement and particle velocity, respectively. Equalization of amplitude and phase responses can be accomplished with the instrumentation shown in figure 3.

Plotted in figure 4 are asymptotic amplitude responses of the SP strain and inertial seismographs. It is noted that matched systems are obtained by

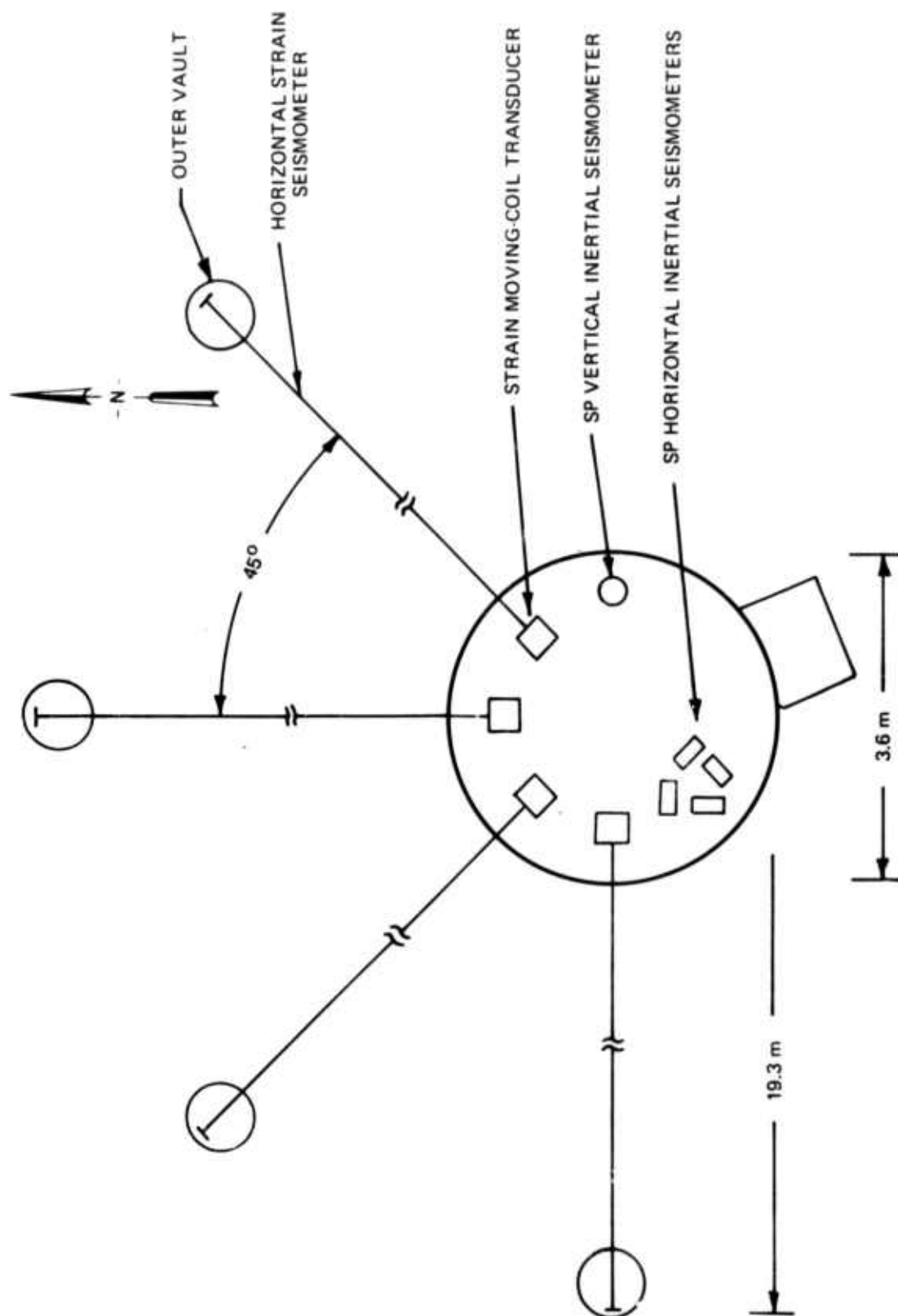


Figure 1. Horizontal strain seismometer installation showing orientation of instruments

G 3933

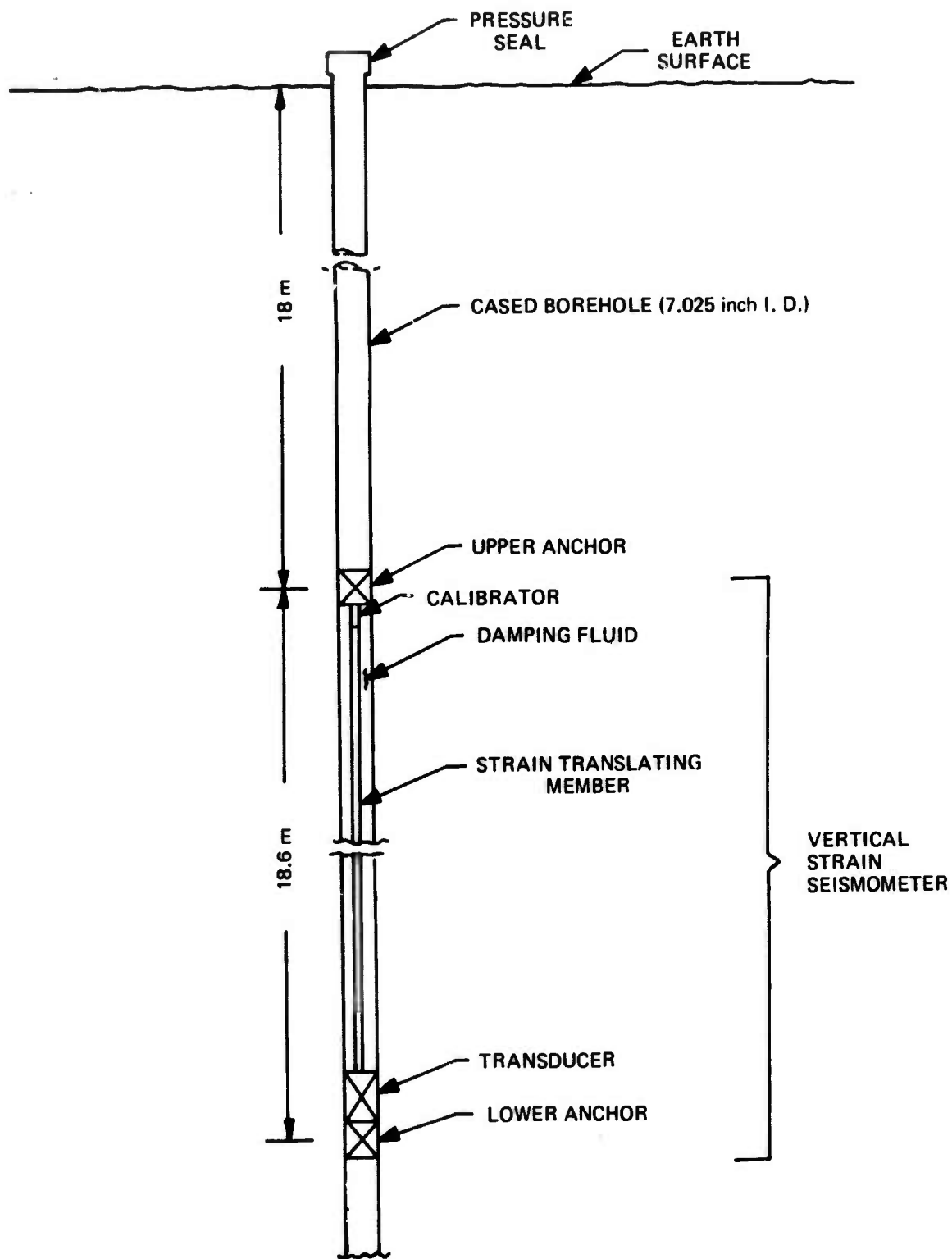


Figure 2. Vertical strain seismometer installation

G 3934

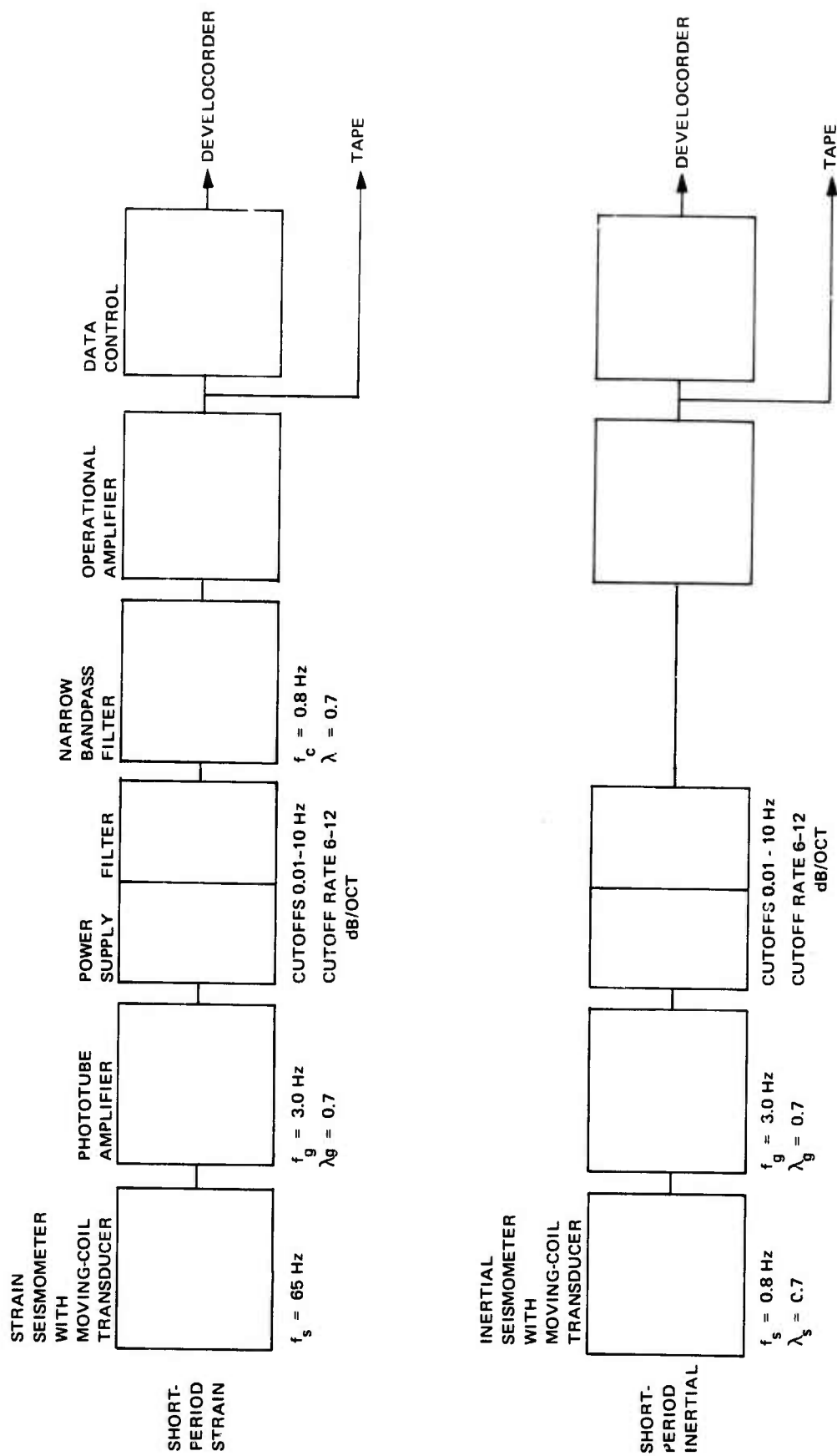
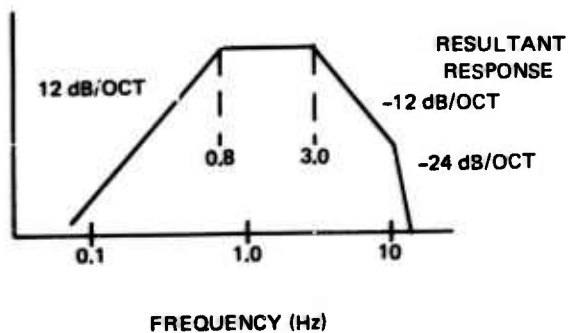
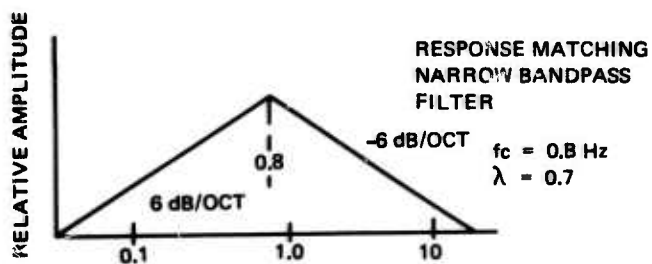
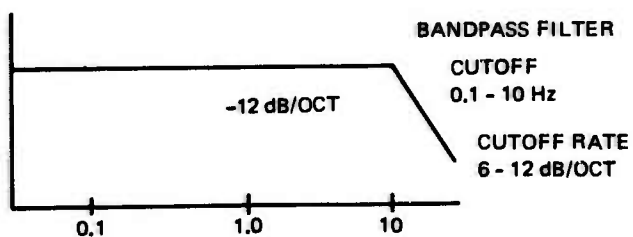
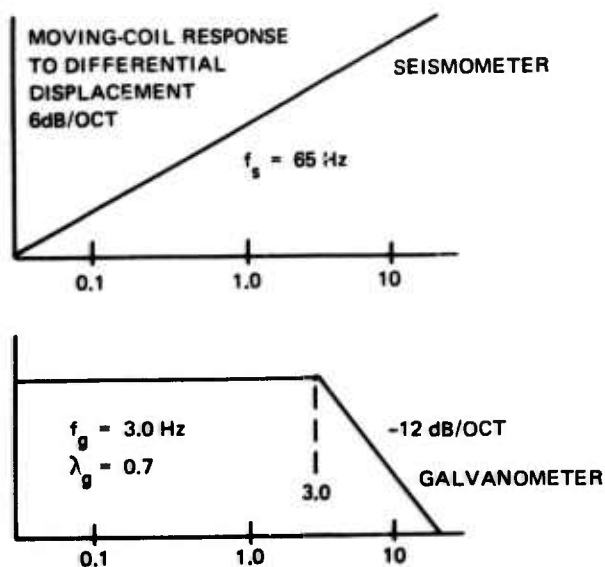


Figure 3. Block diagram of matched horizontal short-period strain and inertial seismographs at WMSO

STRAIN SEISMOGRAPH



INERTIAL SEISMOGRAPH

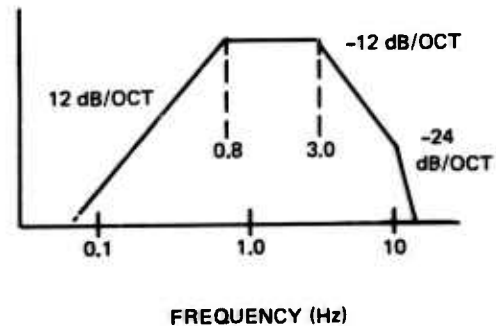
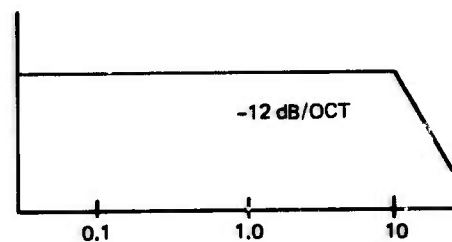
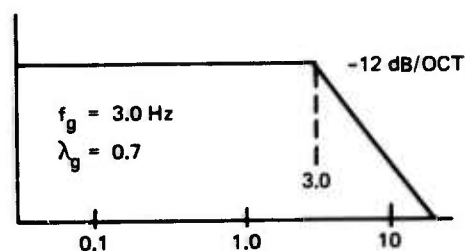
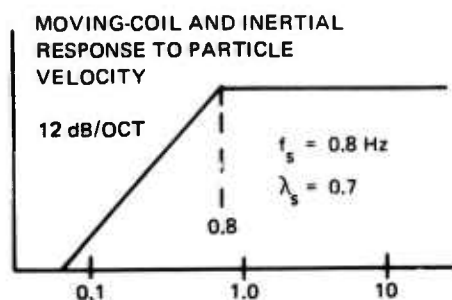


Figure 4. Asymptotic amplitude responses of matched short-period strain and inertial seismographs and their components

G 3936

using similar galvanometers in each system, but using a special narrow band-pass filter to equate the responses of the strain seismometer to differential displacement and the inertial seismometer to particle velocity. Both seismometers have moving-coil transducers.

In later discussions involving interpretation of the data, particle displacement is used as a measure of response. This can be arrived at by integrating the differential displacement in the case of strain seismograph, and the particle velocity in the case of the inertial seismograph.

4. STRAIN-INERTIAL SEISMOGRAPH RESPONSES TO SEISMIC WAVES

The theoretical responses of strain and inertial seismographs to seismic waves computed for a homogeneous half space are examined below. The parameters Poisson's ratio of $1/4$, vertical stress equal to zero, and longitudinal phase velocity of 6 km/sec were used in the computations. The displacements associated with the inertial seismographs were computed for the surface of the earth. The horizontal differential displacement was computed by substituting the horizontal displacement, computed for the surface, into equations (2) or (3). Vertical displacements, computed for depths of 18 and 36 meters below the surface, were substituted into equation (1) to obtain the vertical differential displacement. Expressions for displacement may be obtained from several publications on theoretical seismology (see section 7).

Since the phase angles of ϕ_1 and ϕ_2 of equation (1) are equal for Rayleigh waves, an examination of differential displacement and its relationship to displacement is possible. Furthermore the relationship between horizontal and vertical strain, equation (4), as used to approximate vertical differential displacement may be evaluated. This subject will receive attention throughout this section.

4.1 SURFACE WAVES

Of the surface waves, Love and Rayleigh are of particular importance in seismology. Since they are surface waves, their apparent phase velocities do not differ from their actual phase velocities. The particle displacements caused by Love and Rayleigh waves differ significantly. Love waves produce horizontal displacement normal to the direction of propagation. Rayleigh waves, as considered here, have elliptical particle motion, retrograde with respect to the direction of propagation. Both Love and Rayleigh are treated as plane waves.

4.1.1 Love Waves

Love waves, being horizontally polarized transverse surface waves, SH, produce no vertical displacement and hence no vertical differential displacement. Only the horizontal seismograph responses may, therefore, be considered. The essential difference between the strain and inertial seismograph responses to Love waves lies in their azimuthal responses. By compensating for the phase velocity term in equation (3) the strain and inertial seismograph response patterns illustrated in figure 5 are obtained.

4.1.2 Rayleigh Waves

Figure 6 is a plot of the theoretical values of vertical differential displacement divided by the vertical surface displacement, solid lines, and horizontal differential displacement divided by the horizontal surface displacement, dashed line, for fundamental mode Rayleigh waves plotted as a function of frequency. The effect of changing the length of the vertical strain rod is also shown.

The slope of the curves, except for vertical differential displacement at the higher frequencies, is 6 dB per octave. This slope is an inherent property of strain independent of wave type. The response of the vertical strain seismometer to Rayleigh waves, however, shows a departure from this slope. As the frequency increases from 5 to 10 Hz the magnitude of the vertical differential displacement decreases to zero, changes sign, then increases. Here the constant proportionality between horizontal and vertical strain is not applicable to differential displacement. This is illustrated in figure 7 where the summed outputs of the horizontal strain seismographs (ΣNE, NW) and the vertical strain seismograph (SZ) output are about equal for 4 sec microseisms, but unequal for 0.25 sec cultural noise.

The departure of vertical differential displacement from a constant slope can be anticipated by examining vertical displacement as a function of the product of frequency and depth, figure 8. Along the abscissa of figure 8 is magnitude of displacement normalized to the surface magnitude. If we assume a frequency of 1.0 Hz then the values of the ordinate represent depth in meters. Since the phase of the vertical displacement due to Rayleigh waves does not change with depth, the difference between the displacements, for example, at 18 and 36 meters below the surface, marked with dots on the Rayleigh displacement curve of figure 8, is the normalized differential displacement that will be recorded by a vertical strain seismograph operating at those depths. If we assume a frequency of 10 Hz the values of the ordinate must be divided by 10 to obtain the depth in meters. Considering again 18 and 36 meters below the surface, the triangles on the Rayleigh displacement curve represent the normalized magnitudes at 10 Hz. At 10 Hz the displacement at 36 meters is seen to be greater than at 18 meters, whereas it was less at 1.0 Hz. That is, relative to the vertical displacement at the surface, there is a reversal in polarity of the vertical differential displacement.

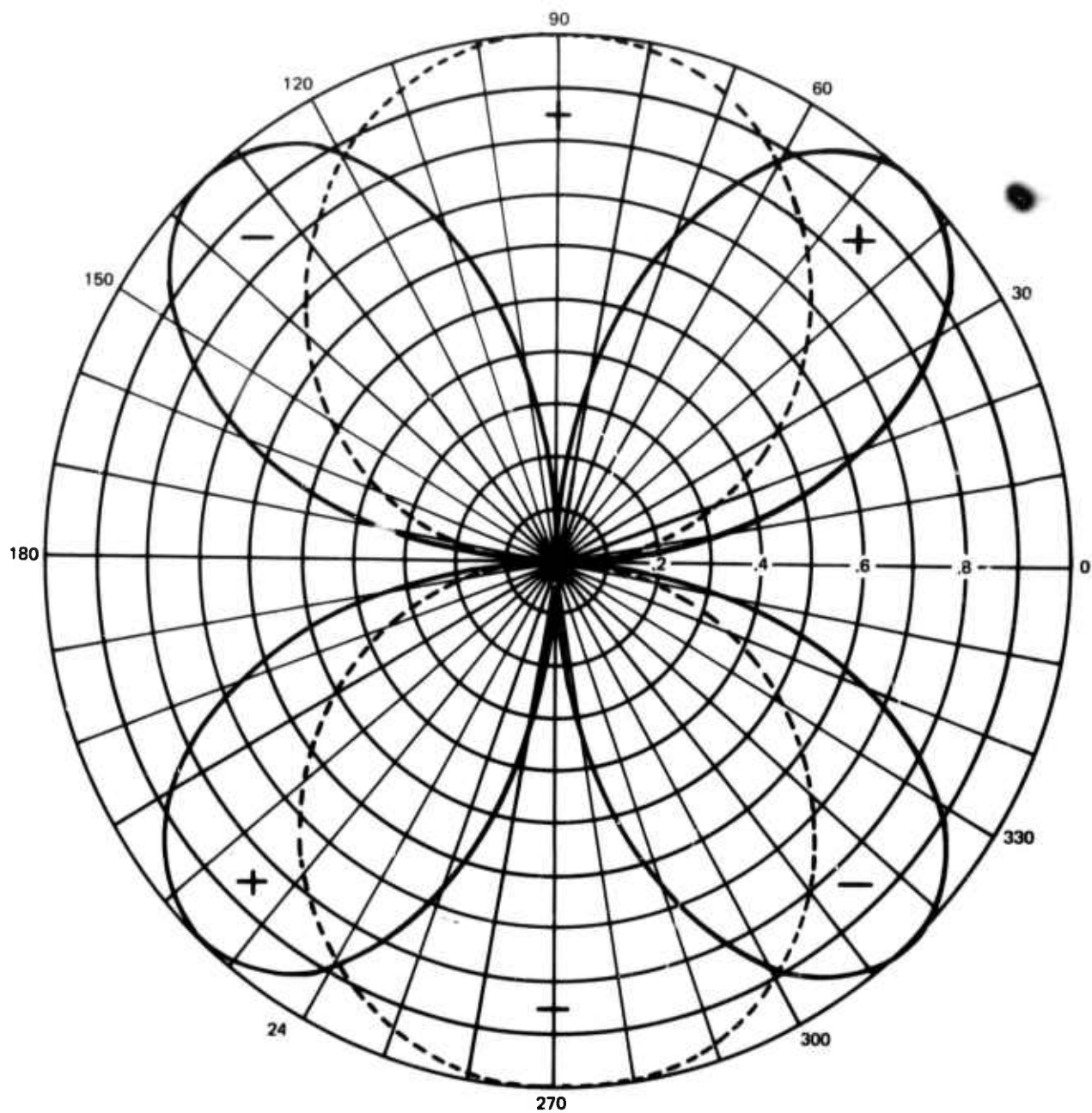


Figure 5. Azimuthal response of a horizontal strain seismometer, solid curve, and a horizontal inertial seismometer, dashed line curve, to horizontally polarized transverse waves (SH)

G 3937

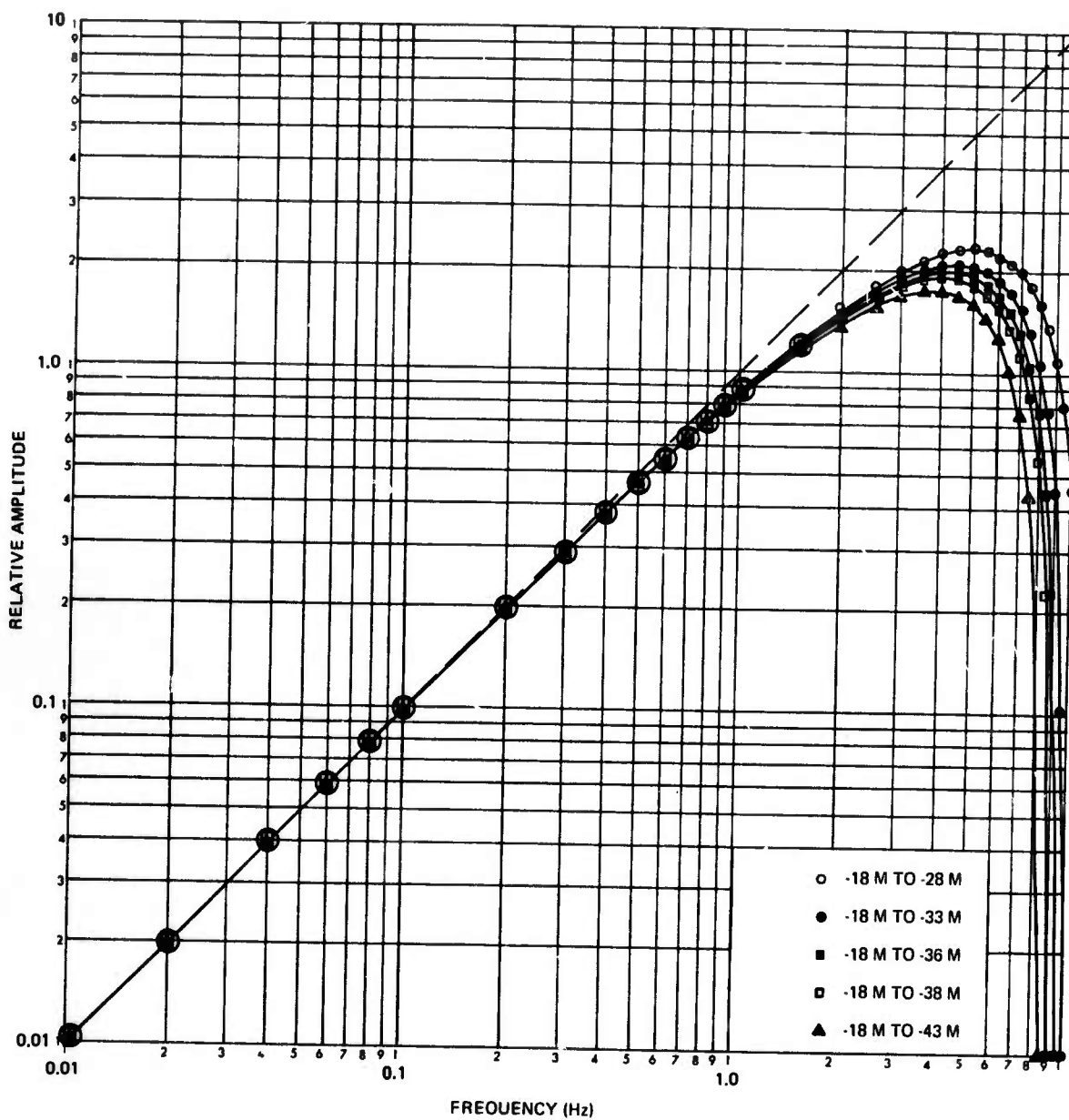


Figure 6. Ratios of horizontal and vertical differential displacement to surface displacement due to Rayleigh waves plotted as a function of frequency. The dashed line is the horizontal ratio and is for an 18-meter strain rod. The solid lines are the vertical ratios for different positions and lengths of the strain rod

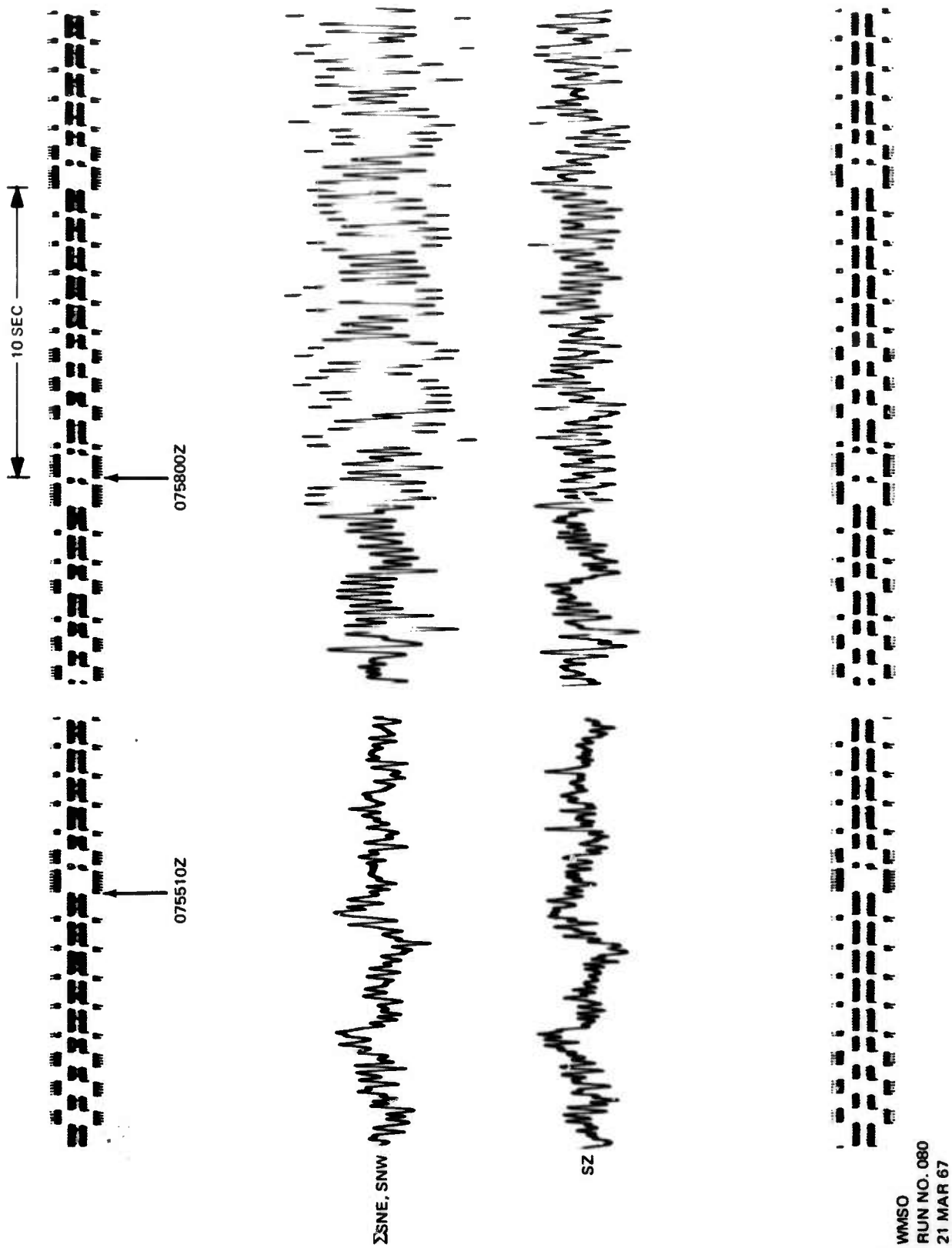


Figure 7. Seismogram illustrating the difference between responses of summed orthogonal horizontal strains (Σ SNE, SNW) and vertical strain (SZ) to high frequency Rayleigh waves when equal for longer period microseisms

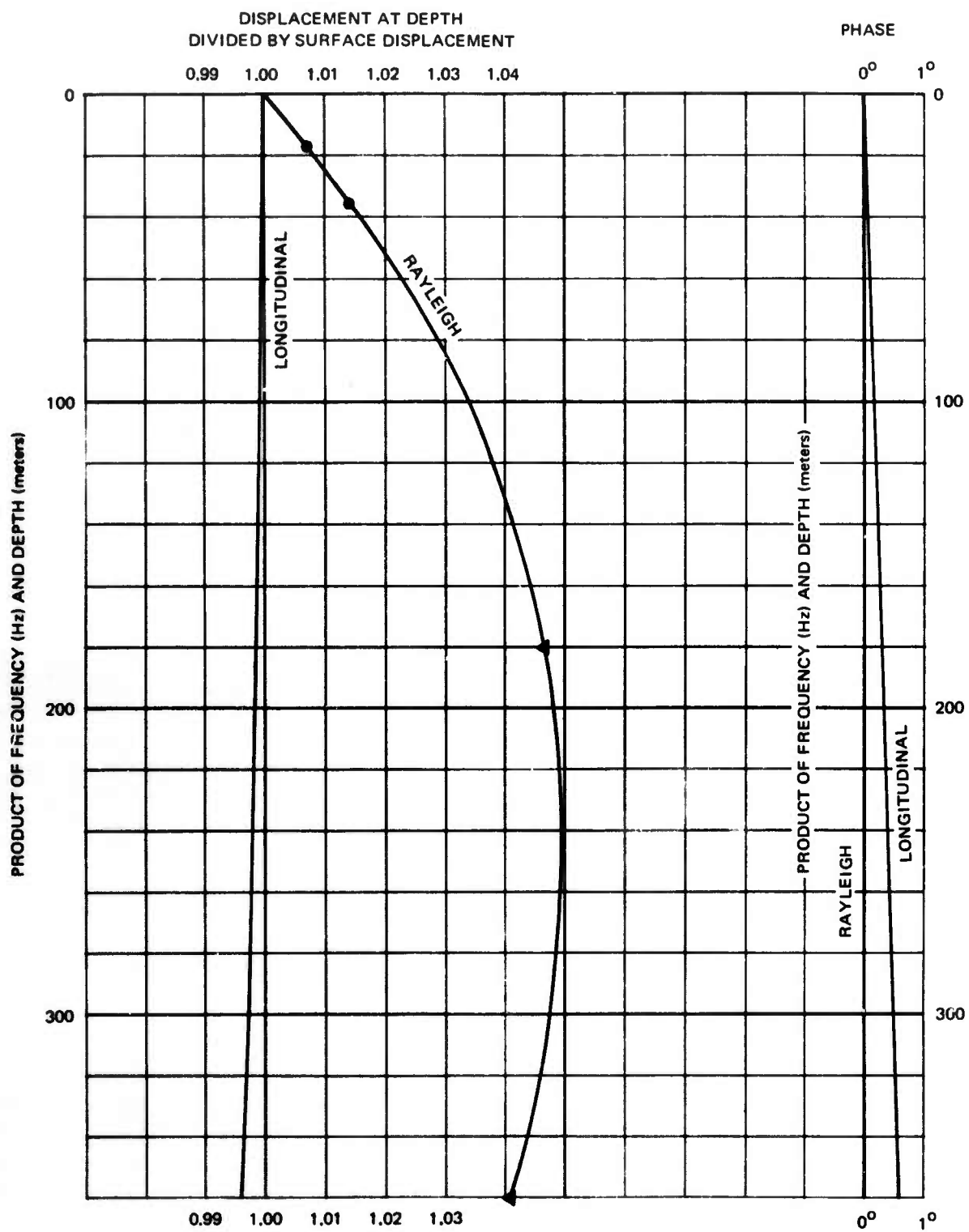


Figure 8. Displacement phase-depth relationships for Rayleigh and longitudinal waves. Longitudinal waves incident at 30 degrees

G 3940

Also, it can be seen that there must be a frequency where the displacement at 18 and 36 meters will be equal, hence there will be no vertical differential displacement.

The phase relationship among the components of displacement and differential displacement due to Rayleigh waves also deserves consideration. The vertical and horizontal components of displacement have a phase difference of $\pi/2$ due to the elliptical particle motion of Rayleigh. The vertical and horizontal differential displacements, however, have a phase difference of π except at high frequencies near 10 Hz where the phase difference is zero. The difference, π , between the components of differential displacement might be expected from the proportionality of vertical and horizontal strain at the free surface, but it is not obvious from the $\pi/2$ phase difference between the vertical and horizontal components of displacement. As stated earlier, the phase of vertical displacement due to Rayleigh does not change with depth, therefore, the vertical displacement and differential displacement will be either in phase or π out of phase. Horizontal differential displacement, on the other hand, will always have a $\pi/2$ phase with respect to horizontal displacement resulting from any traveling wave. This $\pi/2$ phase combined with the $\pi/2$ phase difference between horizontal and vertical displacement for Rayleigh results in the expected π phase difference between horizontal and vertical differential displacement.

The azimuthal response patterns of the horizontal strain and inertial seismographs to Rayleigh waves, which may be considered apparent longitudinal waves in a horizontal plane, are shown in figure 9.

In addition to the fundamental mode, higher mode Rayleigh waves are found to exist both in earthquake surface waves and microseisms. In figure 10, theoretical displacement normalized to surface displacement is plotted as a function of depth for several Rayleigh modes of a period of 1.0 seconds. The displacements were computed for an earth model of WMSO (Fix 1967). From the curves, it can be seen that a vertical strain seismograph will not necessarily record the different modes at the same amplitude even if the vertical displacements of each mode at the surface are the same.

4.2 BODY WAVES

Body waves consist of longitudinal and transverse waves. The strain and inertial seismograph responses to these waves, in contrast to surface waves, are generally dependent on the angle at which the waves are incident. Therefore, the seismograph responses to both longitudinal and transverse waves will be examined as a function of incidence angle. The values of differential displacement have been computed for a frequency of 1.0 Hz. The relative magnitudes of the displacements and differential displacements, however, may be used for all frequencies when the seismograph systems have been matched.

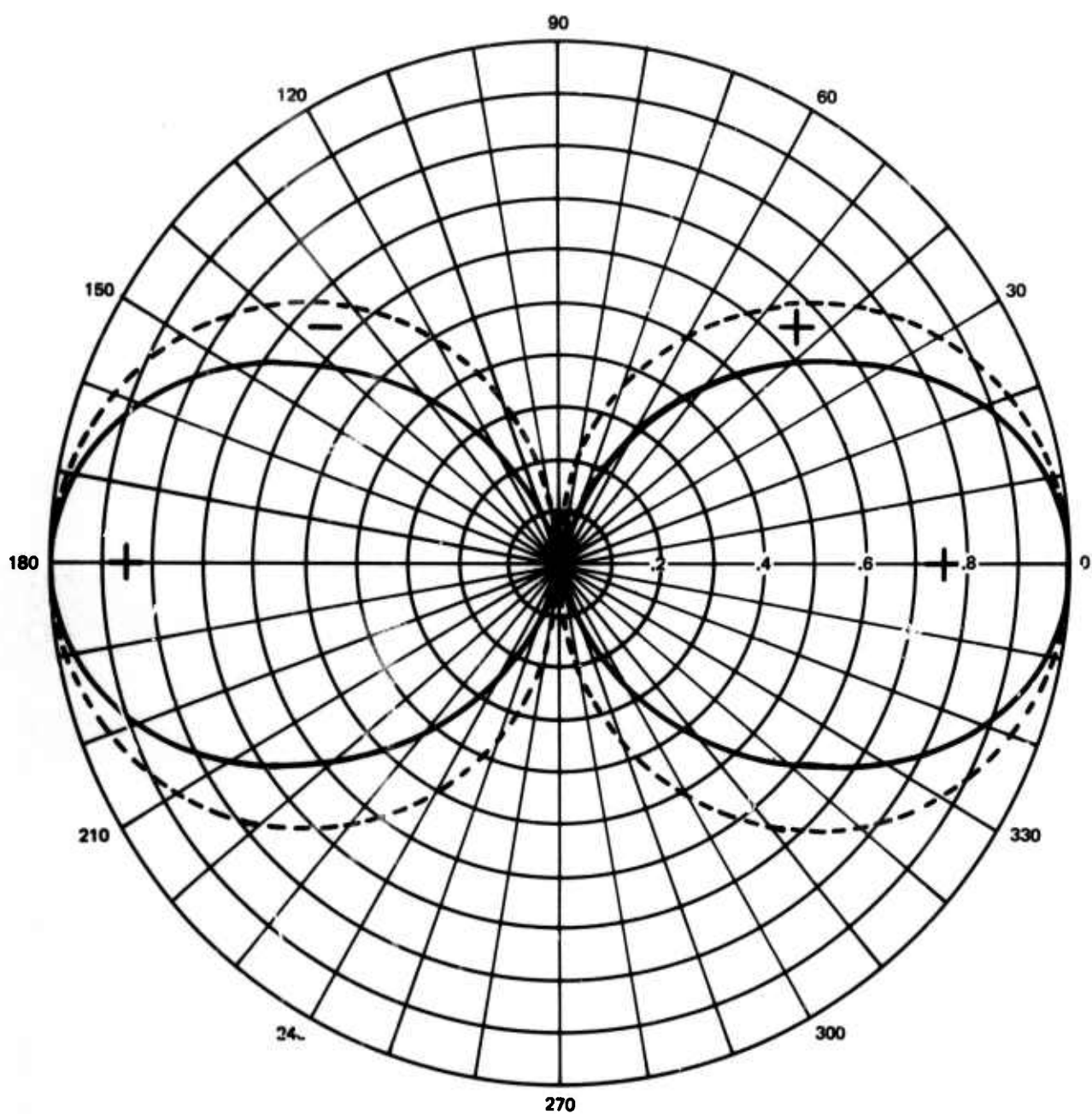


Figure 9. Azimuthal response of a horizontal strain seismometer, solid curve, and a horizontal inertial seismometer, dashed curve, to apparent longitudinal waves

G 3941

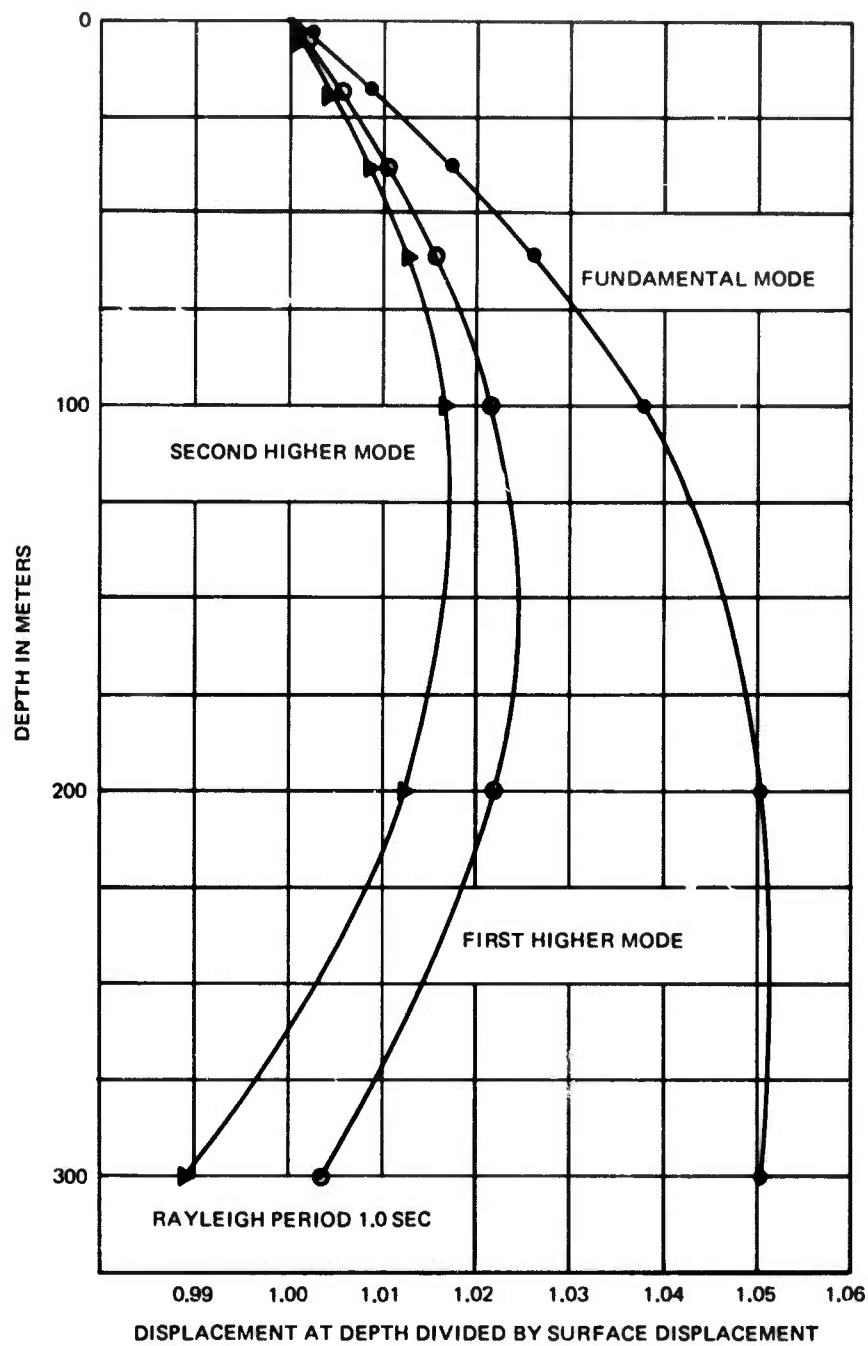


Figure 10. Displacement - depth relationship for Rayleigh waves using an earth model for WMSO

G 3942

4.2.1 Longitudinal Waves

In figure 11 the theoretical trace amplitudes of strain and inertial seismograms that would result from longitudinal disturbances are plotted as a function of the angle of incidence. The values of vertical and horizontal differential displacement have been increased by the factors 144 and 28, respectively, to equalize the strain seismograph outputs to those of the inertials for 1.0 Hz fundamental mode Rayleigh waves.

Several interesting observations can be made from the plots. The horizontal displacement and both horizontal and vertical differential displacement are seen to decrease, starting at an incidence near 65 degrees, as the angle of incidence decreases. Thus, the more distant an earthquake the less sensitive the strain seismographs will be to P-waves. The vertical inertial seismograph, on the other hand, becomes more sensitive.

The curves of vertical and horizontal differential displacement are shaped almost identically as suggested by the relationship between horizontal and vertical strain. However, at vertical incidence there will be no horizontal differential displacement, whereas there will be some vertical differential displacement.

The phase angles of the vertical and horizontal differential displacement are not the same at all angles of incidence, figure 12. In the case of longitudinal waves, vertical differential displacement results not only from an amplitude difference as with Rayleigh, but also from a phase difference in the displacements at the two locations between which differential displacement is measured, figure 8. The latter causes a $\pi/2$ phase difference between vertical displacement and differential displacement rather than 0 or π as in the case of Rayleigh waves.

The azimuthal response pattern of the strain and inertial seismographs for longitudinal waves are the same as for Rayleigh waves, figure 9.

4.2.2 Transverse Waves

Transverse body waves may be polarized either horizontally (SH) or vertically (SV). The response of a seismometer, either horizontal or vertical, strain or inertial, will differ significantly between the two components of transverse waves. Each component, therefore, will be examined separately.

4.2.2.1 SH Component

The primary difference between the body wave, SH, and surface wave, Love, is that SH is not necessarily horizontally propagated. Similar to Love waves, SH produces no vertical displacement or vertical differential displacement.

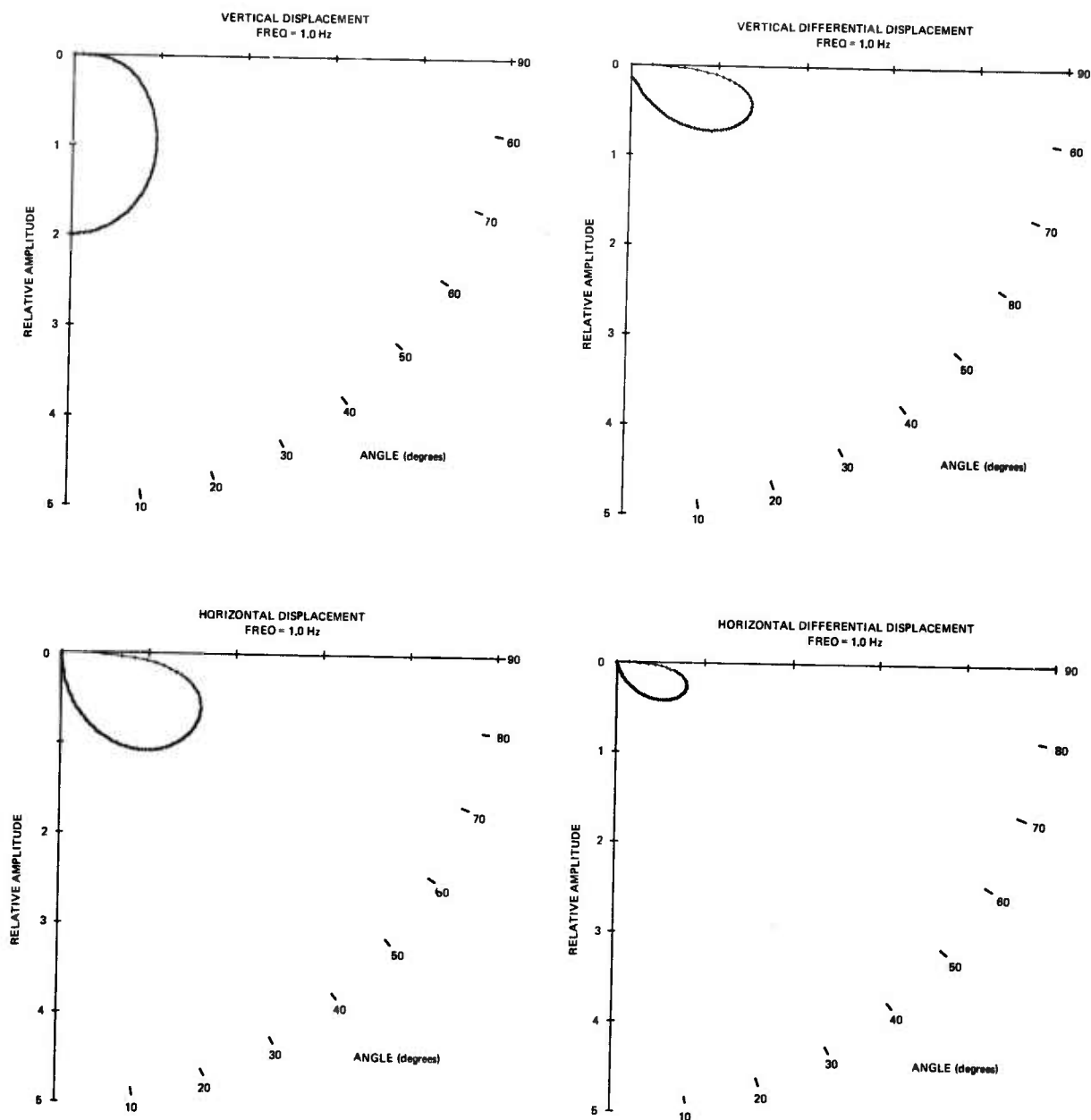


Figure 11. Polar plots of the relative vertical displacement, vertical differential displacement, horizontal displacement, and horizontal differential displacement due to incident longitudinal waves plotted as a function of the angle of incidence. The values of vertical and horizontal differential displacement have been multiplied by 144 and 28 respectively

G 3943

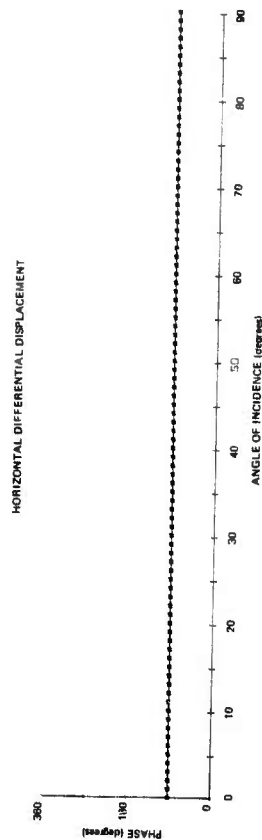
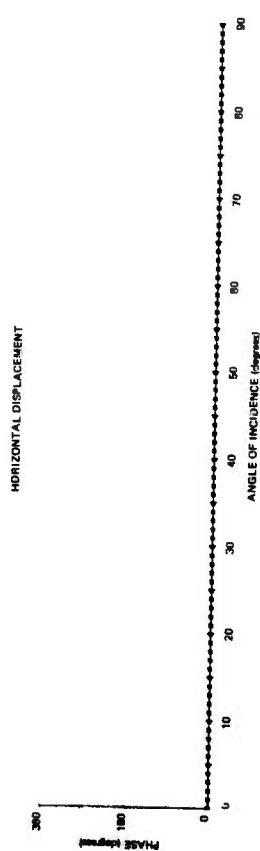
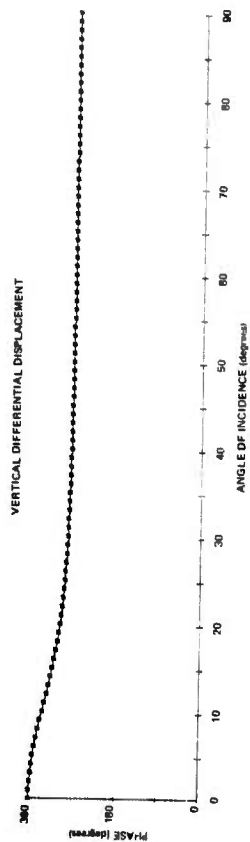
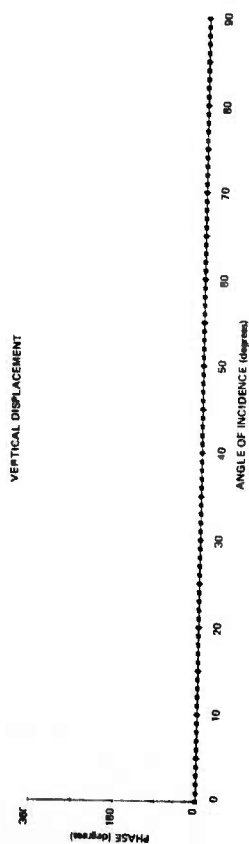


Figure 12. Phase of the vertical displacement, vertical differential displacement, horizontal displacement, and horizontal differential displacement due to incident longitudinal waves as a function of the angle of incidence at a frequency of 1.0 Hz

In figure 13 the theoretical trace amplitudes of horizontal strain and inertial seismograms that would result from SH disturbances are plotted as a function of the angle of incidence. Here, the incident wave is assumed to arrive from a direction 45° from the orientation of the inertial seismometer and strain rod. This is the direction, for both SH and Love, of maximum horizontal strain seismograph sensitivity. That is, SH has the same azimuthal response pattern as Love waves, figure 5.

Unlike the displacement due to longitudinal waves, the horizontal displacement resulting from SH is essentially independent of incidence. Therefore, the horizontal differential displacement varies with incidence by the sine of the angles of incidence.

4.2.2.2 SV Component

In figure 14 the theoretical trace amplitudes of strain and inertial seismograms that would result from vertically polarized transverse disturbances are plotted as a function of the angles of incidence. A striking feature of these plots is a large increase in amplitude near 35° incidence, which is seen on all but the vertical displacement. This occurs where the longitudinal wave resulting from the incident SV is reflected horizontally. The phase, figure 15, of both displacement and differential displacement also is seen to behave peculiarly near and beyond 35° incidence. Since the large amplitude occurs in horizontal but not vertical displacement, it could be mistakenly identified as SH on inertial seismograms especially if SH is also present. The vertical strain seismogram, however, will readily show the presence of SV, figure 16.

SV, unlike SH, may be considered an apparent longitudinal wave; therefore, the azimuthal response pattern of the horizontal seismographs are again those illustrated in figure 9.

The constant proportionality between vertical and horizontal strain, in the case of SV, does not hold for differential displacement over all angles of incidence.

4.2.3 Earthquake Phases

The angle at which an earthquake body phase, either longitudinal or transverse, will be incident at a seismograph is dependent on the focal depth and epicentral distance to the seismograph. For simplicity in the following discussion, a surface focus will be assumed; therefore, the incidence of any phase will become dependent on the epicentral distance alone. Since the strain and inertial seismograph responses may be expressed as a function of incidence and wave type, they may also be examined in terms of earthquake phases at given epicentral distances as shown in figures 17 and 18. All waves have been assumed to arrive from the azimuth of maximum inertial seismograph sensitivity.

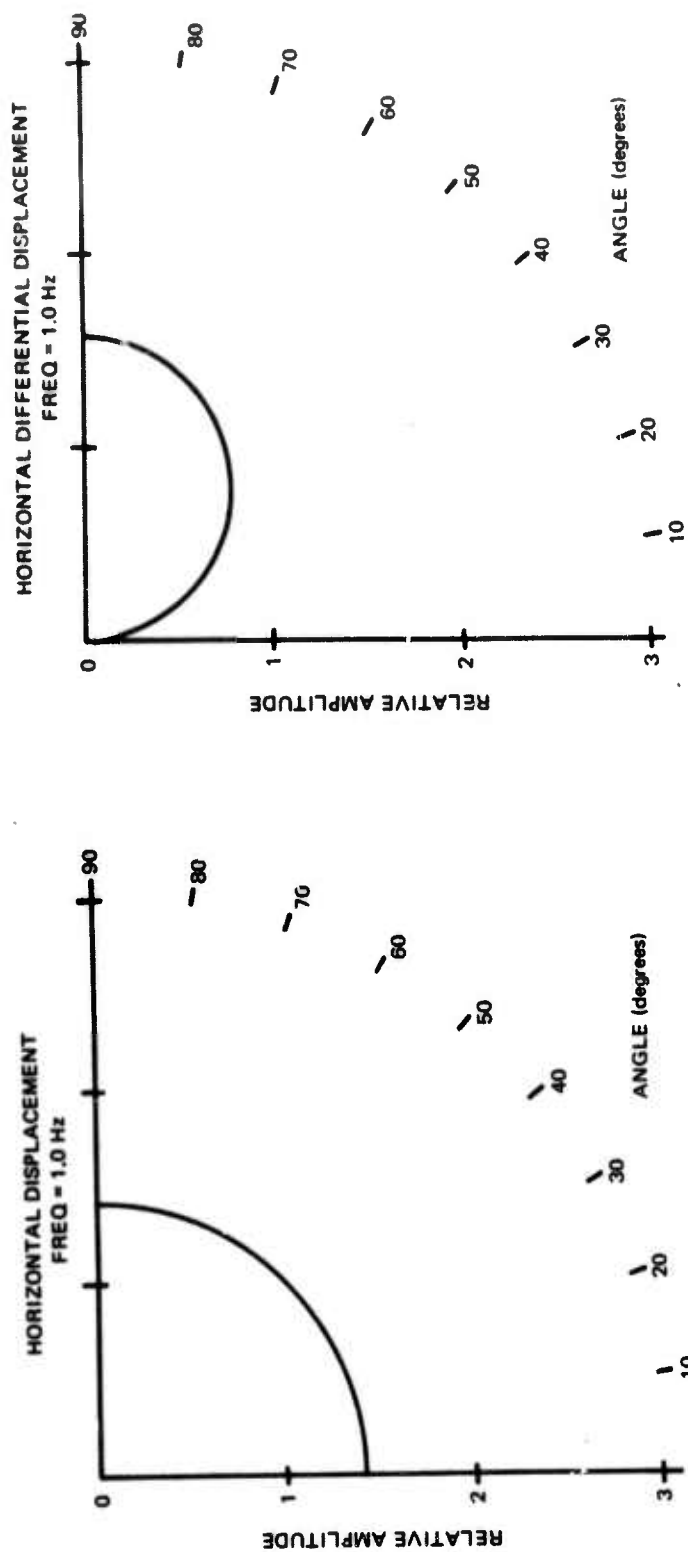


Figure 13. Polar plots of the relative horizontal displacement and horizontal differential displacement due to incident SH waves plotted as a function of the angle of incidence. The values of horizontal differential displacement have been multiplied by 20.

G 3945

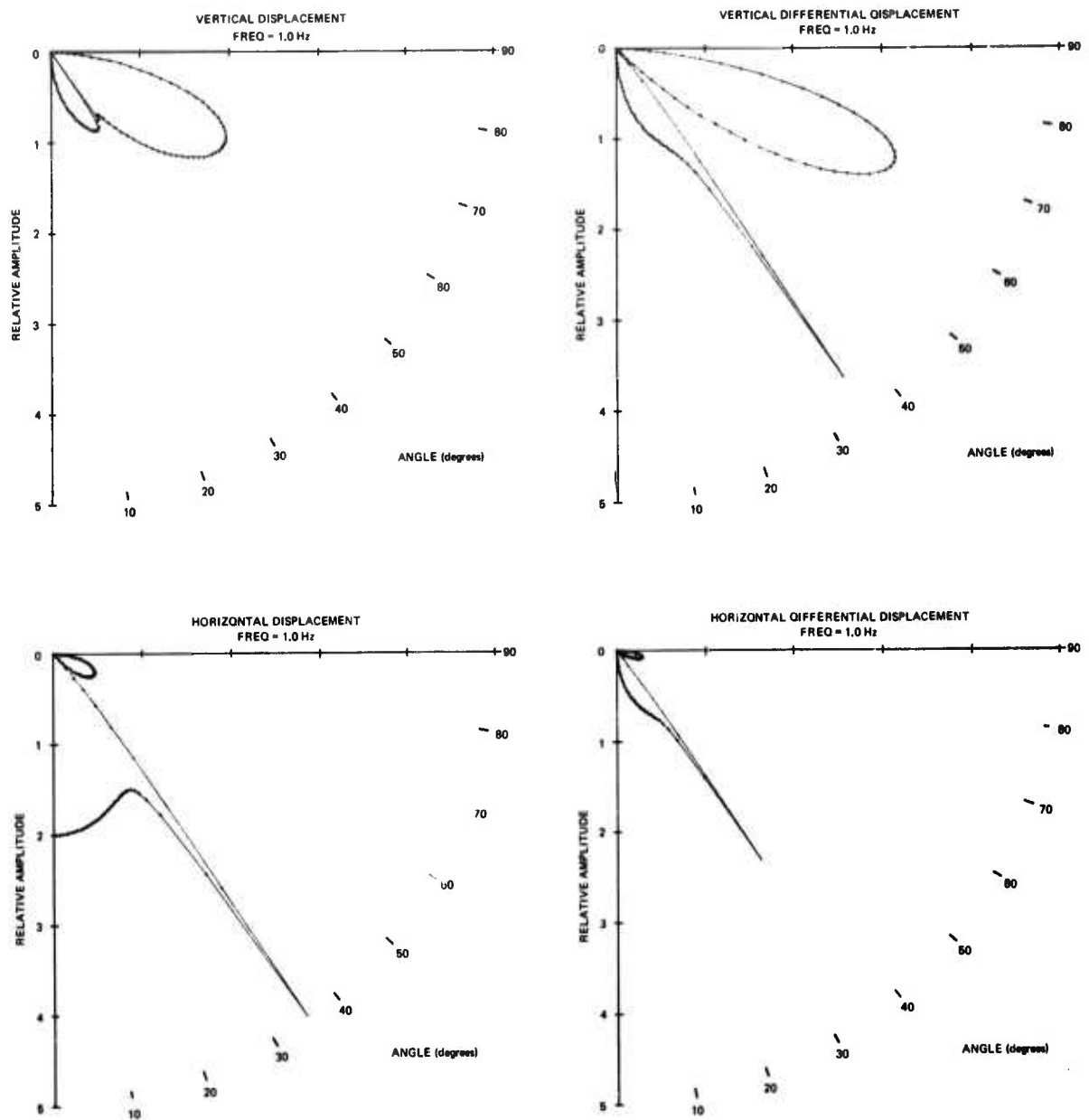


Figure 14. Polar plots of the relative vertical displacement, vertical differential displacement, horizontal displacement, and horizontal differential displacement due to incident SV waves plotted as a function of the angle of incidence. The values of vertical and horizontal differential displacement have been multiplied by 144 and 28 respectively

G 3946

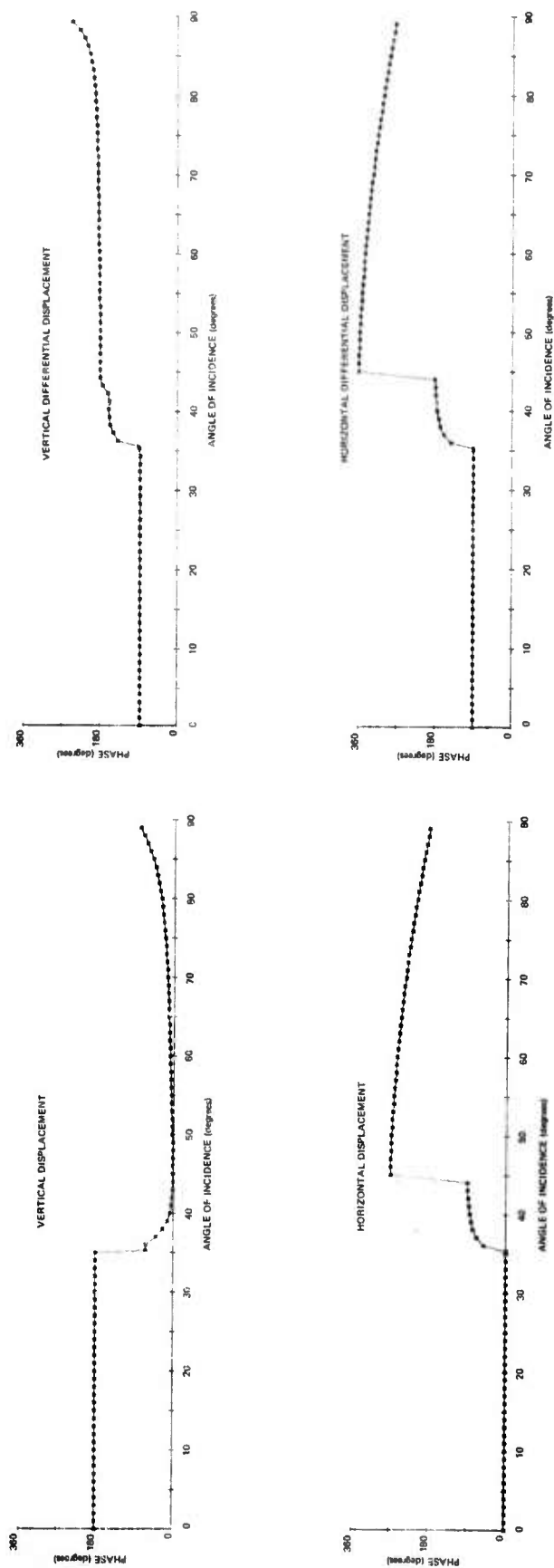


Figure 15. Phase of the vertical displacement, vertical differential displacement, horizontal displacement, and horizontal differential displacement due to incident SV waves as a function of the angle of incidence at a frequency of 1.0 Hz

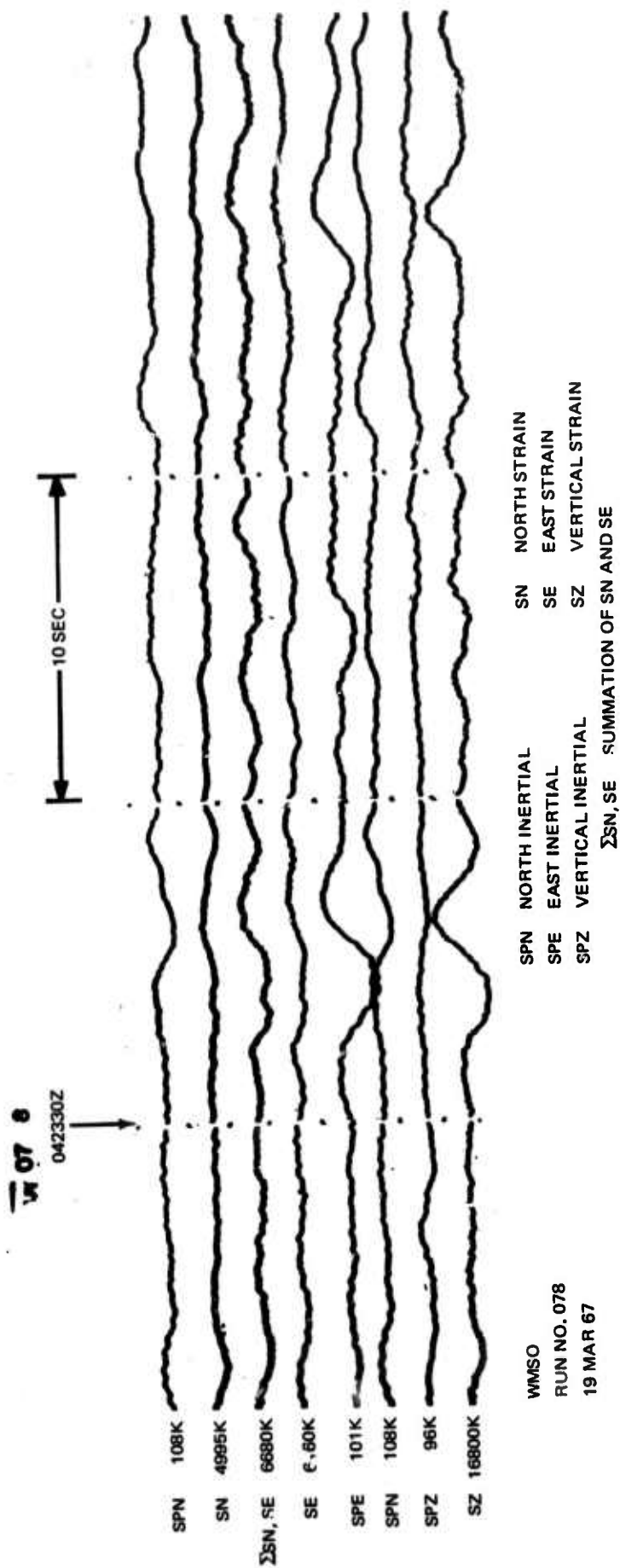


Figure 16. Seismogram illustrating the sensitivity of a vertical strain seismograph to the SV component of transverse waves. The recording is of the S-phase from an earthquake whose epicenter was in the Kurile Islands

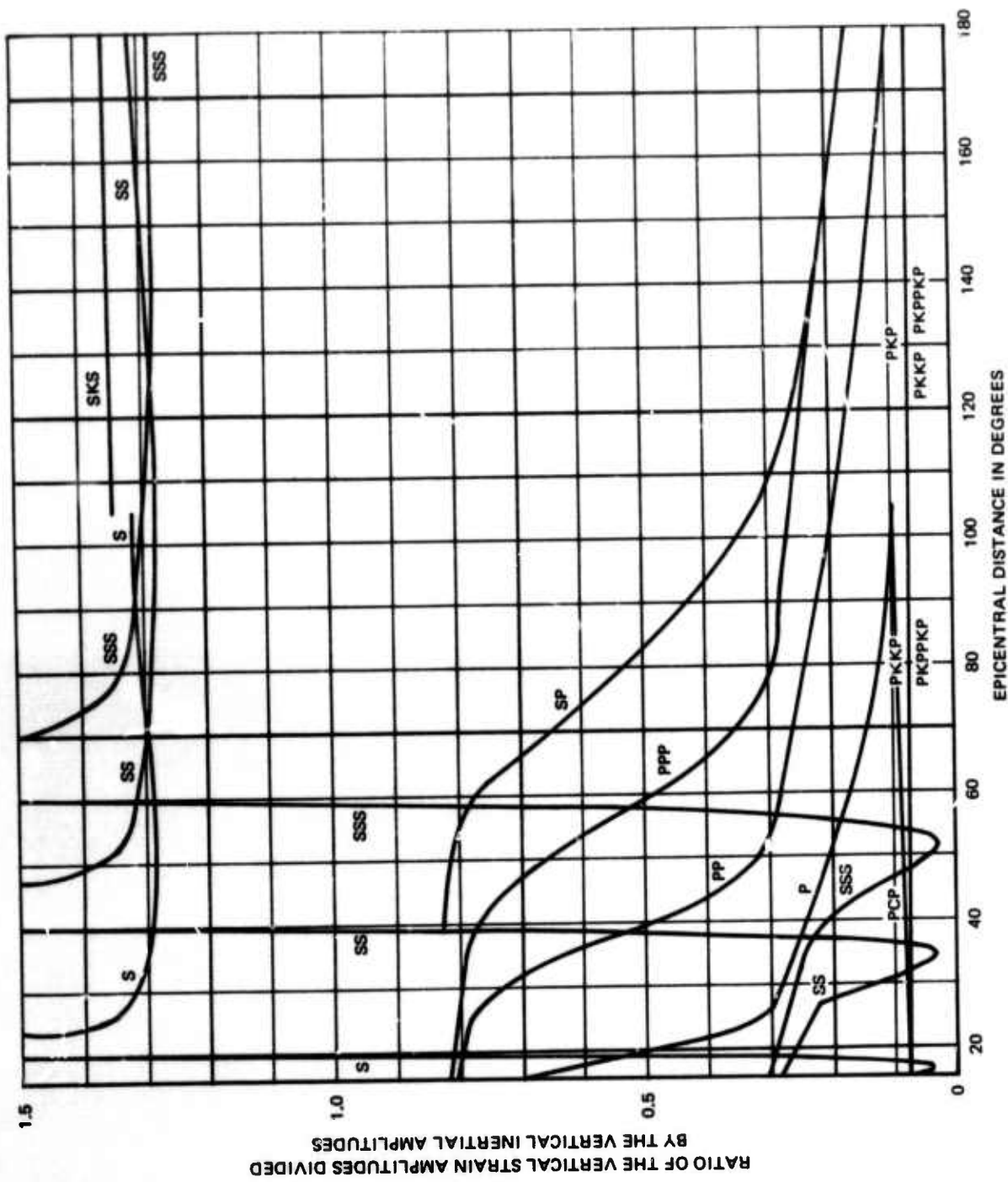


Figure 17. Ratios of the theoretical amplitudes of the vertical strain to vertical inertial for several earthquake body phases. The ratios are based on a value of unity for Rayleigh waves. The SV component of transverse waves is used

G 3949

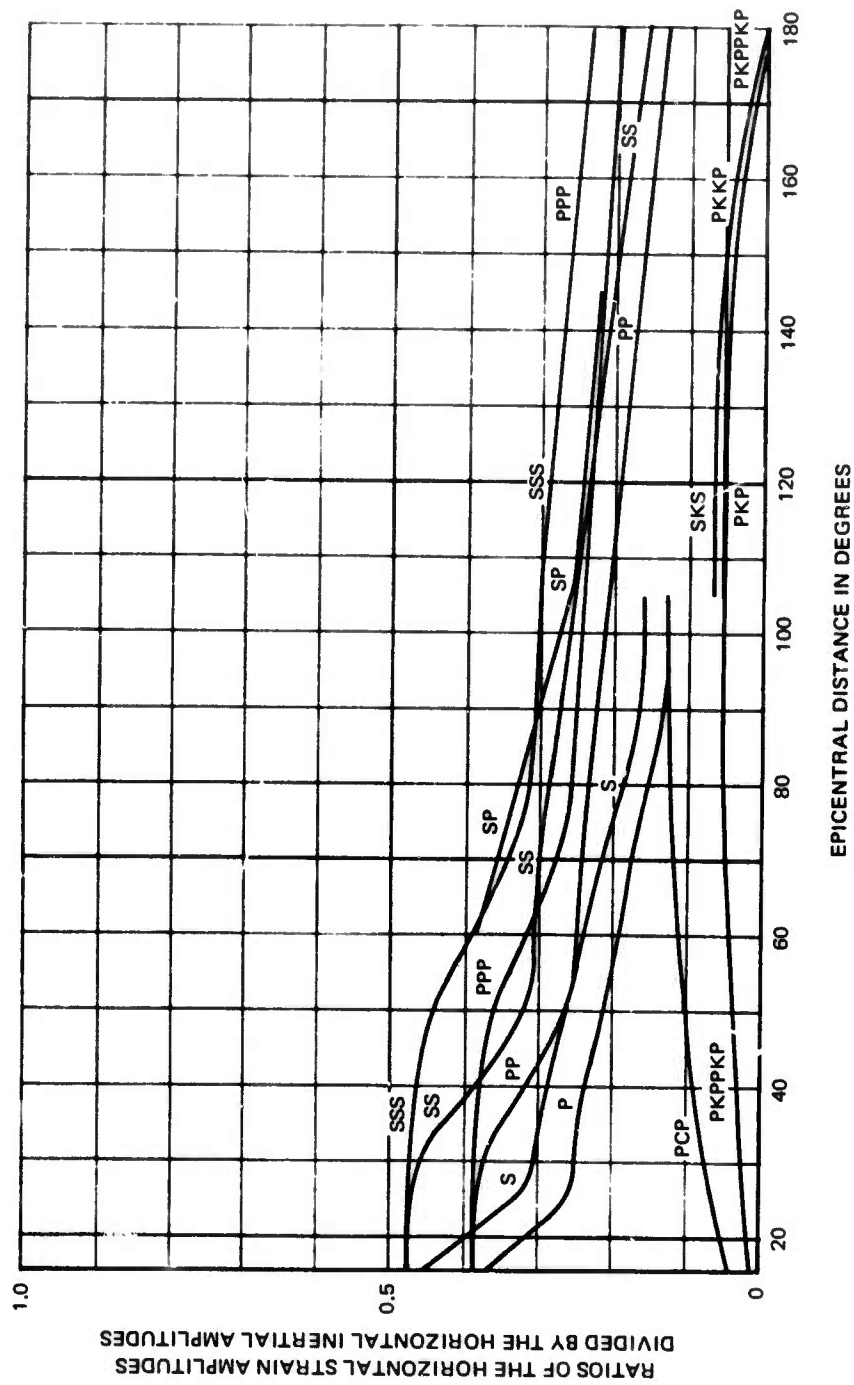


Figure 18. Ratios of the theoretical amplitudes of the horizontal strain to horizontal inertial for several earthquake body phases. The ratios are based on a value of unity for Rayleigh waves. The SH component of transverse waves is used

In figure 17 the ratios of the theoretical amplitudes of the vertical strain to the vertical inertial for several earthquake phases are plotted as a function of epicentral distance. The ratios are based on a value of unity for fundamental mode Rayleigh waves, not shown on the plot. The SV component of the transverse phase S, SS, SSE, and SKS has been used since vertical seismographs do not record SH.

The amplitude of longitudinal phases recorded by the vertical strain whose paths either include the earth's core or reflected from the core are seen to be very small relative to the inertial amplitudes. Also, the vertical strain amplitudes resulting from the P phase, and longitudinal phases reflected from the crust, e. g., PP and PPP, are seen to decrease with increasing distance. That is, the vertical strain seismograph has a low response to most body phases and, therefore, cannot be used by itself to detect them.

Similarly, the ratios of the theoretical amplitude of the horizontal strain to horizontal inertial, figure 18, show the horizontal strain seismograph response to behave essentially like that of the vertical strain. Again, the ratios are based on a value of unity for fundamental mode Rayleigh waves. The SH component rather than SV was used for the transverse phases. The ratios for the transverse phases show the horizontal strain amplitudes to decrease, with respect to the inertial amplitudes, with increasing distance as in the case for longitudinal phases.

5. APPLICATION OF STRAIN SEISMOGRAPHS

The application of strain seismograph outputs to the enhancement of signals and identification of seismic waves is discussed in three parts. In the first part the combined outputs of the horizontal strain and inertial seismographs are examined as an azimuthally sensitive system. Part two examines the potential of combined omnidirectional vertical strain and vertical inertial seismograph outputs to cancel microseisms. The third part discusses the identification of seismic waves, both earthquake phases and microseisms, by the amplitude and phase relationships among strain and inertial seismograms.

5.1 HORIZONTAL STRAIN-INERTIAL COMBINATION

Figure 19 shows the azimuthal response to Rayleigh waves that can be obtained by summing the outputs of horizontal strain and inertial seismographs oriented in the same direction. By normalizing magnifications and summing, the response to Love waves, illustrated in figure 20, can be obtained. The above curves are rotated 180 degrees by changing the polarity of either the strain or inertial seismograph.

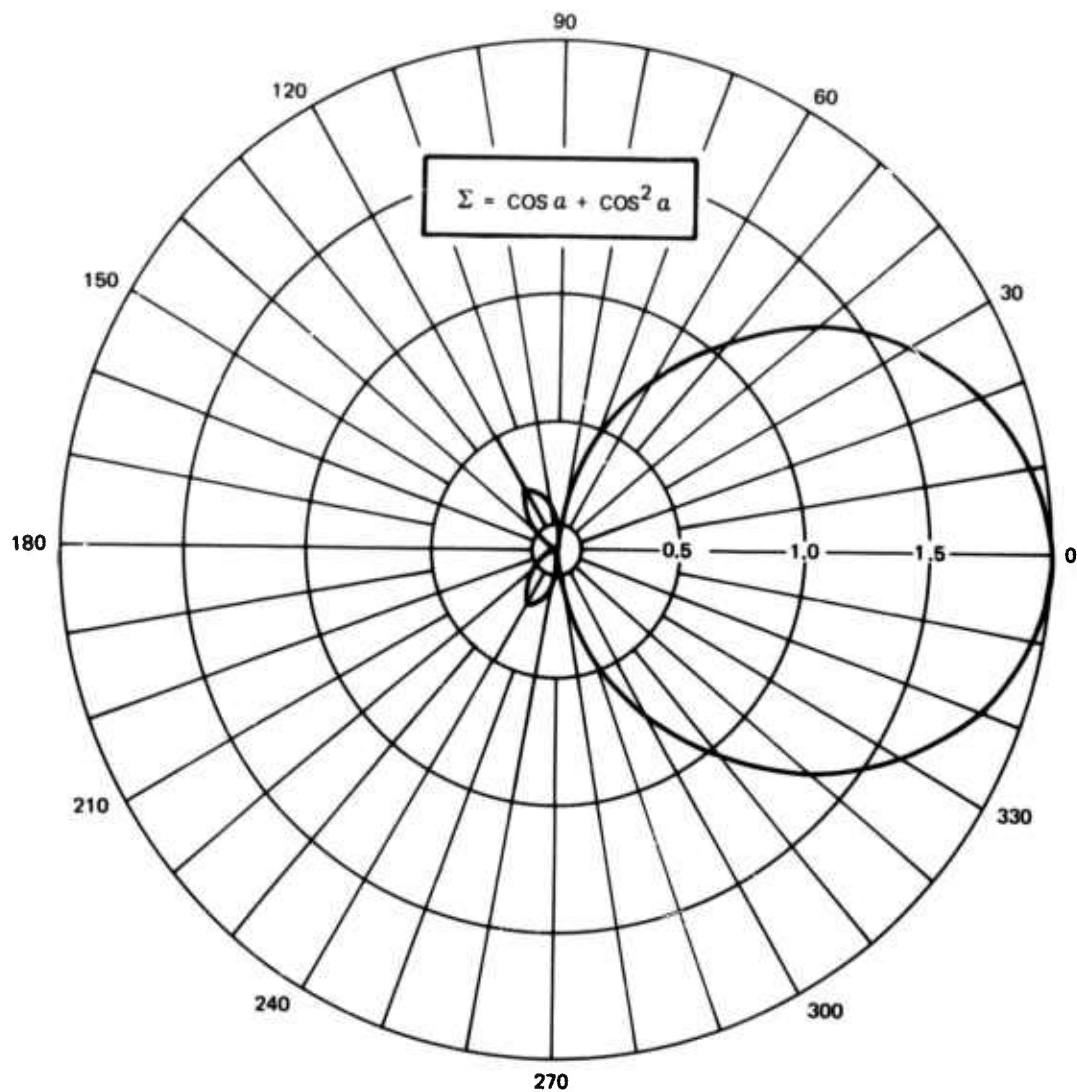


Figure 19. Azimuthal response to Rayleigh waves of the summed outputs of horizontal strain and inertial seismographs that are oriented in the same direction

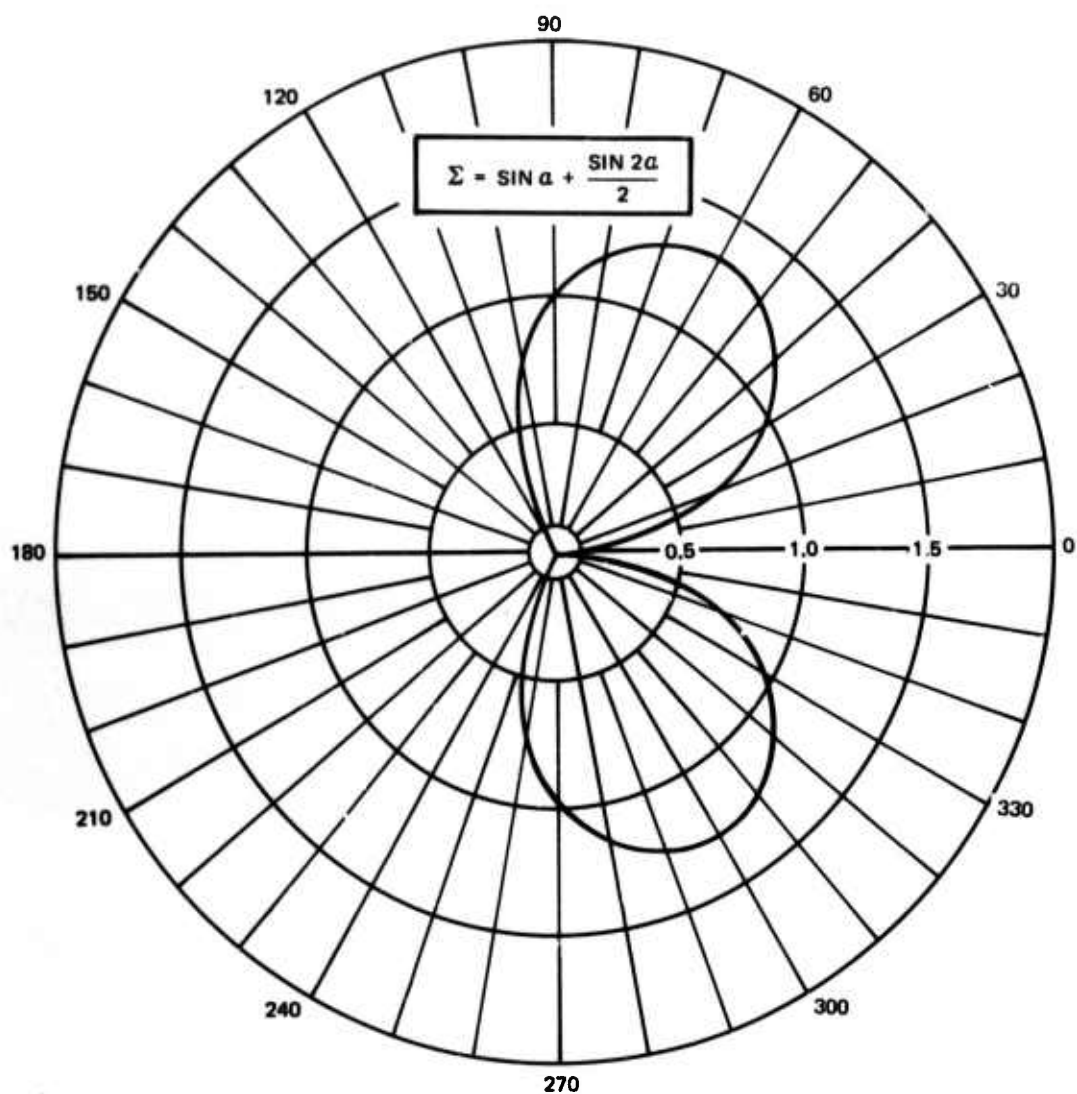


Figure 20. Azimuthal response to Love waves of the summed outputs of the horizontal strain and inertial seismographs that are oriented in the same direction

G 3952

These azimuthal responses lead to a variety of applications of the combined horizontal strain-inertial seismograph outputs. The applications include cancellation of microseisms, signal enhancement, and the discrimination between simultaneous arrivals from more than one earthquake.

5.1.1 Microseismic Rejection

Cancellation of unidirectional microseisms attained by summing the outputs of the strain and inertial seismographs is illustrated in figure 21 by the SW component of the WMSO directional array. The W component also exhibits cancellation indicating the microseisms were arriving slightly east of northeast. The WMSO directional array consists of four pairs of horizontal strain and inertial seismograph combinations summed so as to provide the maximum response to Rayleigh waves, figure 19, in the directions N, NE, E, SE, S, SW, W, and NW.

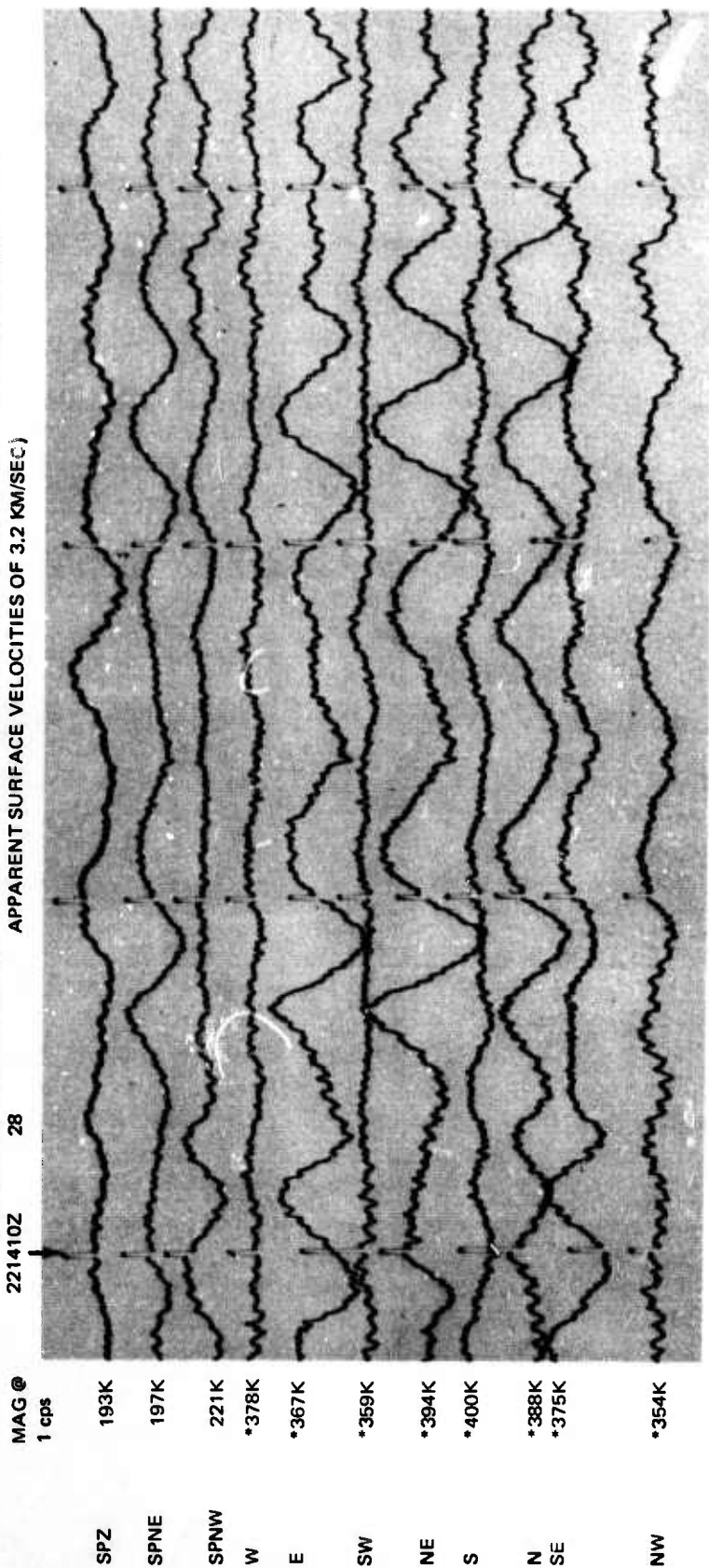
A broader variable azimuthal response can be obtained by summing the effective output of a single horizontal inertial with that of either a vertical strain or summed orthogonal horizontal strain seismographs. The advantages of such a system lie in the limited number of seismographs needed and the ability to azimuthally rotate the response pattern. The disadvantage is a broad response shown in figure 22. This response is a cardioid. The effective output of a single horizontal inertial oriented in any arbitrary direction can be obtained from the outputs of any two orthogonal horizontal inertials through a coordinate transformer. A sine-cosine potentiometer may be used for this purpose. Cancellation of microseisms employing a sine-cosine potentiometer is illustrated in figure 23.

Cancellation of microseisms from a given direction can be used to improve the signal-to-noise ratio of signals arriving from a direction different from that of the microseisms. This capability is illustrated by the west component of the WMSO directional array, figure 24. The strain (SE) and inertial (SPE) recordings of signal and noise arriving from opposite directions were added to simulate a small event arriving during a period of high level microseisms. Trace (SPE) shows the simulated inertial recording of both the signal and microseisms. Trace (W) shows the restoration and improvement of the signal attained by adding the strain seismograph output.

A strain-inertial combination may also be employed to enhance teleseismic SH body waves. Since the strain seismograph response to these waves is low, the inertial recording will be essentially unchanged by the strain contribution. Therefore, cancellation of apparent longitudinal wave microseisms (Rayleigh) arriving 90° from the azimuth of an earthquake will result in enhancement of the SH waves.

$$\text{*MAGNIFICATION} = \frac{\text{STRAIN MAGNIFICATION}}{28} + \text{INERTIAL MAGNIFICATION} \quad \text{WHERE}$$

$$\frac{\text{STRAIN MAGNIFICATION}}{28} \equiv \frac{\text{EQUIVALENT INERTIAL MAGNIFICATION (EQUATED FOR SEISMIC WAVES OF APPARENT SURFACE VELOCITIES OF 3.2 KM/SEC)}}{28}$$



SPZ	VERTICAL INERTIAL	NE	NORTHEAST COMPONENT OF THE DIRECTIONAL ARRAY
SPNE	NORTHEAST HORIZONTAL INERTIAL	S	SOUTH COMPONENT OF THE DIRECTIONAL ARRAY
SPNW	NORTHWEST HORIZONTAL INERTIAL	N	NORTH COMPONENT OF THE DIRECTIONAL ARRAY
W	EAST COMPONENT OF THE DIRECTIONAL ARRAY	SE	SOUTHEAST COMPONENT OF THE DIRECTIONAL ARRAY
E	WEST COMPONENT OF THE DIRECTIONAL ARRAY	NW	NORTHWEST COMPONENT OF THE DIRECTIONAL ARRAY
SW	SOUTHWEST COMPONENT OF THE DIRECTIONAL ARRAY		

Figure 21. Seismogram illustrating the ability of the strain directional array to azimuthally discriminate between microseisms exhibiting directional properties

WMSO
RECORD NO. 076
17 MAR 67

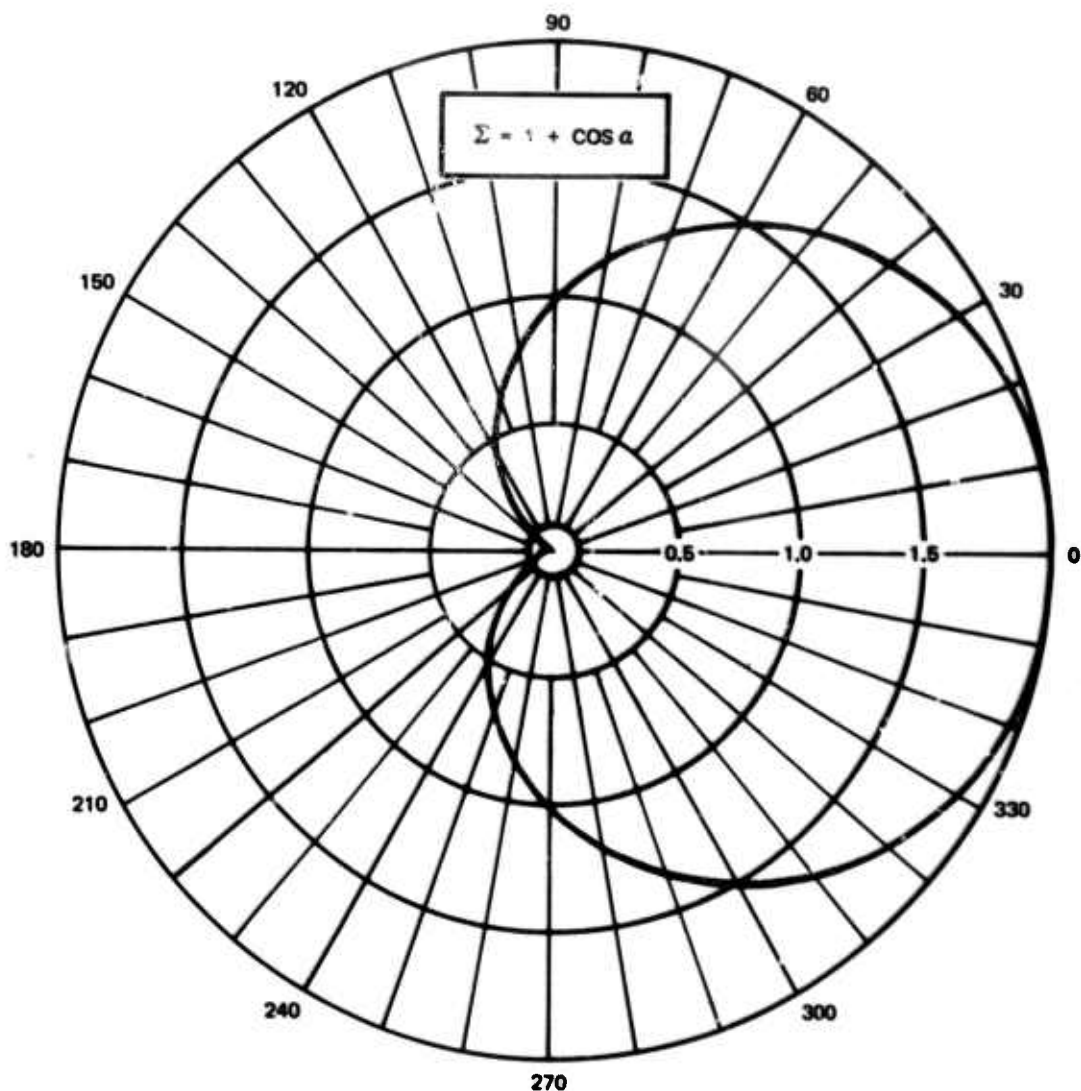


Figure 22. Azimuthal response to Rayleigh waves of the summed outputs of a horizontal inertial seismograph and either a vertical strain or two orthogonal horizontal strain seismographs

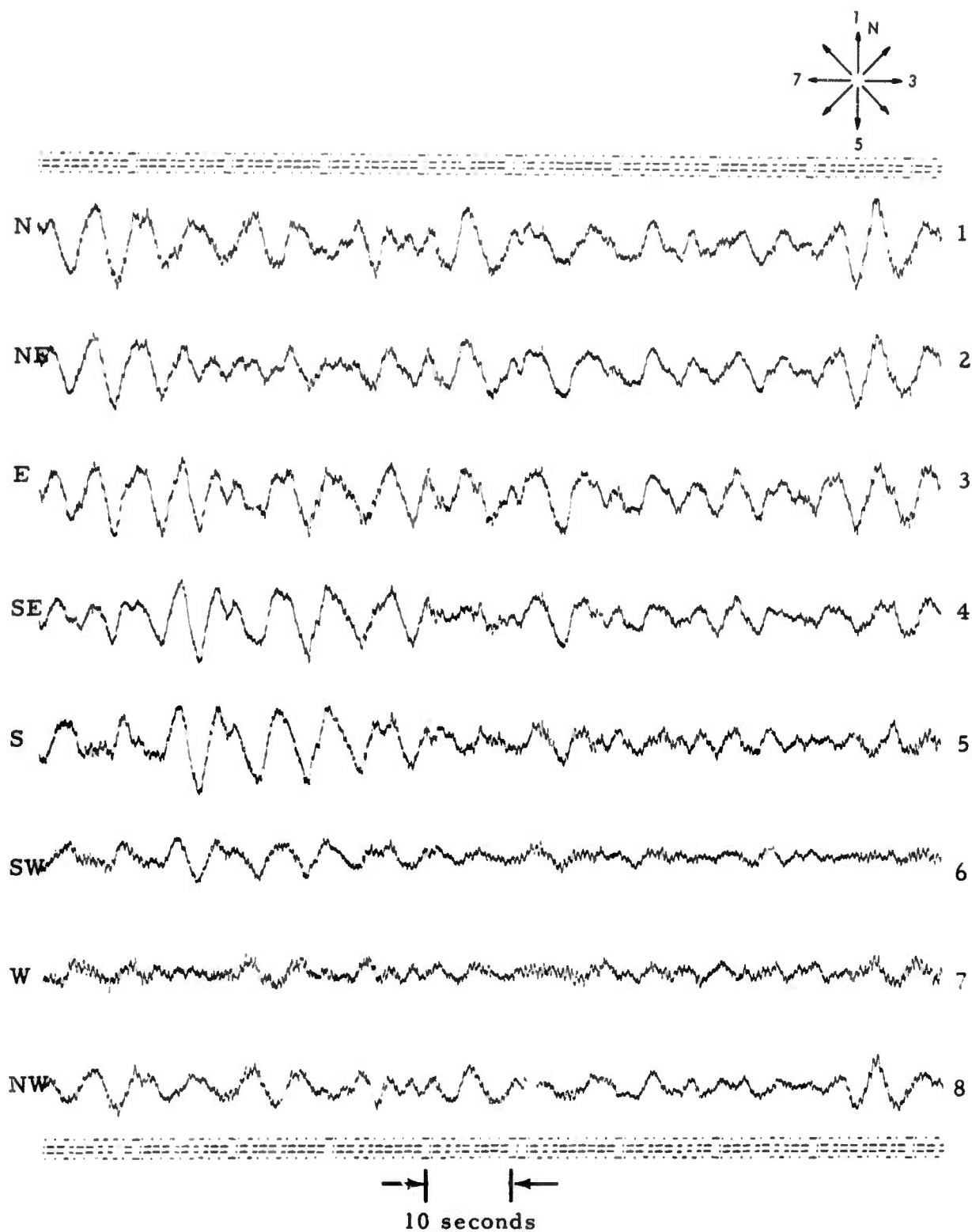


Figure 23. Seismograms showing results obtained from the sine-cosine technique. Maximum cancellation of 4 to 6 second microseisms occurred on the west and southwest traces (6 and 7), indicating that the microseisms are arriving from the east and the northeast

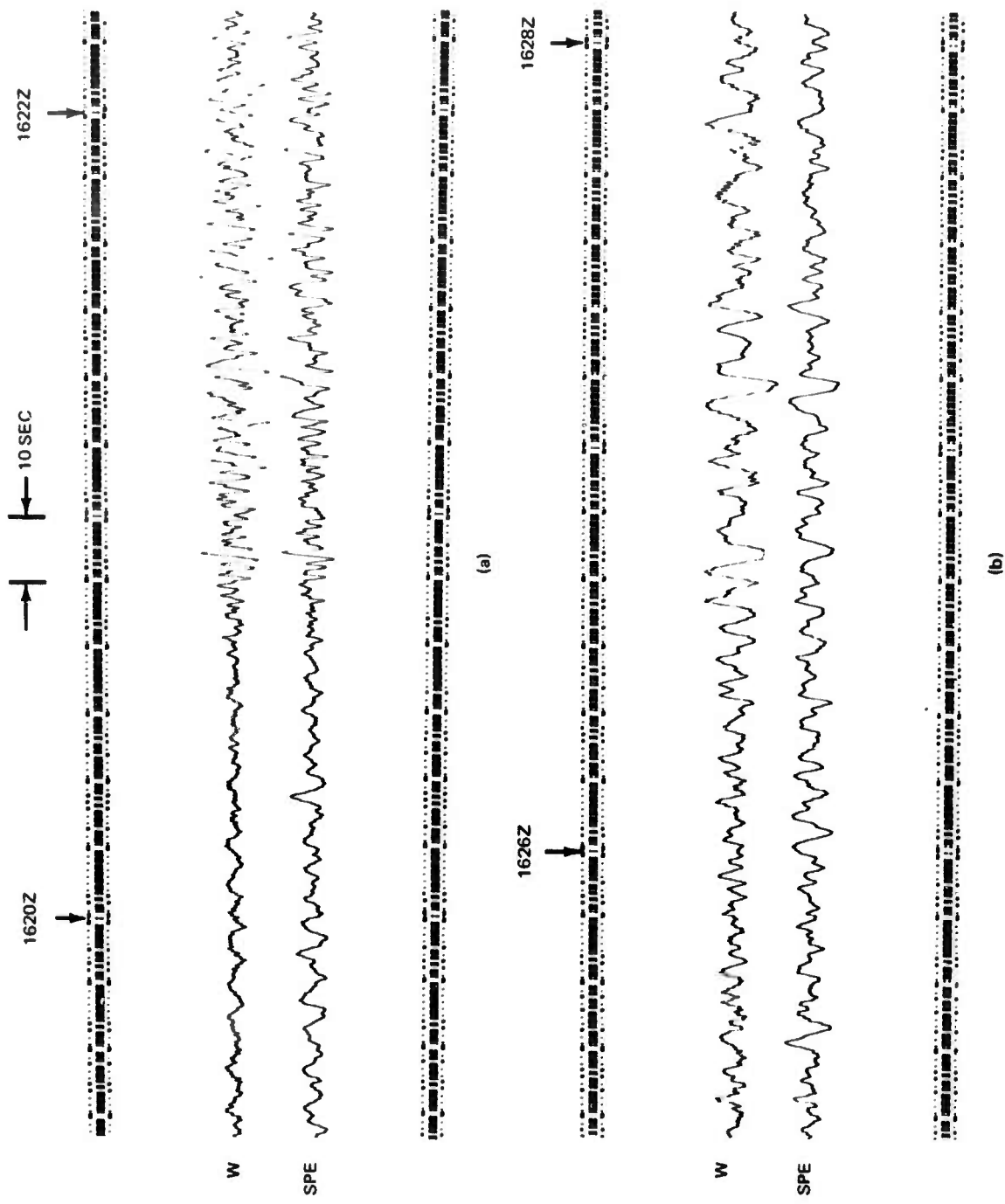


Figure 24. Seismograms illustrating the reduction of microseisms by the west component of the WMSO directional array (W) thereby enhancing the horizontal component of body phases (figure 24a) and surface waves (24b) from an earthquake. The horizontal east inertial (SPE) recording is also shown

5.1.2 Signal Addition

Signal enhancement is not necessarily just a consequence of microseismic cancellation. As the azimuthal response curves suggest, signal may add while microseisms cancel. The degree of enhancement by signal addition is, of course, dependent on signal wave type and incidence. For example, the strain contribution of P- and S-waves will increase with decreasing epicentral distance. Figure 25 illustrates the increasing enhancement of P-waves by the NW component of the WMSO directional array as the epicentral distance decreases. All the epicenters were northwest of WMSO.

Horizontal strain-inertial combinations are most suited to the enhancement of surface waves. This is due to the relatively high response of strain seismographs to surface waves. Also, the ratio of the horizontal to vertical displacement resulting from these waves is high compared to the ratio for teleseismic longitudinal waves. Figure 26 illustrates the enhancement of long-period surface waves from an earthquake in Central Alaska by the north component of the WMSO directional array. The individual strain and inertial recordings are also shown.

In the above sample, enhancement was obtained by summing the strain and inertial signals. If, however, there had been another earthquake, say from South America, whose surface waves arrived coincident with those from the Alaskan earthquake, a result, unique to the strain-inertial combination, would be obtained. This is illustrated in figure 27 where surface waves from an earthquake near the Peru-Ecuador border were superimposed on those from the Alaskan event. The surface waves from South America have been cancelled by the strain-inertial combination leaving those from the Alaskan earthquake. Had the polarity of either the strain or inertial seismograph output been reversed, the signal from Alaska would have been cancelled while the signal from South America would have been added. That is, the strain-inertial combination can be used to discriminate between earthquakes recorded simultaneously.

Time delay techniques on the outputs of a spacial array of inertial seismographs might yield results somewhat similar to those above; however, these techniques are relatively complicated requiring many seismographs.

Therefore, the effectiveness and simplicity of the horizontal strain-inertial combination to azimuthally discriminate between, cancel and enhance surface waves suggest this seismograph combination can be used more efficiently and perhaps, more effectively than inertial seismographs alone in the identification of earthquakes by surface waves.

5.2 VERTICAL STRAIN-INERTIAL COMBINATION

Romney (1964) suggested that the combined outputs of vertical strain and vertical inertial seismographs might yield an improved P-wave signal-to-noise

$$*MAGNIFICATION = \frac{STRAIN\ MAGNIFICATION}{28} + INERTIAL\ MAGNIFICATION \quad \text{WHERE}$$

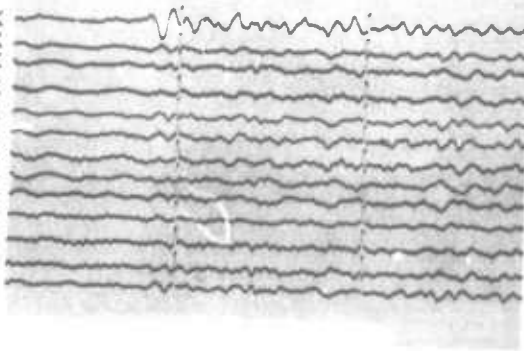
$$\frac{STRAIN\ MAGNIFICATION}{28} \equiv EQUIVALENT\ INERTIAL\ MAGNIFICATION\ (EQUATED\ FOR\ SEISMIC\ WAVES\ APPARENT\ SURFACE\ VELOCITIES\ OF\ 3.2\ KM/SEC)$$

06 APR 67

10 SEC

SPZ
SPN
SPE
SPNE
SPNW
N
NE
E
SE
S
SW
W
NW

108K
95K
98K
106K
106K
187K
194K
186K
192K
187K
196K
193K
191K

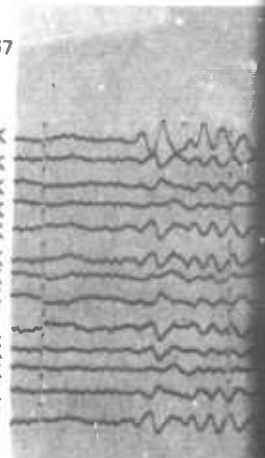


NEAR S. COAST OF HONSHU $\Delta = 90.4^\circ$ Az - 316°

12 JUN 67

SPZ
SPN
SPE
SPNE
SPNW
N
NE
E
SE
S
SW
W
NW

100K
100K
98K
100K
100K
187K
190K
191K
193K
189K
195K
200K
193K

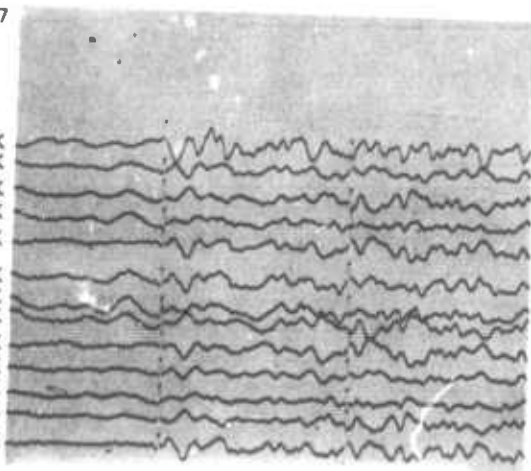


KURILE IS. Δ

29 APR 67

SPZ
SPN
SPE
SPNE
SPNW
N
NE
E
SE
S
SW
W
NW

96K
98K
101K
100K
101K
189K
193K
190K
189K
183K
194K
190K
188K

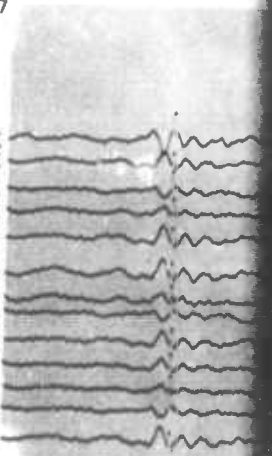


ANDREANOF IS. ALEUTIAN IS. $\Delta = 57.6^\circ$ Az - 313°

30 APR 67

SPZ
SPN
SPE
SPNE
SPNW
N
NE
E
SE
S
SW
W
NW

96K
98K
101K
100K
101K
189K
193K
190K
189K
183K
194K
190K
188K

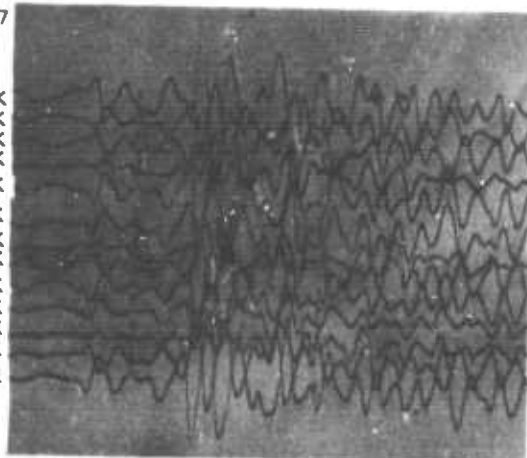


SOUTH ALASKA

29 APR 67

SPZ
SPN
SPE
SPNE
SPNW
N
NE
E
SE
S
SW
W
NW

96K
98K
101K
100K
101K
189K
193K
190K
189K
183K
194K
190K
188K

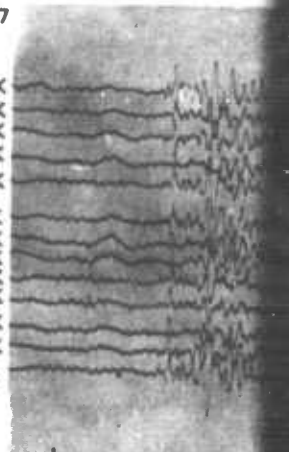


QUEEN CHARLOTTE IS. REG. $\Delta = 28.2^\circ$ Az - 315°

27 APR 67

SPZ
SPN
SPE
SPNE
SPNW
N
NE
E
SE
S
SW
W
NW

91K
93K
99K
92K
99K
192K
192K
183K
187K
191K
196K
181K
187K

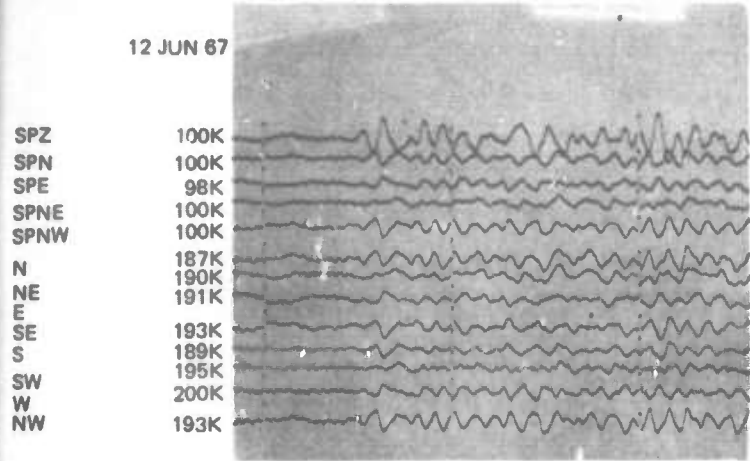


COLORADO $\Delta =$

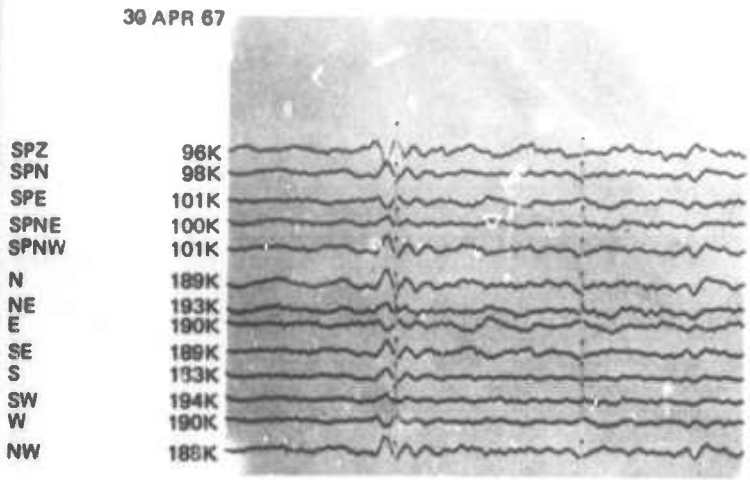
A

IAL MAGNIFICATION WHERE

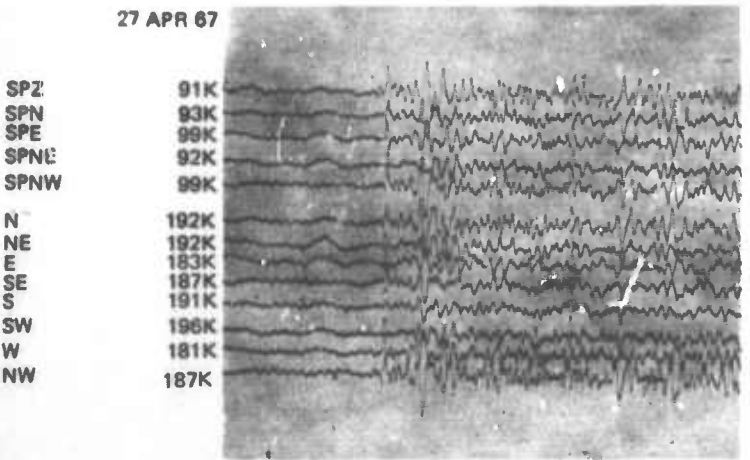
MAGNIFICATION (EQUATED FOR SEISMIC WAVES OF
 CITIES OF 3.2 KM/SEC



KURILE IS. $\Delta = 75.4^{\circ}$ Az - 318°



SOUTH ALASKA $\Delta = 43.5^{\circ}$ Az - 323°



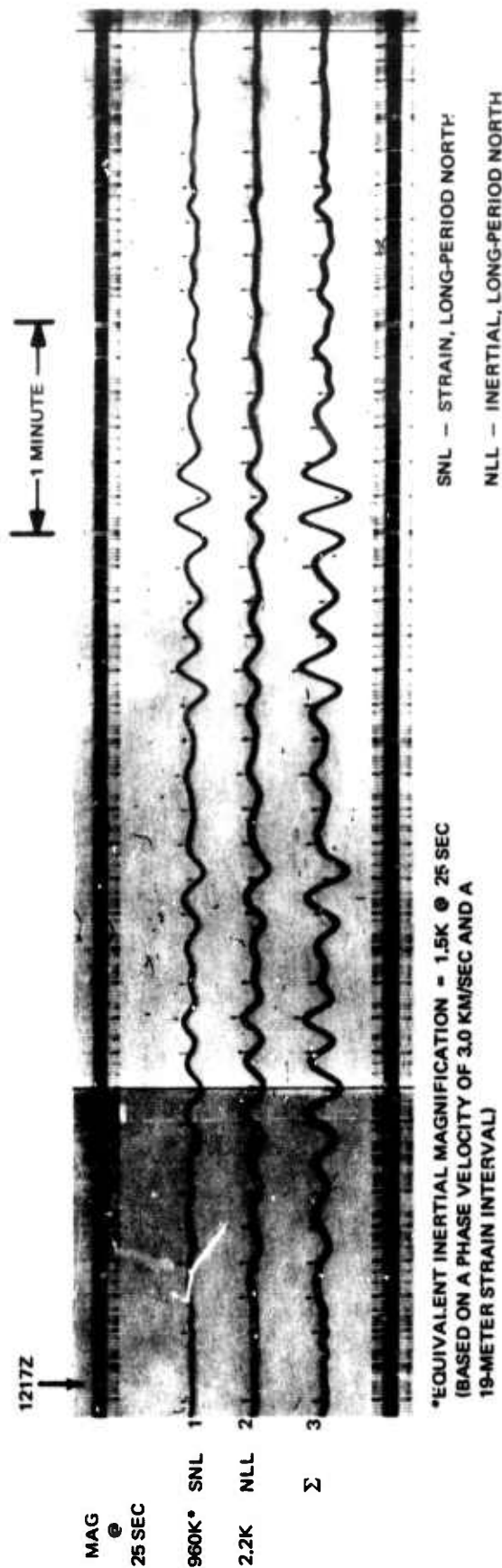
COLORADO $\Delta = 7.1^{\circ}$ Az - 319°

B

Figure 25. Seismograms illustrating increased improvement
 in recorded P-waves by the NW component of the WMSO
 directional array as the epicentral distance decreases

G 3957

DATE: 23 JUNE 1967
 ORIGIN TIME: 11:54:52.7Z
 CENTRAL ALASKA
 64.7 N, 148.7° W
 AZ = 333°
 Δ = 42°
 MAG 4.6
 h ≈ 30 KM



WMO
 MAG TAPE NO. 1
 RUN NO. 174
 23 JUNE 1967

Figure 26. Enhancement of surface waves from Central Alaska by the north component of the WMSO directional array

EVENT 1 - DATE: 23 JUNE 1967
 ORIGIN TIME: 11:54:52.7Z
 CENTRAL ALASKA
 64.7 N, 148.7° W
 AZ = 333°
 Δ = 42°
 MAG 4.6
 h \approx 30 KM

EVENT 2 - DATE: 21 JUNE 1967
 ORIGIN TIME: 06:49:56.6Z
 PERU-EQUADOR BORDER
 2.2 S, 77.6 W
 AZ = 183°
 Δ = 42°
 MAG 5.3
 h = 49 KM

MAG
 ●
 25 SEC

5 MINUTES

3.2K NLL EVENT 1

1.0K NLL EVENT 2

NLL EVENT 1 + 2

Σ [SNL EVENT 1 + 2
 + (NLL EVENT 1 + 2)]

SNL - STRAIN, LONG-PERIOD NORTH
 NLL - INERTIAL, LONG-PERIOD NORTH

WMO
 MAG TAPE NO. 1

Figure 27. Azimuthal discrimination of surface waves from Central Alaska and South America superimposed to simulate simultaneous recording. The surface waves from South America have been rejected, enhancing those from Central Alaska

G 3959

ratio over that of the vertical inertial seismograph alone. This possibility arises from the differences in the responses of the two seismographs to various wave types. As seen earlier from figure 17, the ratios of the amplitudes recorded by the vertical strain seismograph to those by the vertical inertial seismograph for teleseismic P-waves decrease as the epicentral distance increases. Thus, the combined outputs of the two vertical seismographs can be appropriately filtered to cancel Rayleigh wave noise while only partially distorting the vertical inertial recording of an incident P-wave. This distortion results from the phase difference, shown in figure 12, between the strain and inertial seismograph recordings of the P-wave.

Romney also noted that the complexity of the filter necessary to effectively combine the outputs of the two vertical seismographs for an improved S/N ratio will depend largely on the degree to which microseisms consist of a given mode of Rayleigh waves. If the microseisms consist of a mixture of wave types and modes, the required filter may be very complicated or even unrealizable. This can be seen by examining the difference between both the vertical strain and vertical inertial seismograph responses to different wave types.

Recent investigations employing deep well and surface inertial seismographs indicate that microseisms do consist of a mixture of wave types in the short-period range 0.3 to 6.0 seconds. Data recorded by the strain seismographs at WMSO also indicate the presence of a mixture of wave types in microseisms. The coherence between the outputs of the vertical strain and inertial seismographs has been computed to be low for recorded samples of microseisms. The outputs of the two seismographs have also been filtered so as to provide equal amplitudes for Rayleigh waves. They have then been combined in an attempt to reduce the microseismic level as shown in figure 28. Only limited reduction in noise has been attained by this method. The summed outputs of the horizontal strain seismographs have been substituted for that of the vertical strain seismograph in the above tests, but yielded the same results.

Failure to improve the signal-to-noise ratio by this method at WMSO does not preclude the possibility of successful application at other locations with a different noise field.

5.3 SEISMIC WAVE IDENTIFICATION

5.3.1 Earthquake Phases

Strain and inertial seismograms can be used to assist in the identification of earthquake phases. Theoretical ratios of the amplitudes of the vertical strain output to vertical inertial output for several earthquake phases as a function of epicentral distance were given in figure 17. These ratios can be used to approximate the epicentral distance of an earthquake and to distinguish between phases of the same wave type. The signal-to-noise ratio of the strain

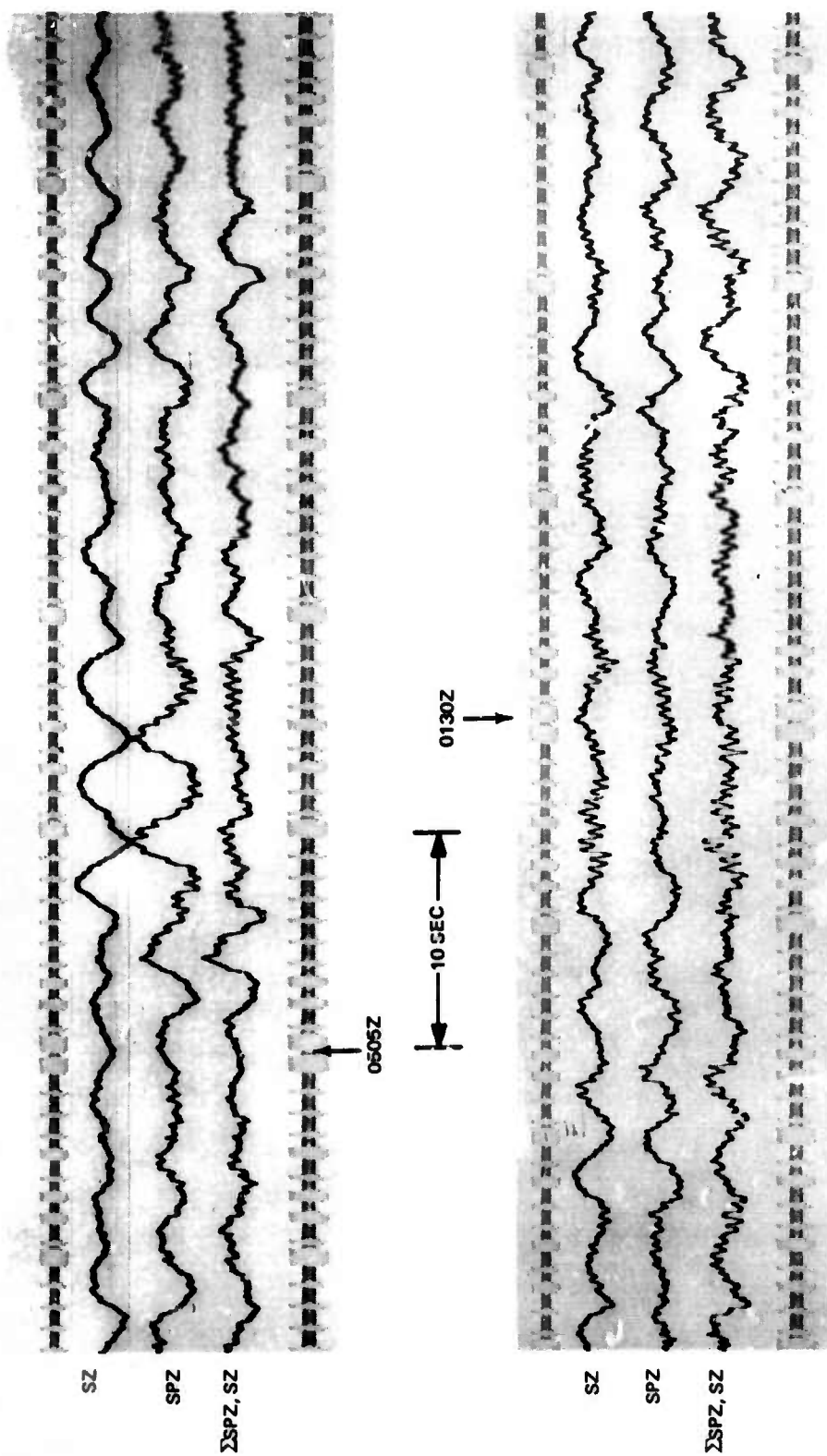


Figure 28. Seismograms illustrating limited reduction of microseisms over sustained periods of time attained by the summation (Σ SPZ, SZ) of the filtered outputs of a vertical strain (SZ) and a vertical inertial (SPZ) seismograph

WMO
RECORD NO. 028
28 JAN 66

G 3960

recording will, of course, limit accuracy. Furthermore, caution must be exercised to assure that only the recorded energy of a given phase is measured rather than the coda of a previous phase which will be contaminated with other wave types.

Some very useful information can be obtained by inspection of the seismograms. The phases pP and PCP may arrive seconds to minutes after the P arrival dependent primarily on the depth and distance, respectively, of the hypocenter. Unless one knows the hypocenter, no prediction can be made as to which phase will arrive first or that either one will necessarily be recorded. The character of the recorded phases is not necessarily a diagnostic feature. The strain seismograph response to these phases, however, differs significantly out to an epicentral distance near 70 degrees. Since PCP is a core reflection, it is steeply incident. The incidence angle of pP, however, will be slightly greater than that of the P. Therefore, the ratios of the amplitudes of the strain to inertial recording of pP will be about the same as P, but much less for PCP. This is illustrated in figure 29.

The phase relationship between two orthogonal horizontal strains can be used to distinguish Love from Rayleigh. Regardless of the azimuth, Rayleigh waves will be recorded in phase, Love waves 180° out of phase. The presence of both Love and Rayleigh can be detected in figure 30 by the horizontal strain, SN and SE, whereas they are indistinguishable on the horizontal inertials SPN and SPE.

Observations of a departure of surface waves from a great circle path have been made and documented by Evernden (1954). If the azimuth of an earthquake is known the relationship of the amplitudes of horizontal strain and inertial seismograms can be used to compute any deviation from the great circle path. This is possible due to the different azimuthal responses of the seismographs.

5.3.2 Microseisms

Strain seismograms can be used in the study of microseisms in two important capacities. The first is the determination of the azimuths from which microseisms arrive. Combined horizontal strain-inertial seismograph outputs described earlier, figures 19 and 20, and examination of the coherence between the seismograph outputs as a function of frequency are methods by which azimuthal properties of microseisms can be studied. The second application of strain seismograms in the study of microseisms is the determination of the seismic waves that constitute microseisms. Unfortunately, the complexity of microseisms, regarding the presence of and energy distribution as a function of time among multiple wave types and modes, prohibit a simple determination of their composition. The differences, however, between the response of strain and inertial seismographs and even between horizontal and vertical strain seismographs can be used to identify predominant wave types.

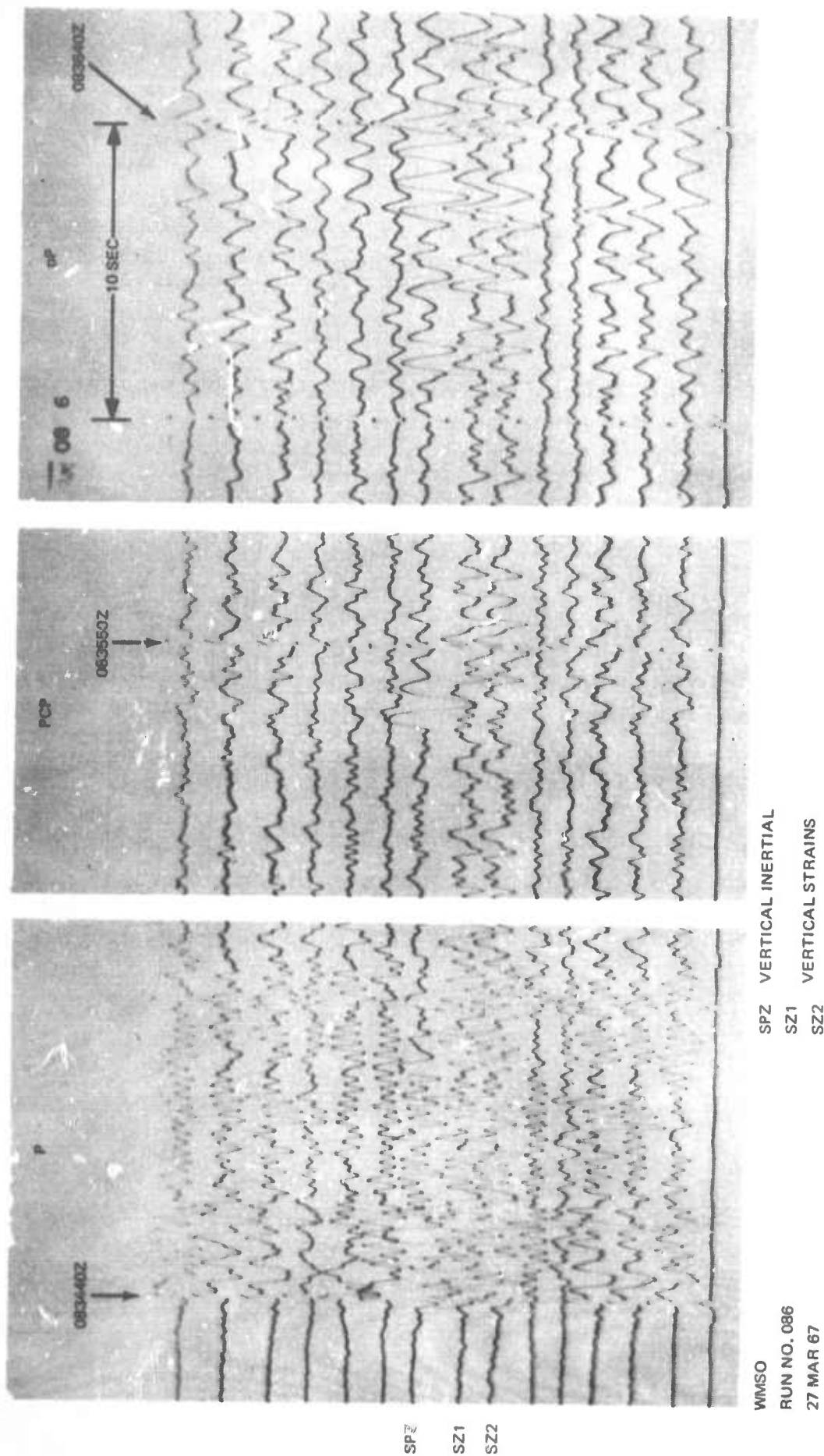


Figure 29. Seismograms illustrating how vertical strain and inertial recordings can be used to discriminate between the phases pP and PCP by inspection. The strain/inertial amplitude ratio for pP is about the same as for P, but much smaller for PCP. The earthquake epicenter was in the western part of Brazil

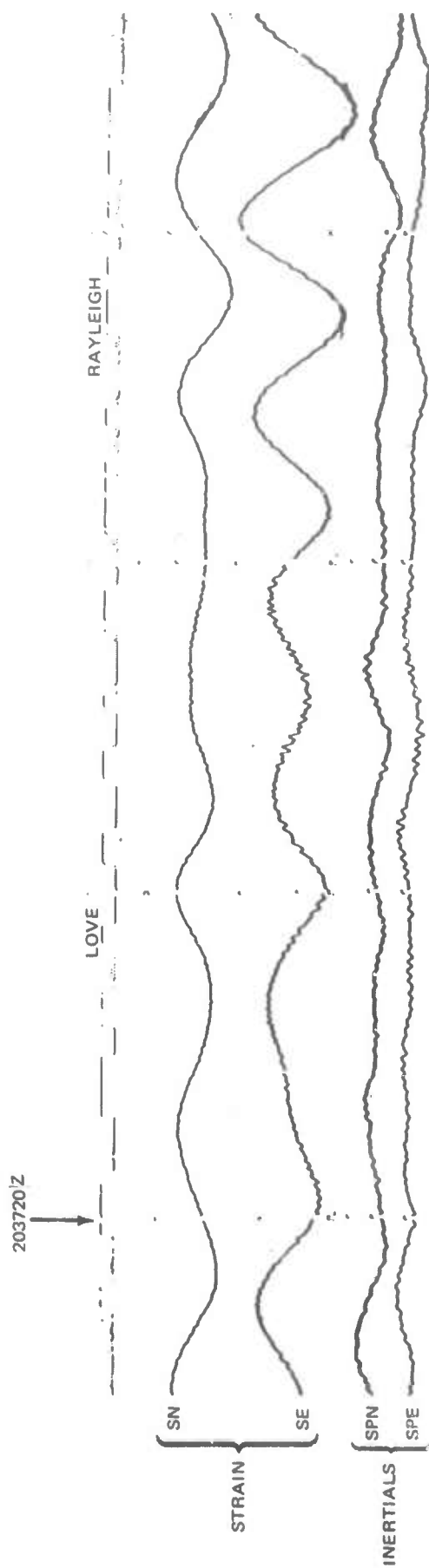


Figure 30. Seismogram illustrating the 180° phase difference between the orthogonal horizontal strains (SN and SE) for Love waves, and 0° phase difference for Rayleigh waves. The phase difference between the orthogonal horizontal inertials (SPN and SPE) for both Love and Rayleigh will be dependent on azimuth

6. SYSTEM DESCRIPTION AND OPERATING PROCEDURES

A description of the WMSO strain-inertial seismograph systems and installation, in addition to the procedures necessary to calibrate and operate the seismograph systems are discussed below. Included are recording requirements and procedures for obtaining seismograph frequency responses.

6.1 SYSTEM DESCRIPTION

As stated earlier, the WMSO strain-inertial seismograph system contains four SP horizontal strain seismometers, four SP horizontal inertial seismometers, one LP horizontal inertial seismometer, one vertical strain seismometer, one SP vertical inertial seismometer, and one LP vertical inertial seismometer. The system is capable of recording earth motion in the period range of 0.1 sec to 200 sec.

The strain-inertial seismograph system is composed of three primary groups: the vault group, the remote group, and the central group. A block diagram of the system is shown in figure 31, and the operating parameters are listed in table 1.

The vault group includes the strain and inertial seismometers. The horizontal strain seismometers and horizontal and vertical inertial seismometers are located in a central subsurface concrete vault with four strain-member housings extending radially toward the northeast, north, northwest, and west. The concrete vault and strain-member housings are rigidly anchored to competent bedrock. The vault is sealed against rapid pressure changes that produce noise in the frequency band of interest.

The vertical strain seismometer is located in a borehole about 30 m north of the concrete vault. The borehole is cased with a 178 mm i.d. steel casing and is 39 m deep.

The strain and inertial seismometer characteristics are listed in table 2.

The first stages of amplification and filtering are achieved in the remote group. The outputs from the seismometer transducers are amplified by either SP or LP Phototube Amplifiers (PTA's), Geotech Model Nos. 4300 and 5240A, respectively. In the SP system, 3.0 Hz Galvanometers, Model 4100-213M, are used in the strain PTA's and Model 4100-213 in the inertial PTA's. The PTA Power Supplies, Model 4304, house SP Band-pass Filters, Model 6824-1. In the LP system, 100 sec Harris Galvanometers, Model 8530-5, are used in both the strain and inertial PTA's. The PTA Power Supplies, Model 14486, house the LP Band-pass Filters, Model 6824-14. The signals from the strain seismometer transducers drive both the SP and LP galvanometers. The LP and SP galvanometer characteristics are listed in table 3. The outputs of the PTA's then undergo additional filtering

Table 1. Strain-inertial seismograph operating parameters

Seismo- graph	f _o (Hz)	f _g (Hz)	λ _o	λ _g	Band-pass Filter, Models 6824-1 and -14		Narrow Band-pass Filter, Models 28900-01 and -02	
					Cutoff low-high (Hz)	Cutoff rate low-high (dB/oct)	Center frequency (Hz)	Cutoff rate low-high (dB/oct)
Strain SP horizontal	65	3.0	-	0.7	.01-10	6-12	0.8	6-6 0.7
Strain SP vertical	60	3.0	-	0.7	.01-10	6-12	0.8	6-6 0.7
Inertial SP horizontal	0.8	3.0	0.7	0.7	.01-10	6-12	-	- -
Inertial SP vertical	0.8	3.0	0.7	0.7	.01-10	6-12	-	- -
Strain LP horizontal	65	0.009	-	1.0	.005--05	6-12	0.059	6-6 0.64
Strain LP vertical	80	0.009	-	1.0	.005--05	6-12	0.059	6-6 0.64
Inertial LP horizontal	0.059	0.009	0.64	1.0	.005--05	6-12	-	- -
Inertial LP vertical	0.059	0.009	0.64	1.0	.005--05	6-12	-	- -

λ_o = Seismometer damping ratio
λ_g = Galvanometer damping ratio
λ_f = Filter damping ratio

NOTE: SP = short-period
LP = long-period
f_o = natural frequency of seismometer
f_g = natural frequency of galvanometer

Table 2. Strain and inertial seismometer characteristics

Seis- mometer	Geotech model	Natural frequency (Hz)	Type of transducer	Internal resistance (Ω)	Type of calibrator	Internal resistance (Ω)
Strain, horizontal	14103A	65	velocity	1000	electromagnetic	80
Strain, vertical	14936	60	"	1000	"	2000
Inertial SP horizontal	7515	0.8	"	110	"	98
Inertial SP vertical	6480	0.8	"	110	"	98
Inertial LP horizontal	8700C	0.056	"	565	"	0.2
Inertial LP vertical	7505A	0.056	"	565	"	0.2

NOTE: SP = short-period
LP = long-period

Table 3. Strain-inertial seismograph galvanometer characteristics

	Geotech model No.		Galvanometer model No.	Natural frequency (Hz)	Internal resistance (Ω)	CDRX (Ω)
	PTA	Pwr supply				
Strain SP horizontal	4300	4304	4100-213M	3.0	22	300 to 500
Strain SP vertical	4300	4304	4100-213M	3.0	22	300 to 500
Inertial SP horizontal	4300	4304	4100-213	3.0	22	82
Inertial SP vertical	4300	4304	4100-213	3.0	22	82
Strain LP horizontal	5240A	14486	8530-5	0.009	1118	1000
Strain LP vertical	5240A	14486	8530-5	0.009	1118	1000
Inertial LP horizontal	5240A	14486	8530-5	0.009	1118	1000
Inertial LP vertical	5240A	14486	8530-5	0.009	1118	1000

NOTE: SP = short-period
LP = long-period

and amplification in the central group.

In the central group the strain signal is routed through a Model 28900 narrow band-pass filter which matches the strain to the inertial seismograph response. The signals are then routed to the Amplifier Module, Model 23043. The signals are amplified and the orthogonal horizontal strain signals are summed. The signals are then fed into (1) the primary Develocorder through the Data Control Modules, Model 5792, (2) a magnetic-tape recorder, and (3) the directional array summation circuits (horizontal strain outputs only). In the summation circuits of the directional array the strain signals are summed in two polarities with the inertial signals, and the resultant is transmitted to the strain directional array Develocorder through Data Control Modules, Model 5792.

The inertial signals are routed to the Amplifier Modules, Model 23043. The signals are then fed into (1) the primary Develocorder through the Data Control Modules, Model 5792, (2) a magnetic tape recorder, and (3) the strain directional array summation circuits. A schematic diagram of a typical two-channel directional array is shown in figure 32.

6.2 SYSTEM CALIBRATION PROCEDURES

The calibration procedures for the strain-inertial systems are described in detail below. Recommended recording procedures are also given. The instructions apply specifically when using the Calibration Control Unit, Model 17123, to calibrate the strain-inertial seismograph system. When used with other systems, modification of these procedures might be necessary. A front panel view of the control unit is shown in figure 33.

6.2.1 Determination of Calibration Constants

6.2.1.1 Strain Seismometers

Calibrator constants for strain seismometers are determined by accurately measuring the displacement produced by a known sinusoidal current passing through a calibration coil. The displacement is measured using a variable-capacitance transducer (VCT) with a known sensitivity. Procedures are as follows:

- a. Set up the VCT for operation near the moving coil transducer of the seismometer to be calibrated.
- b. Measure the VCT sensitivity by displacing the capacitor plates using the micrometer-driven 100:1 motion reducer and measuring the output voltage with an oscilloscope.
- c. Compute the sensitivity of the VCT in volts per micron.

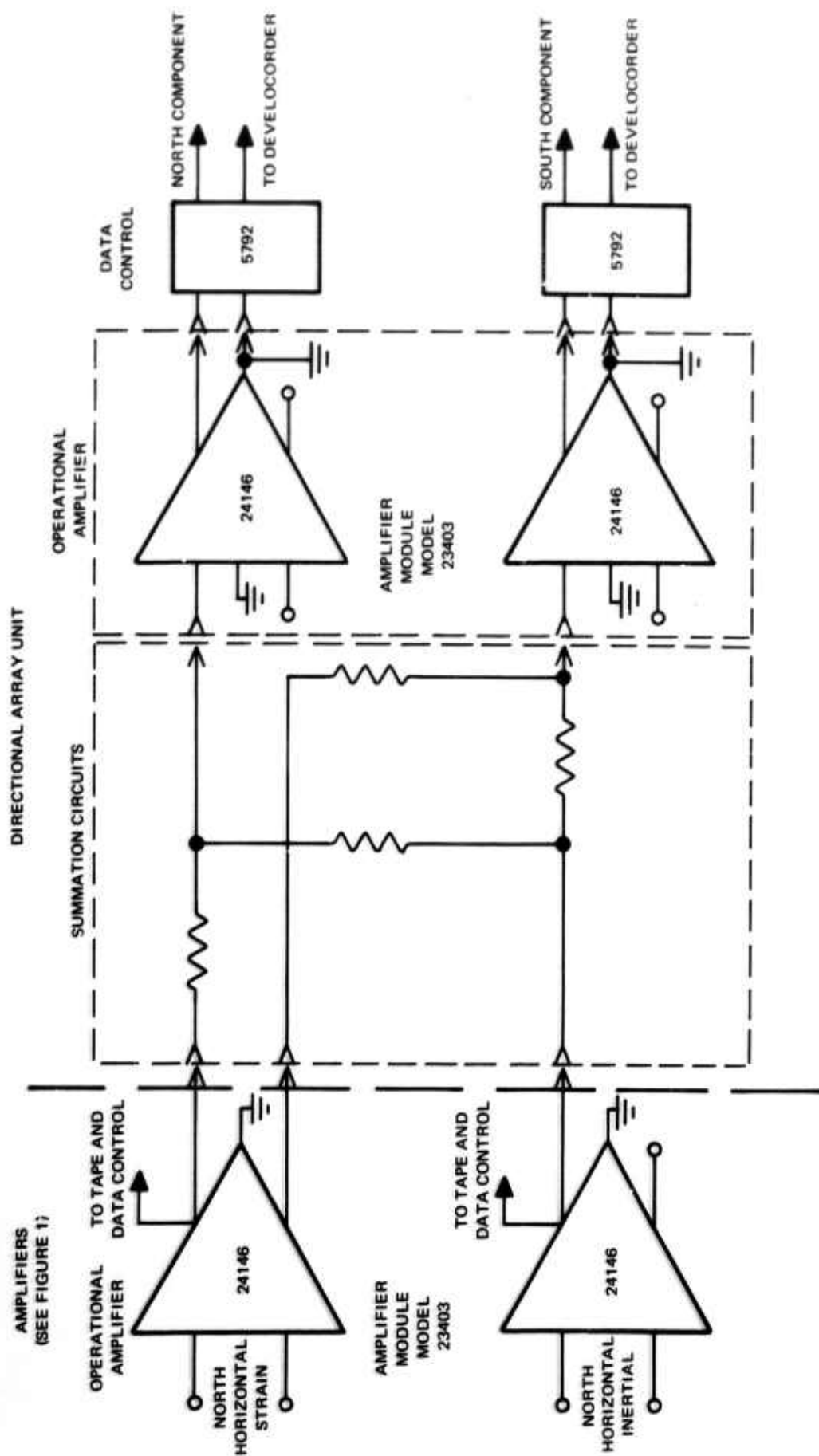


Figure 32. Schematic diagram of a typical two channel strain directional array

G 3964

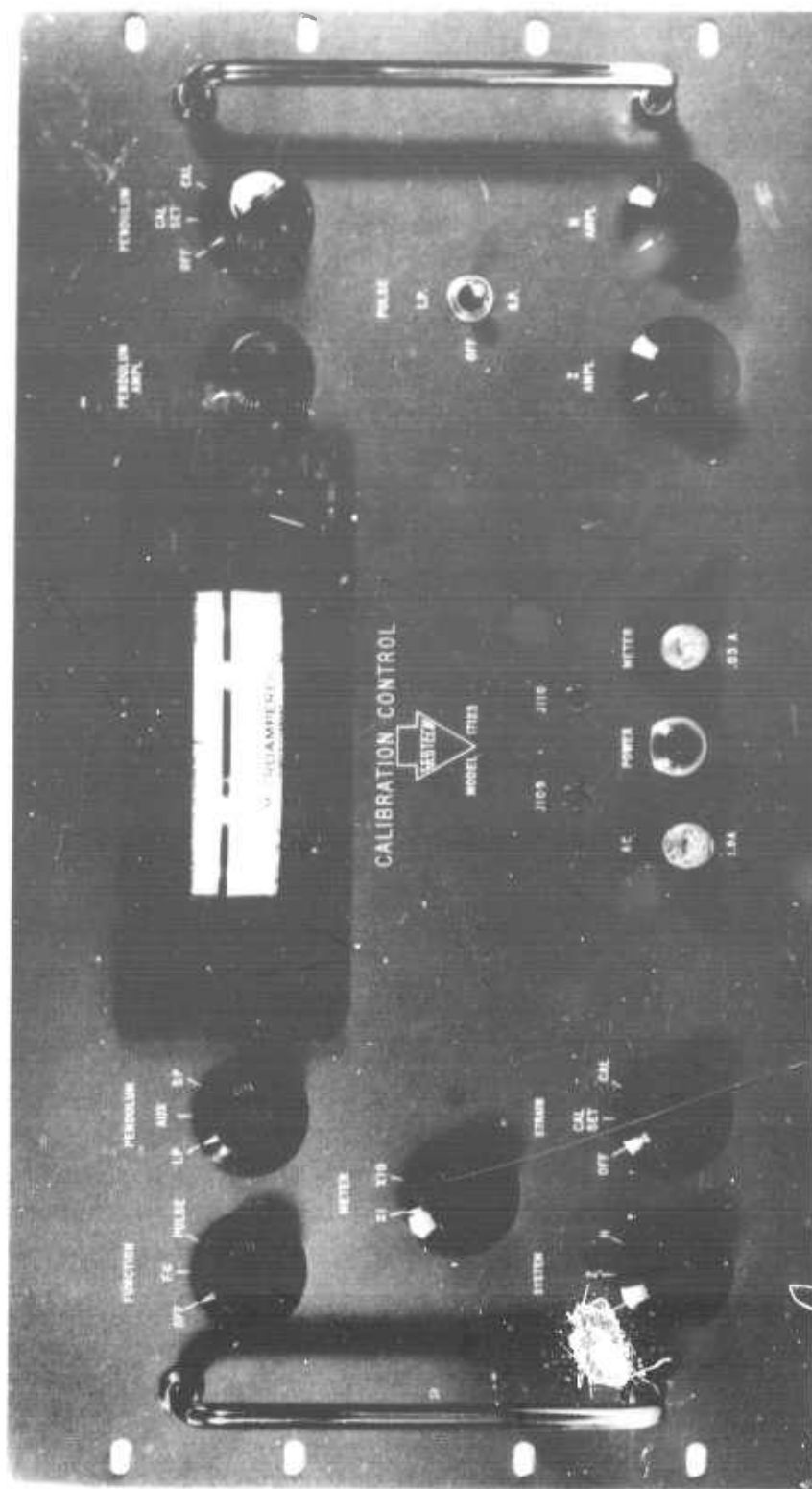


Figure 33. Calibration Control Unit, Model 17123

G 1602

d. Apply a 1.0 Hz sine wave calibration to the seismometer being calibrated. Use sufficient calibration current to obtain at least a 5 to 1 signal-to-noise ratio on the VCT output.

e. Measure the output voltage of the VCT with the same oscilloscope used to determine the VCT sensitivity.

f. Determine the calibrator constant using the following formula:

$$C = \frac{e}{si}$$

where C is the calibrator constant in microns per ampere

s is the sensitivity of the VCT in volts per micron

e is the output of the VCT in volts, peak-to-peak, due to i

i is the calibration current in amperes, peak-to-peak.

A typical range of values of the calibrator constant is 0.4 to 0.8 mμ/mA for the vertical and horizontal seismometers with the calibrator compressing a 6 m length of strain member, and 0.07 to 0.15 mμ/mA for horizontals with a 1 m calibrator.

6.2.1.2 Inertial Seismometers

Refer to paragraph 4.4 of the Operation and Maintenance Manuals, Vertical Seismometer, Model 6480, and Horizontal Seismometer, Model 7515, for detailed procedures for determining the motor constant (G) of the calibrators on the inertial seismometers.

6.2.2 Daily Calibration Procedures

6.2.2.1 Horizontal Strain Seismographs

To perform a daily calibration check of horizontal strain systems (including summation), proceed as follows:

- a. Operate all switches on the control unit to OFF, where applicable.
- b. Rotate H AMPL control R115 counterclockwise to its stop.
- c. Set the amplitude control of the function generator to the maximum clockwise position and the output frequency to 1.0 Hz.
- d. Set SYSTEM switch S105 to H.

e. Connect an oscilloscope in balanced mode to jacks J109 and J110 on the control unit.

f. Set STRAIN switch S107 to the CAL SET position.

NOTE

Calibration current is determined by measuring the voltage drop across a precision 100 ohm resistor (R128) in series with the calibration line. Therefore, 100 mV p-p measured between jacks J109 and J110 is equivalent to calibration current of 1 mA p-p.

g. Using the H AMPL control (R115), adjust the trace amplitude on the scope until the desired voltage is obtained. Calibration motion produced can be determined using the calibration constants for each seismometer.

h. Set the STRAIN switch S107 to CAL. After 20 seconds, set this switch to the OFF position.

i. Measure the trace amplitudes on the records (including SUM) to determine system magnifications.

j. Repeat steps a through i for long-period calibration except in step c use 0.04 Hz for the calibrating frequency and in step h use at least 300 seconds for the duration of calibration.

6.2.2.2 Vertical Strain Seismograph

To perform a daily calibration check of vertical strain instrumentation, proceed as follows:

- a. Operate all switches on the control unit to OFF, where applicable.
- b. Set SYSTEM switch S105 to P.
- c. Rotate PENDULUM AMPL control R109 counterclockwise to its stop.
- d. Set the function generator amplitude control to the maximum clockwise position and the output frequency to 0.1 Hz or below.

NOTE

Sinusoidal currents measured with microammeter M101 will not be accurate at frequencies greater than 0.1 Hz.

- e. Set FUNCTION switch S101 on the control unit to F. G.
- f. Set PENDULUM switch S102 to AUX.
- g. Set METER switch S106 to the Xi position, and the microammeter switch to the range appropriate for the calibration current desired (in microamperes).
- h. Set PENDULUM switch S103 to CAL SET.
- i. Adjust PENDULUM AMPL control R109 until the desired calibration current is indicated on microammeter M101.
- j. Set the function generator output frequency to 1.0 Hz.
- k. Place PENDULUM switch S103 to CAL. After 20 seconds set this switch to OFF.
- l. Set FUNCTION switch S101 to OFF.
- m. Measure the trace amplitude on the record to determine magnification.
- n. Repeat steps a through m for LP calibration, except in step j use 0.04 Hz for the calibration frequency and in step k use at least 300 seconds for the duration of calibration.

6.2.2.3 Inertial Seismographs

To perform a daily calibration check of inertial instrumentation, proceed as in 6.2.2.2 except in step f, set PENDULUM switch S102 to SP for short-period or LP for long-period instrument calibration.

6.2.3 Determination of Seismograph Response Curves

6.2.3.1 Amplitude Response for Strain Seismographs

To determine the amplitude responses of the strain instruments, including the summation, proceed as follows:

- a. Attenuate the data signal from the system to be calibrated until

the background noise is less than 1.0 mm on the record.

b. Apply a calibration current of sufficient magnitude to obtain readable trace deflections at all calibration points. Use procedures as contained in paragraphs 6.2.2.1 or 6.2.2.2 above, as applicable.

NOTE

The frequency which produces the greatest amplitude on strain channels is 1.5 Hz. To avoid nonlinearities in the amplifying systems, the balanced mode output voltage of the Narrow Band-pass Filter, Model 28900-01, should not exceed 7 V p-p at 1.5 Hz.

c. Calibrate at the following frequencies:

0.15 Hz	2.5 Hz
0.2	3.0
0.3	4.0
0.5	5.0
0.8	6.0
1.0	8.0
1.5	10.0
2.0	

Calibration duration should be 20 seconds for frequencies of 1.0 Hz and above and sufficient to record at least five complete cycles at frequencies below 1.0 Hz. Depending on the seismograph being calibrated, move the appropriate switch from CAL to CAL SET after recording each frequency.

d. Measure and record the trace amplitude at each frequency.

e. Determine the magnification at each frequency using the following formula:

$$m = \frac{A \times 10^6}{Y} = \frac{A}{C_i} \times 10^6 \quad \text{where:}$$

m is seismograph magnification

A is the recorded amplitude in millimeters, peak-to-peak

Y is the equivalent differential displacement in millimicrons

C is the calibrator constant in millimicrons per milliamp

and i is the calibration current in milliamps, peak-to-peak.

f. Plot magnification versus frequency on graph paper (3 x 3 log) to obtain the frequency response.

g. Repeat steps a through f for LP amplitude responses except substitute the following frequencies in step c:

0.01 Hz	0.04 Hz
0.015	0.05
0.02	0.06
0.025	0.08
0.03	0.10

Calibration duration should be sufficient to record at least five complete cycles for each frequency. Also, the balanced mode output voltage of the Narrow Band-pass Filter, Model 28900-02, should not exceed 15.0 V at 0.025 Hz, the frequency of greatest amplitude.

6.2.3.2 Amplitude Response for Inertial Seismographs

To obtain the amplitude response curve for an inertial system, proceed as in 6.2.3.1 above with the following exceptions:

a. In steps b and g, the frequency which produces the greatest amplitude is 0.6 Hz for SP and 0.01 Hz for LP inertial channels. PTA output voltages at these frequencies should not exceed 15 V p-p.

b. In step e, the formula used to compute the magnification at each frequency is as follows:

$$m = \frac{4\pi^2 f^2 A M}{G i \times 10^3} \quad \text{where}$$

M is the seismograph magnification

f is the frequency of the calibration in Hz

A is the recorded trace deflection in millimeters, peak-to-peak

M is the inertial mass of the seismometer in kilograms

(18 kg for SP and 10 kg for LP seismometers)

G is the calibrator motor constant in newtons per ampere

and i is the calibration current in amperes, peak-to-peak.

6.2.3.3 Phase Measurement Techniques

The phase of both the strain and inertial seismographs is measured using a variable-phase function generator. Use of the generator is described in Technical Report No. 65-90, Electrical Phase Study.

6.2.3.4 Determination of the Amplitude and Phase Response Match Between Strain and Inertial Seismographs

Figures 34 and 36 show the theoretical amplitude and phase response curves for the SP strain and inertial seismographs. Figures 35 and 37 show the theoretical amplitude and phase response curves for the LP strain and inertial seismographs.

Theoretical data for each component were computed and are listed in tables 4 through 11.

The differentiating effect of the strain seismometer causes the strain amplitude response curve to differ from the inertial curve by 6 dB/octave. Also, the strain phase response lags the inertial response by 90°. The strain amplitude curve may be compensated for this effect by multiplying each magnification value determined in 6.2.3.1, step e, by the frequency of the calibration. Figures 34 and 35 show compensated curves for the SP and LP strain seismographs. The strain phase responses may be compensated by simply adding 90° to each value determined. These compensated responses may then be directly compared to their inertial counterparts to determine the equality (or match) of the strain and inertial seismograph responses.

6.2.4 Determination of Strain Seismograph Polarity

The polarity of a strain seismograph is determined by manually displacing one end of the seismometer to simulate a reduction of the distance between

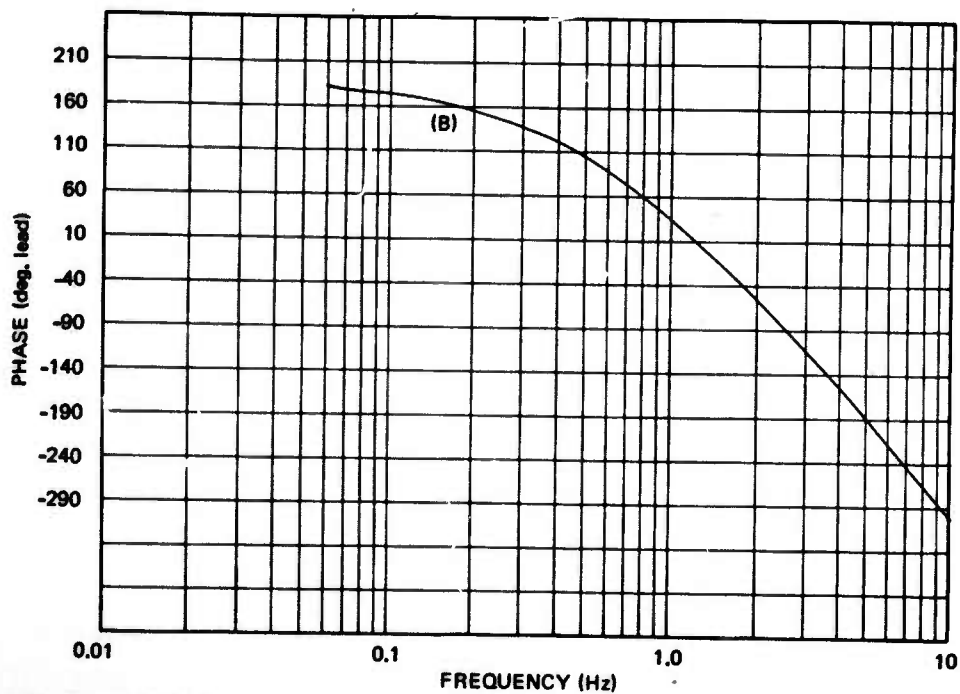
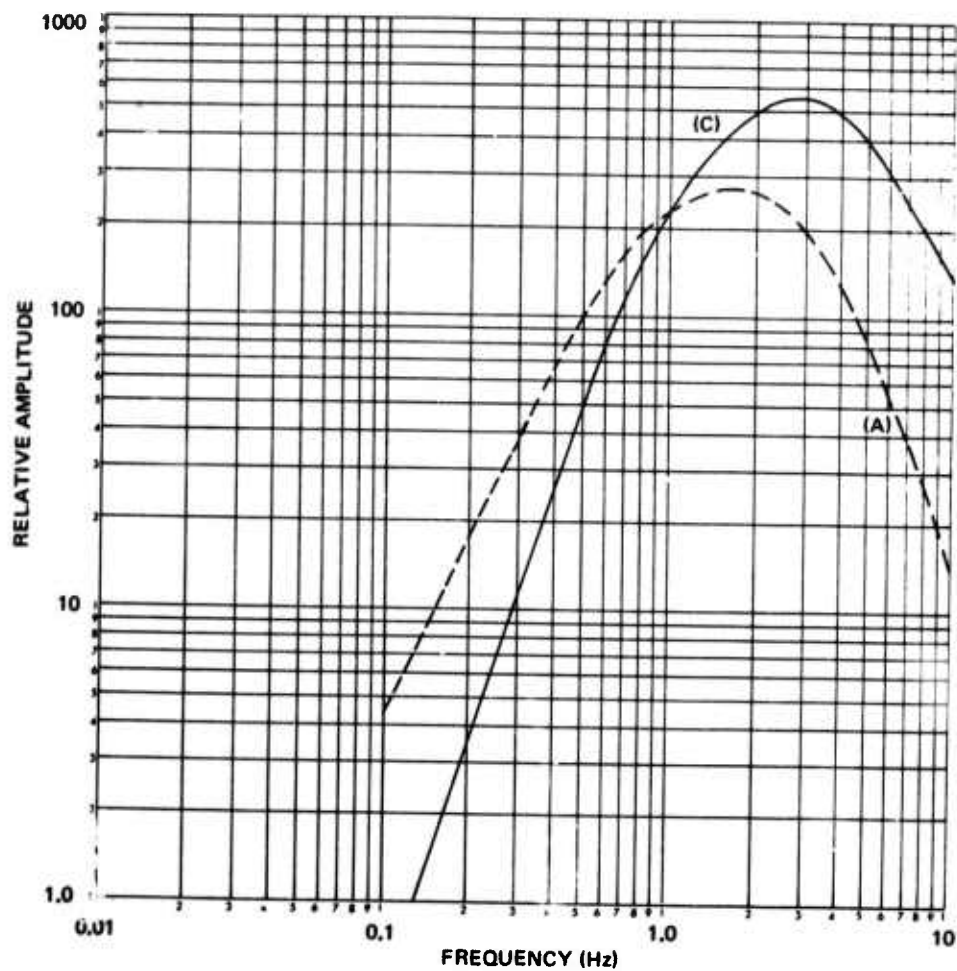


Figure 34. Curves A and B are theoretical amplitude and phase response curves for the short-period strain seismograph at constant differential ground displacement. Curve C is curve A compensated 6 dB/octave to allow determination of match between strain and inertial seismograph responses

G 3965

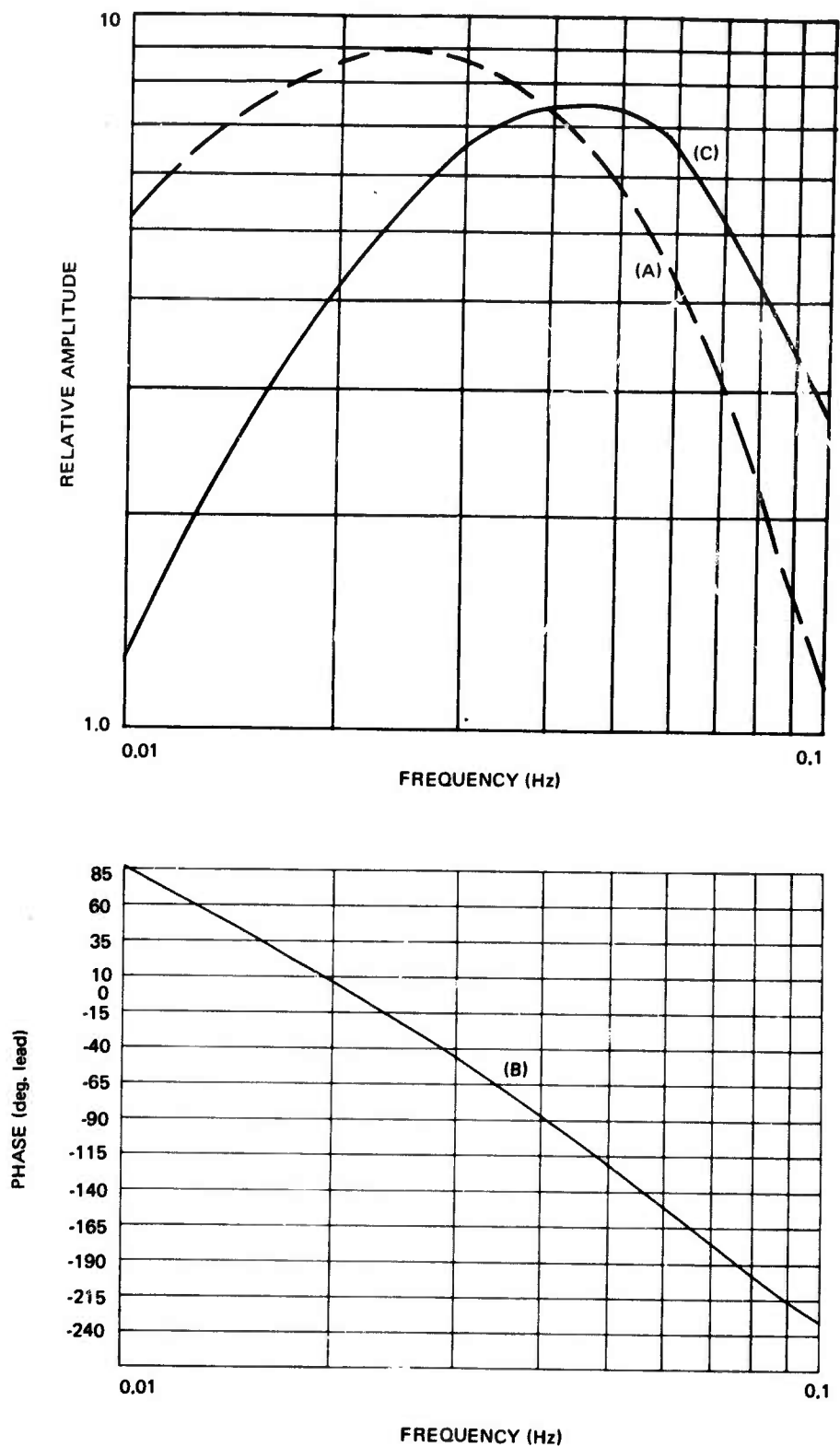


Figure 35. Curves A and B are theoretical amplitude and phase response curves for the long-period strain seismograph at constant differential ground displacement. Curve C is curve A compensated 6 dB/octave to allow determination of match between strain and inertial seismograph responses

G 3966

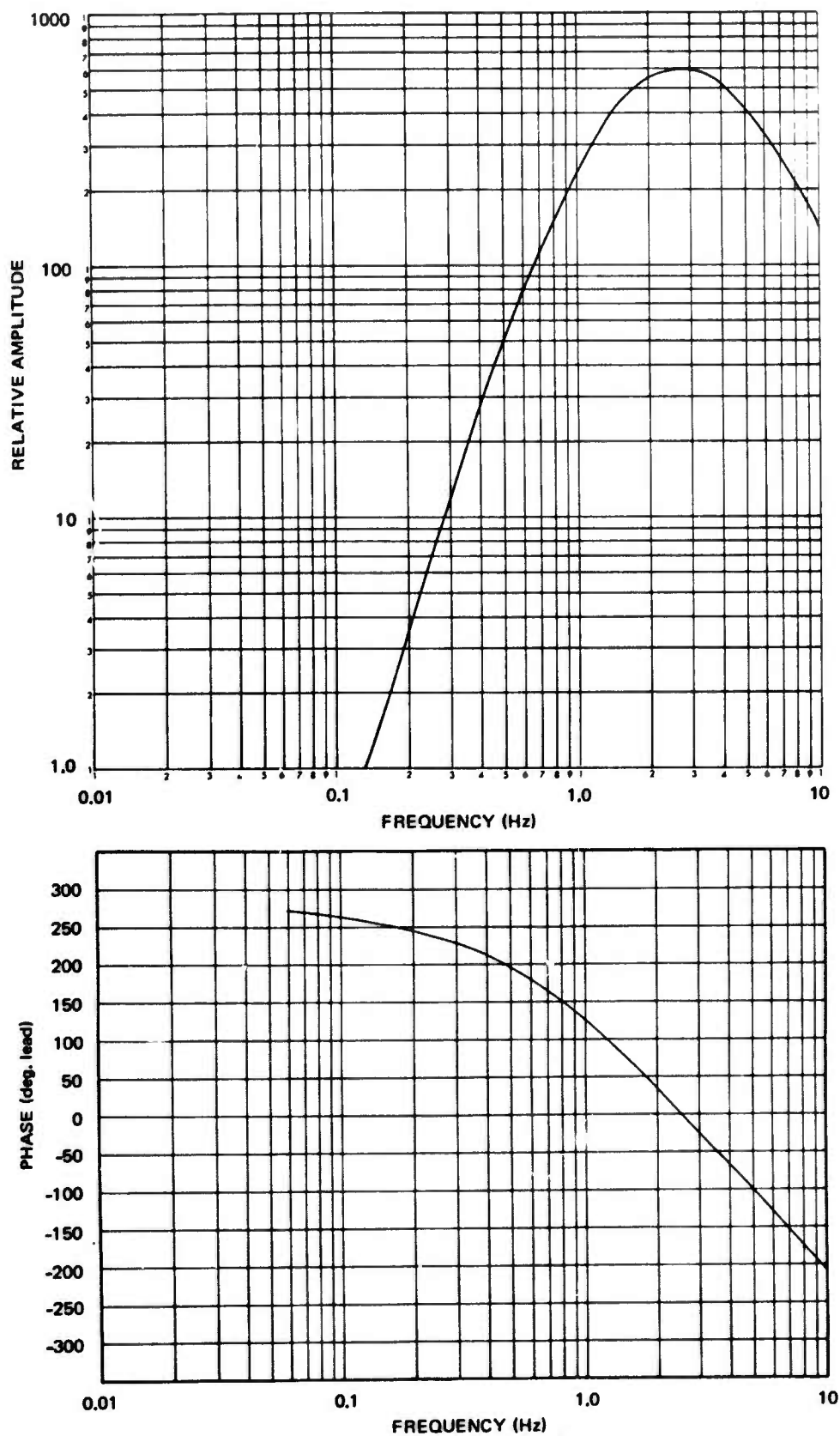


Figure 36. Theoretical amplitude and phase response curves for the short-period inertial seismograph for constant ground displacement

G 3967

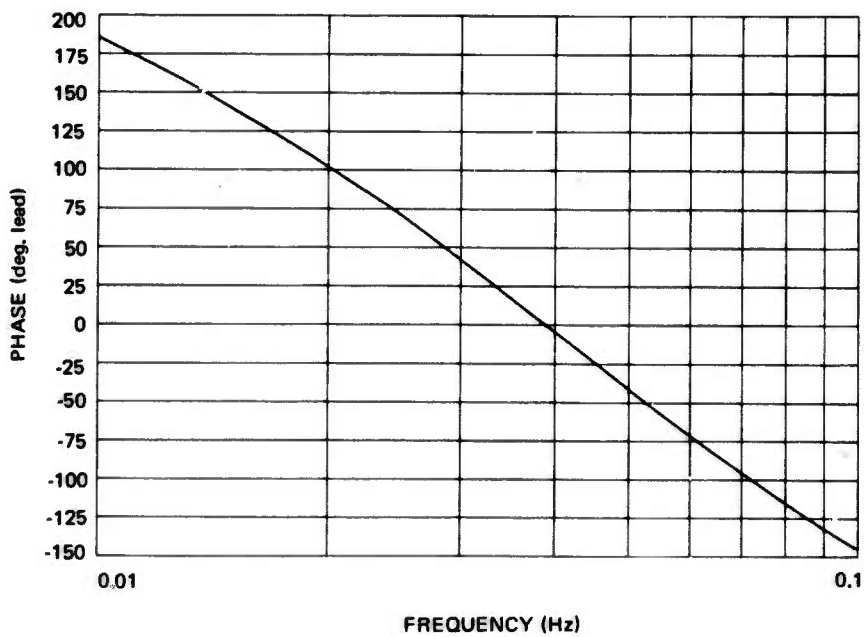
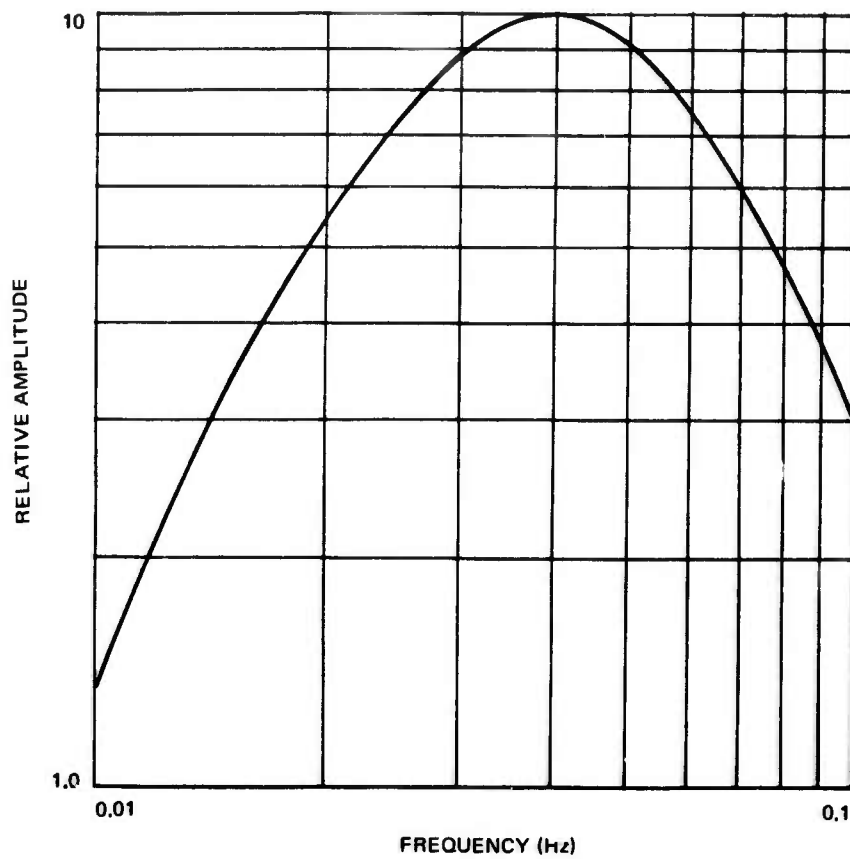


Figure 37. Theoretical amplitude and phase response curves for the long-period inertial seismograph at constant ground displacement

G 3968

Table 4. Theoretical SP strain seismograph amplitude response data for constant differential ground displacement

Frequency	Seis- mometer	PTA galvanometer	PTA filter 6824-1	Filter 28900	Operational amplifier	Develocorder galvanometer	Total
0.06	0.06	1.0	0.99	0.073	1.0	1.0	0.0043
.08	.08	1.0	1.0	.098	1.0	1.0	.0079
.10	.10	1.0	1.0	.12	1.0	1.0	.012
.15	.15	1.0	1.0	.183	1.0	1.0	.027
.20	.20	1.0	1.0	.245	1.0	1.0	.049
.25	.25	1.0	1.0	.31	1.0	1.0	.078
.30	.30	1.0	1.0	.36	1.0	1.0	.11
.40	.40	1.0	1.0	.49	1.0	1.0	.20
.50	.50	.99	1.0	.59	1.0	1.0	.29
.60	.60	.99	1.0	.66	1.0	1.0	.39
.80	.80	.98	1.0	.707	1.0	1.0	.55
1.0	1.0	.97	1.0	.67	1.0	1.0	.65
1.5	1.5	.97	1.0	.51	1.0	1.0	.74
2.0	2.0	.92	1.0	.40	1.0	1.0	.74
2.5	2.5	.84	1.0	.31	1.0	1.0	.65
3.0	3.0	.71	1.0	.26	1.0	.97	.54
4.0	4.0	.5	.99	.19	1.0	.96	.36
5.0	5.0	.34	.96	.15	1.0	.94	.23
6.0	6.0	.24	.90	.13	1.0	.91	.15
8.0	8.0	.14	.84	.096	1.0	.85	.077
10.0	10.0	.09	.707	.078	1.0	.78	.039

Table 5. Theoretical SP strain seismograph phase response data
for constant differential ground displacement

Frequency	Seis- mometer	PTA galvanometer	PTA filter 6824-1	Filter 28900	Operational amplifier	Develocorder galvanometer	Total
.06	90°	-2°	9°	84°	0°	0°	181°
.08	90	-2	6	82	0	0	176
.10	90	-2	5	81	0	0	174
.15	90	-4	3	76	0	-1	164
.20	90	-5	1	71	0	-2	155
.25	90	-6	0	65	0	-2	147
.30	90	-8	-1	59	0	-2	138
.40	90	-11	-2	48	0	-3	122
.50	90	-14	-3	36	0	-3	106
.60	90	-16	-4	24	0	-4	90
.80	90	-21	-5	0	0	-5	59
1.0	90	-27	-7	-17	0	-7	32
1.5	90	-43	-12	-43	0	-10	-18
2.0	90	-60	-16	-56	0	-13	-55
2.5	90	-75	-20	-64	0	-16	-85
3.0	90	-90	-25	-69	0	-19	-113
4.0	90	-112	-34	-74	0	-26	-156
5.0	90	-127	-43	-78	0	-32	-190
6.0	90	-137	-54	-79	0	-38	-218
8.0	90	-149	-72	-82	0	-50	-268
10.0	90	-155	-89	-84	0	-62	-300

Table 6. Theoretical LP strain seismograph amplitude response data
for constant differential ground displacement

Frequency	Seis- mometer	PTA galvanometer	PTA filter 6824-14	Filter 28900	Operational amplifier	Develocorder galvanometer	Total
.01	1.0	.4475	1.100	.166	1.0	1.0	.0817
.015	1.5	.2647	1.20	.250	1.0	1.0	.119
.02	2.0	.1683	1.220	.330	1.0	1.0	.135
.025	2.5	.1147	1.170	.420	1.0	1.0	.141
.03	3.0	.0825	1.12	.495	1.0	1.0	.137
.04	4.0	.0481	1.000	.620	1.0	1.0	.119
.05	5.0	.0313	.8720	.690	1.0	1.0	.0944
.06	6.0	.022	.75	.707	1.0	1.0	.0700
.07	7.0	.0162	.64	.690	1.0	1.0	.0500
.08	8.0	.0124	.55	.650	1.0	1.0	.0355
0.1	10.0	.008	.4120	.550	1.0	1.0	.0182

Table 7. Theoretical LP strain seismograph phase response data
for constant differential ground displacement

Frequency	Seis- mometer	PTA galvanometer	PTA filter 6824-14	Filter 28900	Operational amplifier	Develocorder galvanometer	Total
.01	90°	-96°	15°	78°	0°	0°	87°
.015	90	-118	-2	71	0	0	41
.02	90	-132	-16	64	0	0	6
.025	90	-140	-28	56	0	0	-22
.03	90	-146	-38	48	0	0	-46
.04	90	-155	-53	32	0	0	-86
.05	90	-160	-65	14	0	0	-121
.06	90	-163	-76	-1	0	0	-150
.07	90	-165	-86	-15	0	0	-176
.08	90	-167	-95	-26	0	0	-198
0.1	90	-170	-110	-41	0	0	-231

Table 8. Theoretical SP inertial seismograph amplitude response data
for constant ground displacement

Frequency	Seis- mometer	PTA galvanometer	PTA filter 6824-1	Operational amplifier	Develocorder galvanometer	Total
0.06	0.076	1.0	.99	1.0	1.0	0.0257
.08	0.063	1.0	1.0	1.0	1.0	.063
.10	0.12	1.0	1.0	1.0	1.0	.12
.15	0.46	1.0	1.0	1.0	1.0	.46
.20	0.95	1.0	1.0	1.0	1.0	.98
.25	1.9	1.0	1.0	1.0	1.0	1.9
.30	3.3	1.0	1.0	1.0	1.0	3.3
.40	7.8	1.0	1.0	1.0	1.0	7.8
.50	14.7	.99	1.0	1.0	1.0	14.5
.60	23.8	.99	1.0	1.0	1.0	23.5
.80	45.3	.98	1.0	1.0	1.0	44.5
1.0	67	.97	1.0	1.0	1.0	65
1.5	127	.97	1.0	1.0	1.0	123
2.0	160	.92	1.0	1.0	1.0	147
2.5	194	.84	1.0	1.0	1.0	163
3.0	234	.71	1.0	1.0	.97	162
4.0	304	.50	0.99	1.0	.96	144
5.0	375	.34	0.96	1.0	.94	115
6.0	467	.24	0.90	1.0	.91	92
8.0	615	.14	0.84	1.0	.65	62
10.0	780	.09	0.707	1.0	.78	38

Table 9. Theoretical SP inertial seismograph phase response data
for constant ground displacement

Frequency	Seis- mometer	PTA galvanometer	PTA filter 682/-1	Operational amplifier	Develocorder galvanometer	Total
0.06	264°	-2°	9°	0°	0°	271°
.08	262	-2	6	0	0	266
.10	258	-2	5	0	0	261
.15	255	-4	3	0	-1	253
.20	249	-5	1	0	-2	243
.25	244	-6	0	0	-2	236
.30	239	-8	-1	0	-2	228
.40	228	-11	-2	0	-3	212
.50	216	-14	-3	0	-3	196
.60	204	-16	-4	0	-4	180
.80	181	-21	-5	0	-5	150
1.0	163	-27	-7	0	-7	122
1.5	136	-43	-12	0	-10	71
2.0	123	-60	-16	0	-13	34
2.5	114	-75	-20	0	-16	3
3.0	110	-90	-25	0	-19	-24
4.0	104	-112	-34	0	-26	-68
5.0	102	-127	-43	0	-32	-100
6.0	100	-137	-54	0	-38	-129
8.0	98	-149	-72	0	-50	-173
10.0	96	-155	-89	0	-62	-210

Table 10. Theoretical LP inertial seismograph amplitude response data
for constant ground displacement

<u>Frequency</u>	<u>Seis- mometer</u>	<u>PTA galvanometer</u>	<u>PTA filter 6824-14</u>	<u>Operational amplifier</u>	<u>Develocorder galvanometer</u>	<u>Total</u>
.01	.275	.4475	1.100	1.0	1.0	.135
.015	1.03	.2647	1.20	1.0	1.0	.328
.02	2.66	.1683	1.220	1.0	1.0	.546
.025	5.46	.1147	1.170	1.0	1.0	.734
.03	9.45	.0825	1.12	1.0	1.0	.872
.04	20.8	.0481	1.000	1.0	1.0	1.00
.05	33.8	.0313	.8720	1.0	1.0	.923
.06	46.4	.022	.75	1.0	1.0	.766
.07	58.0	.0162	.64	1.0	1.0	.601
.08	69.4	.0124	.55	1.0	1.0	.474
0.1	89.5	.008	.4120	1.0	1.0	.295

Table 11. Theoretical LP inertial seismograph phase response data
for constant ground displacement

Frequency	Seis- mometer	PTA galvanometer	PTA filter 6824-14	Operational amplifier	Develocorder galvanometer	Total
.01	260°	-96°	+15°	0°	0°	185°
.015	260	-118	-2	0	0	140
.02	251	-132	-16	0	0	103
.025	239	-140	-28	0	0	71
.03	227	-146	-38	0	0	43
.04	204	-155	-53	0	0	-4
.05	184	-160	-65	0	0	-41
.06	168	163	-76	0	0	-71
.07	155	-165	-86	0	0	-96
.08	146	-167	-95	0	0	-116
0.1	135	-170	-110	0	0	-145

anchor points. The polarity should be adjusted so that this provides an upward trace deflection. If, however, the output of a strain seismograph is combined with that of an inertial seismograph, the specific application of the combined outputs will govern the polarity of the strain seismograph.

6.3 RECORDING PROCEDURES

6.3.1 Recorder Requirements

To record both SP and LP strain-inertial data simultaneously, the following recorders are needed: two SP Develocorders, two LP Develocorders, and two magnetic-tape recorders. The Develocorders are used to record on line LP and SP primary data and directional-array data. The magnetic-tape recorders are used to record LP and SP data for off line processing.

6.3.2 Recorder Signal Levels

6.3.2.1 Develocorders

The magnifications on the Develocorders are governed by the particular application of the strain-inertial system. The data recorded on the two primary Develocorders are used mainly for discrimination of wave type and direction. The two directional array Develocorders are used primarily for enhancement of the horizontal components of seismic signal by seismic noise rejection, and to determine direction of seismic signals and noise. Listed below are recommended operating magnifications for the recorders.

Primary SP Develocorder

<u>Trace No.</u>	<u>Magnification @ 1.0 Hz</u>	<u>Trace identification</u>
1	250K	SP north inertial (SPN)
2	7, 000K	SP north strain (SNS)
3	7, 000K	Summation of SNS & SES (Σ SNS, SES)
4	7, 000K	SP east strain (SES)
5	250K	SP east inertial (SPE)
6	250K	SP north inertial (SPN)
7	250K	SP vertical inertial (SPZ)
8	24, 500K	SP vertical strain (SZS)
9	250K	SP northeast inertial (SPNE)
10	7, 000K	SP northeast strain (SNES)
11	7, 000K	Summation of SNES & SNWS (Σ SNES, SNWS)
12	7, 000K	SP northwest strain (SNWS)
13	250K	SP northwest inertial (SPNW)
14	-	Anemometer (Wind)

SP Directional Array Develocorder

<u>Trace No.</u>	<u>Magnification @ 1.0 Hz</u>	<u>Trace identification</u>
1	250K	SP vertical inertial (SPZ)
2	250K	SP north inertial (SPN)
3	250K	SP east inertial (SPE)
4	250K	SP northeast inertial (SPNE)
5	250K	SP northwest inertial (SPNW)
6	500K *	North element of strain directional array (N)
7	500K *	Northeast element of strain directional array (NE)
8	500K *	East element of strain directional array (E)
9	500K *	Southeast element of strain directional array (SE)
10	500K *	South element of strain directional array (S)
11	500K *	Southwest element of strain directional array (SW)
12	500K *	West element of strain directional array (W)
13	500K *	Northwest element of strain directional array (NW)

*Magnification = $\frac{\text{Strain magnification}}{28 (@1.0 \text{ Hz})} + \text{inertial magnification where}$

$\frac{\text{Strain magnification}}{28 (@1.0 \text{ Hz})} \equiv \text{equivalent inertial magnification (equated for seismic wave of apparent surface velocities of 3.2 km/sec)}$

Primary LP Develocorder

<u>Trace No.</u>	<u>Magnification @ 0.04 Hz</u>	<u>Trace identification</u>
1	10K	LP north inertial (LPN)
2	7, 000K	LP north strain (SNL)
3	7, 000K	Summation of SNL & SEL (Σ SNL, SEL)
4	7, 000K	LP east strain (SEL)
5	10K	LP east inertial (LPE)
6	10K	LP north inertial (LPN)
7	10K	LP vertical inertial (LPZ)
8	21, 000K	LP vertical strain (SZL)
9	10K	LP northeast inertial (LPNE)
10	7, 000K	LP northeast strain (SNEL)
11	7, 000K	Summation of SNEL and SNWL (Σ SNEL, SNWL)
12	7, 000K	LP northwest strain (SNWL)
13	10K	LP northwest inertial (LPNW)
14		Anemometer (Wind)

LP Directional Array Develocorder

<u>Trace No.</u>	<u>Magnification @ 0.04 Hz</u>	<u>Trace identification</u>
1	10K	LP vertical inertial (LPZ)
2	10K	LP north inertial (LPN)
3	10K	LP east inertial (LPE)
4	10K	LP northeast inertial (LPNE)
5	10K	LP northwest inertial (LPNW)
6	20K *	North element of LP strain directional array (NL)
7	20K *	Northeast element of LP strain directional array (NEL)
8	20K *	East element of LP strain directional array (EL)
9	20K *	Southeast element of LP strain directional array (SEL)
10	20K *	South element of LP strain directional array (SL)
11	20K *	Southwest element of LP strain directional array (SWL)
12	20K *	West element of LP strain directional array (WL)
13	20K *	Northwest element of LP strain directional array (NWL)

* Magnification = $\frac{\text{Strain magnification}}{700 (@0.04 \text{ Hz})} + \text{inertial magnification}$ where

$\frac{\text{Strain magnification}}{700 (@0.04 \text{ Hz})} \equiv \text{equivalent inertial magnification (equated for seismic wave of apparent surface velocities of 3.2 km/sec)}$

6.3.2.2 Magnetic -Tape Recorders

The recording levels on the magnetic-tape recorders are governed by the objective of off line processing. For example, low-level seismic signal enhancement by seismic noise rejection requires recording the seismic noise data at least 10 dB above the magnetic-tape noise. The recommended operating level of seismic noise in terms of the WMSO magnetic-tape system output for both SP and LP strain and inertial seismographs are given in figure 38. Strain and inertial data recorded on magnetic tape are listed below.

SP Magnetic-Tape Recorder

<u>Channel No.</u>	<u>Channel identification</u>
1	BCD station time
2	SP north inertial (SPN)
3	SP east inertial (SPE)
4	SP north strain (SNS)
5	SP east strain (SES)
6	SP vertical strain (SZS)
7	Compensation
8	SP northeast inertial (SPNE)
9	SP northwest inertial (SPNW)
10	SP northeast strain (SNES)
11	SP northwest strain (SNWS)
12	SP vertical inertial (SPZ)
13	Summation of SNS and SES (Σ SNS, SES)
14	Voice comment

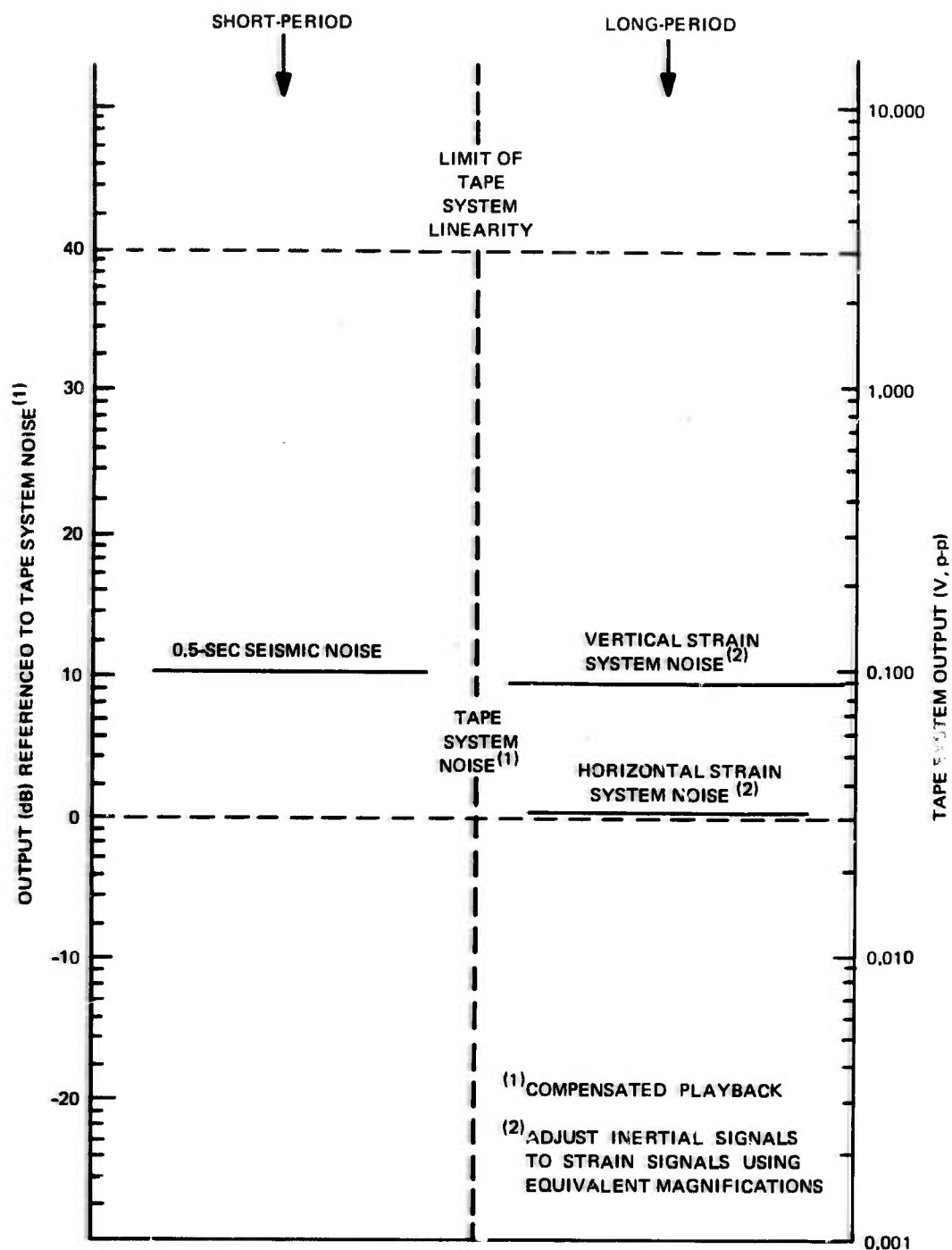


Figure 38. Recommended operating levels for the magnetic tape recorders in the strain inertial system

G 3969

LP Magnetic-Tape Recorder

<u>Channel No.</u>	<u>Channel identification</u>
1	BCD station time
2	LP north inertial (LPN)
3	LP east inertial (LPE)
4	LP north strain (SNL)
5	LP east strain (SEL)
6	LP vertical strain (SZL)
7	Compensation
8	LP northeast inertial (LPNE)
9	LP northwest inertial (LPNW)
10	LP northeast strain (SNEL)
11	LP northwest strain (SNWL)
12	LP vertical inertial (LPZ)
13	Summation of SNL and SEL (Σ SNL, SEL)
14	Voice comment

7. SELECTED REFERENCES

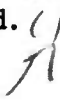
- Benioff, Hugo, 1935, A linear strain seismograph: Bull. Seism. Soc. Am., vol. 25 (4), p.283-309
- _____, and B. Gutenberg, 1952, The response of strain and pendulum seismographs to surface waves: Bull. Seism. Soc. Am., vol. 42, p. 229-237
- Bullen, K. E., 1963, An introduction to the theory of seismology: Cambridge, Cambridge Univ. Press
- Douze, E. J., 1967, Short-period seismic noise: Bull. Seism. Soc. Am., vol. 57, p. 55-81
- Evernden, J. F., 1954, Direction of approach of Rayleigh waves and related problems: Bull. Seism. Soc. Am., vol. 44, p. 159-184
- Ewing, W. M., Jardetzky, W. S., and Press, F., 1957, Elastic waves in a layered media: McGraw Hill Book Company, Inc., New York
- Fix, J. E., 1967, Appendix 2 to Technical Report No. 67-59, Seismic velocity model for the Wichita Mountains Seismological Observatory, Project VT/5081, 1 July to 30 September 1967: Geotech, A Teledyne Company, Garland, Texas
- Huang, Y. T., 1967, Effect of an elastically restrained boundary on SV-wave radiation patterns, Technical Report No. 66-111: Teledyne Industries, Geotech Division, Garland, Texas
- Peck, D. R., and Veith, K. F., 1966, Computation of P-phase travel times, Technical Report No. 66-110: Teledyne Industries, Geotech Division, Garland, Texas
- Romney, Carl, 1964, Combinations of strain and pendulum seismographs for increasing the detectability of P: Bull. Seism. Soc. Am., vol. 54(6), p. 2165-2174
- Shopland, R. C., 1966, Shallow strain seismograph installation at the Wichita Mountains Seismological Observatory: Bull. Seism. Soc. AM., vol. 56, p. 337-360

UNCLASSIFIED

Security Classification

DOCUMENT CONTROL DATA - R & D

(Security classification of title, body of abstract and indexing annotation must be entered when the overall report is classified)

1. ORIGINATING ACTIVITY (Corporate author) Geotech A Teledyne Company 3401 Shiloh Road, Carland, Texas 75040		2a. REPORT SECURITY CLASSIFICATION Unclassified	
		2b. GROUP	
3. REPORT TITLE Strain Seismograph Operating Procedures and Applications			
4. DESCRIPTIVE NOTES (Type of report and inclusive dates) Special Technical Report			
5. AUTHOR(S) (First name, middle initial, last name) Richard H. Kirklin Barry W. Girard			
6. REPORT DATE 1 May 1968		7a. TOTAL NO. OF PAGES 93	7b. NO. OF REFS 11
8a. CONTRACT OR GRANT NO. AF 33(657)-15288		9a. ORIGINATOR'S REPORT NUMBER(S) Technical Report No. 68-2	
b. PROJECT NO. VELA T/5081			
c.		9b. OTHER REPORT NO(S) (Any other numbers that may be assigned this report)	
d.			
10. DISTRIBUTION STATEMENT Qualified users may obtain copies of this report from the Defense Documentation Center, Cameron Station, Alexandria, Virginia, 22314. This document is subject to special export controls and each transmittal to foreign governments or foreign nationals may be made only with prior approval of the Chief, AFTAC.			
11. SUPPLEMENTARY NOTES		12. SPONSORING MILITARY ACTIVITY HQ USAF (AFTAC/VELA Seismological Center) Washington, D. C. 20333	
13. ABSTRACT Procedures necessary to operate the multicomponent strain seismograph facility located at the Wichita Mountains Seismological Observatory (WMSO) and the applications of these seismographs to the enhancement and identification of seismic waves are discussed. The theory of strain seismometers and their response to seismic waves are examined to assist in the interpretation of strain seismograms. A description of the WMSO strain seismograph system is also included. 			

DD FORM 1473
1 NOV 65

UNCLASSIFIED

Security Classification

14.

KEY WORDS

LINK A

LINK B

LINK C

ROLE

WT

ROLE

WT

ROLE

WT

Seismology
Strain Seismographs
Strain Applications
Seismograph Operating Procedures
Interpretation of Strain Seismograms